Università degli Studi di Salerno

DIPARTIMENTO DI MATEMATICA

Scuola Dottorale in Scienze Matematiche, Fisiche e Naturali

Ciclo XIII

Stochastic diffusion processes with jumps for cancer growth and neuronal activity models

Author:
Serena Spina

Research Director:
Prof. Virginia Giorno

Tutor:
Prof. Antonio Di Crescenzo

PhD Director:
Prof. Patrizia Longobardi

A thesis presented for the degree of
Doctor of Philosophy

No substantial part of the universe is so simple that it can be grasped and controlled without abstraction. Abstraction consists in replacing the part of the universe under consideration by a model of similar but simple structure. Models are thus central necessity of scientific procedures.

A. Rosenblueth and N. Wiener, 1945

Contents

Introduction

In the last decades, great attention has been paid to the description of biological, physical and engineering systems subject to various types of jumps. A jump, or catastrophe, is considered as a random event that shifts the state of an evolutionary process in a certain level from which the process can re-start. In the most of literature, a downward jump represents the extinction or reduction of elements in a biological population (due to virus infection or external agent) or of customers in a queue system (due to power failure, reset or system bug).
On the other hand, during the spreading of a rumor one can consider the effect of an external entity that denies the rumor so that the process is reset to the initial state consisting in a unique spreader (the rest of population is ignorant) that renews the spreading process. In Section 0.1, we study two rumor spreading models with denials to give examples of evolutionary processes with jumps.

The notion of catastrophe was introduced by Brockwell in the 80's to evaluate the dangerous of extinction of some wild species subject to phenomenons such as pollution, epidemics, fires or any other external agent. Specifically, Brockwell studied birth-death stochastic processes with catastrophes causing the reduction of the population size n to $n - j$, with a general probability; he introduced models with geometric, binomial and uniform distribution (cf. [12]) and he obtained interesting results regarding the extinction time and the mean size of the population (cf. [14]). After that, most of the literature on such models focuses on studies related to birth-death processes subject to total catastrophes, where the effect of a catastrophe is the total extinction of the population (cf. [26], [27], [40], [41], [55], [70], [82]). These kind of catastrophes, occurring at exponential rate, have been introduced in systems which evolve according to dynamics of some continuous-time Markov chains (cf. [13], [19], [56], [57]). In these papers, the transient and the stationary probabilities, the time of extinction and the first occurrence time of effective catastrophe have been studied.

Taking into account that many of real phenomena are non-stationary, one can consider time non-homogeneous stochastic processes and study them under the effect of jumps; for example, one can study a queueing system whose rates are time-

dependent as well as they are dependent on the number of customers present in the queue. In this direction, in [43] we have considered a inhomogeneous continuous-time Markov chain subject to total catastrophes with time varying intensity; in Section 0.2 we report the performed analysis. In particular, we analyze the system by studying the transition probabilities and the moments of the number of customers in the system. We focus on the problem of the first visit time (FVT) to zero state with particular attention to the busy period of the service center, i.e the time interval during which at least one server is busy. Specifically, we pay attention to the case in which the catastrophe intensity is a periodic function of time obtaining some properties of asymptotic distribution and of the FVT density.

The results obtained in literature for continuous-time Markov chains have suggested the possibility of deriving corresponding results for continuous processes bounded by one reflected boundary and subject to catastrophes that occur at exponential rate. Indeed, in [25], [26], [28], [29] some general results for the transient and steady-state probability density functions of diffusion processes in the presence of catastrophes have been obtained. In particular, some characteristics for jump diffusion processes can be expressed in terms of the same characteristics of the corresponding processes without jumps.

In this thesis, the effect of jumps is introduced in stochastic diffusion processes of interest in neurobiological environment. Specifically, we consider the Gompertz model of cancer growth with jumps to simulate the effect of an intermittent therapy and we study a model of neuronal activity based on the non-homogeneous Ornstein-Uhlenbeck process including the effect of refractoriness periods.

In the remaining part of this chapter, we study two rumor spreading models with denials and we analyze an inhomogeneous continuous-time Markov chain in the presence of catastrophes with periodic intensity function.

The rest of thesis is organized as follows.
In Chapter 1, we introduce stochastic diffusion processes and we remark some characteristics such as the transition probability density function (pdf) and its moments, the first passage time (FPT) problem and the asymptotic behavior of the FPT densities. Then, we construct a stochastic diffusion process with jumps. In particular, we suppose that catastrophes occur at time interval following a general distribution and we suppose that return points are randomly chosen. Moreover, we consider the possibility that, after each jump, the process can evolve with a different dynamics respect to the previous processes; we also suppose that the inter-jump intervals and the return points are not identically distributed. For this type of process, we analyze the transition pdf, its moments and the FPT problem, then we study the Wiener process with jumps, as example.

In the other chapters, we focus on two stochastic diffusion processes with jumps having neurobiological interest. In both cases, firstly we study the dynamic characterizing the phenomenon, then we focus on an appropriate diffusion process on which construct the process with jumps.
Specifically, in Chapter 2, we consider a diffusion process with jumps for cancer growth. Among all processes describing the cancer growth, we consider the Gompertz model; indeed the Gompertz law plays an important role in the dynamic of solid tumor because in several contexts it seems to fit experimental data in a reasonable precise way (cf., for example, [66], [86]). Specifically, the Gompertz equation has proven to be a useful tool to describe human cancer evolution such as the breast and colon cancer (cf., for example, [17], [49], [69], [79], [80]). Moreover, this model is used to study the problem of finding the optimal chemotherapy ([65]) and to describe the interaction between the cancer and the immunological system ([5], [23], [24], [54]). Hence, in order to analyze the effect of a therapeutic program that provides intermittent suppression of cancer cells, we construct a Gompertz process with jumps for which a jump represents a therapeutic application. Firstly, we consider a simple model in which the Gompertz process has the same characteristics between two consecutive jumps, the return points and the inter-jump intervals are random and identically distributed. For this model, we study the transition pdf, the average state of the system (representing the mean size of the tumor) and the number of therapeutic applications to be carried out in time intervals of fixed amplitude ([42]). After this first step, we introduce a more realistic model ([46], [47], [48]). Specifically, we assume:

- the therapeutic program has a deterministic scheduling, so that jumps occur at fixed and conveniently chosen time instants;
- the return points are deterministic;
- when a therapy is applied there is a selection event in which only the most aggressive clones survive (for example this perspective could be applied to targeted drugs that have a much lower toxicity for the patient).

Taking into consideration these aspects, we construct the deterministic and the stochastic processes with jumps. Since each therapeutic application involves a reduction of the tumor mass, but it also implies an increase of the growth speed, the problem of finding a compromise between these two aspects raises. We propose two possible schedulings in order to control the cancer growth. In the first scheduling, we assume that inter-jump intervals have equal size (cf. [46], [47]); this study is useful when one is forced to apply the therapy at equidistant times. In this case, we show interesting properties which allow to choose the most appropriate application times, when the toxicity of the drug is fixed. In the second scheduling (cf. [48]),

we suggest to apply the therapy just before the cancer mass reaches a fixed control threshold. To this aim, we study the FPT problem through a constant boundary and we provide information on how to choose the application times so that the cancer size remains bounded during the treatment. Finally, we compare the deterministic and the stochastic approaches, and we provide a comparison between the two proposed scheduling.

In Chapter 3, we consider a stochastic diffusion process with jumps for the neuronal activity. In particular, to describe the input-output behavior of a single neuron subject to a diffusion-like dynamics, we model the neuronal membrane potential via the Ornstein-Uhlenbeck (OU) diffusion process ([44]). We consider the OU process because it takes account of the exponential decay exhibited by the membrane potential in the absence of input of any type. We assume that inputs, while remaining a constant amplitude, are characterized by time-dependent rates, meaning that some external stimulations are induced on the neuron. Hence, to take into account this feature, we construct a return process on a time non-homogeneous OU process and we study the number of firings and the distribution of interspike intervals, under the assumption of exponential distribution for the firing time.
Moreover, we take into account the effect of refractory periods on the model; a refractory period is a time interval following each spike and during which the neuron is completely or partially unable to respond to stimuli. Hence, we introduce random downtimes which delay spikes, simulating the effect of refractoriness. Finally, a theoretical and numerical analysis of the return process in the presence of constant and exponential refractoriness is performed.

0.1 Rumor spreading with denials

During the spreading of a rumor one can consider the effect of an external entity that denies the rumor so that the process is reset to the initial state consisting in a unique spreader (the rest of population is ignorant) that renews the spreading process. For example, if we consider the rumor as a virus, the denial represents the effect of an anti-virus that restores the initial condition; the hacker reinforces the virus or designs a new virus restarting the spreading process. In business marketing, the rumor is the advertisement of a product, the denial can be an information that discredits it or the launch of a new concurrent product; the society improves the product or defends oneself from the accuses and the process restarts. In a political campaign, the rumor can be the promoting of a candidate, the denial can be the consequence of a scandal, the re-starting is the consequence of the refusal of the scandal.

We insert the concept of denial in rumor spreading models representing a denial as a Poisson event and it resets to start the initial situation from which the process starts following the previous rules. Denials are introduced in the classic Daley-Kendall model and in an its generalization; the steady state densities are analyzed for these models (for details see [45]).

0.1.1 Model A

We consider a population consisting of N individuals which, with respect to the rumor, are subdivided into three classes: ignorants, spreaders and stiflers. We assume that the rumor spreads by direct contact of spreaders with others in the population. Each individual mets another one according to a Poisson process of parameter λ. The contacts between spreaders and the rest of the population are governed by the following set of rules:

- when a spreader contacts an ignorant, the ignorant becomes spreader;
- when a spreader contacts another spreader both become stiflers;
- when a spreader contacts a stifler, the spreader becomes stifler.

Moreover, we assume that a denial occurs following a Poisson process of parameter ξ. A denial transforms all spreaders and stiflers into ignorants except one spreader. We assume that contacts occur independently from denials. We denote by $X(t), Y(t)$ and $Z(t)$ the normalized mean size of population that are ignorants, spreaders and stiflers at time t, respectively.
The initial conditions $X(0) = 1 - \frac{1}{N}$, $Y(0) = \frac{1}{N}$, $Z(0) = 0$ hold and, for all $t > 0$, it is verified the normalizing condition $X(t) + Y(t) + Z(t) = 1$.
Assuming that N is sufficiently large, we can approximate $Y(t)\Big[Y(t) - \frac{1}{N}\Big]$ with $Y^2(t)$, so the rumor spreading mechanism is described by the following equations:

$$\begin{cases} \dfrac{dX(t)}{dt} = -\lambda X(t)Y(t) + \xi\Big[1 - \dfrac{1}{N}\Big] - \xi X(t) \\ \dfrac{dY(t)}{dt} = Y(t)\Big\{\lambda[X(t) - Y(t) - Z(t)] - \xi\Big\} + \dfrac{\xi}{N} \\ \dfrac{dZ(t)}{dt} = \lambda Y(t)[Y(t) + Z(t)] - \xi Z(t). \end{cases} \tag{1}$$

Setting $X = \lim_{t\to\infty} X(t)$, $Y = \lim_{t\to\infty} Y(t)$, $Z = \lim_{t\to\infty} Z(t)$, from (1), recalling the normalizing condition, one obtains

$$\begin{cases} XY - \rho\Big(1 - \frac{1}{N} - X\Big) = 0, \\ \\ Y\Big(-\rho + 2X - 1\Big) + \dfrac{\rho}{N} = 0 \end{cases} \tag{2}$$

with $\rho = \xi/\lambda > 0$. Our aim is to solve system (2) to know the percentage of ignorants X in the stationary regime. Specifically, by solving system (2), we obtain the following expression for the steady-state density of ignorants:

$$X = \frac{N\rho + 3N - 1 - \sqrt{N^2(1-\rho)^2 + 1 + 6N\rho + 2N}}{4N}.$$

Note that $1 - X$ is the percentage of population which know the rumor asymptotically.

For large population, one has

$$\lim_{N\to\infty} X = \begin{cases} \dfrac{\rho+1}{2} & \text{if } \rho < 1 \\ 1 & \text{if } \rho \geq 1. \end{cases}$$

Hence, when N is large, if $\rho < 1$ at most 50% the population is asymptotically informed, whereas if $\rho \geq 1$ the rumor does not spread ($\rho \geq 1$ means that the denial rate is greater or equal than the contact rate).

Moreover, the density of ignorants X increases with ρ and

$$\lim_{\rho\to\infty} X = \frac{N-1}{N} \overset{N\to\infty}{\to} 1.$$

In Table 1 the asymptotic percentage of ignorants is showed for varying N and ρ. In the last row the values of X are listed for $N \to \infty$. Note that X tends to 1 when ρ increases and the speed of this growth increases with N.

Finally, we can calculate ρ such that a fixed percentage $1 - \nu$ of the population

ρ	0.01	0.04	0.08	0.10	0.30	0.50	0.70	0.90	1.00
$N = 50$	0.49	0.50	0.52	0.53	0.63	0.72	0.80	0.87	0.89
$N = 100$	0.49	0.51	0.53	0.54	0.64	0.73	0.82	0.90	0.92
$N = 1000$	0.50	0.52	0.54	0.55	0.65	0.74	0.84	0.94	0.97
$N \to \infty$	0.50	0.52	0.54	0.55	0.65	0.75	0.85	0.95	1

Table 1: For Model A the values of X are listed for different choices of N and ρ.

knows the rumor. Indeed, for $\nu > 1/2$, one has $X = \nu$ if, and only if,

$$\rho = \frac{N(2\nu^2 - 3\nu + 1) + \nu - 1}{N(\nu - 1) + 1} \overset{N\to\infty}{\to} 2\nu - 1.$$

0.1.2 Model B

As before, we consider a population consisting of N individuals, we assume that a rumor spreads by directed contact of spreaders with others in the population and each individual mets another one according to a Poisson process of parameter λ. In this model we suppose that the population is divided into $k + 2$ groups, for $k = 1, 2, \ldots$: ignorants, spreaders that have spreaded the rumor i times (for $i = 0, 1, \ldots, k - 1$) and stiflers. The spreader which has told the rumor i times is called i-th spreader. The 0-th spreader is the individual who has not yet told the rumor. Hence, the 0-th spreader is the initial spreader that starts the diffusion process or an ignorant who has just become spreader. Moreover, we suppose that a spreader can spread the rumor only k times when he mets an ignorant; so, when the $(k-1)$-th spreader mets an ignorant, he transmits the rumor and then he becomes stifler. The contacts are governed by the following set of rules:

- for $i = 0, 1, \ldots, k-2$, when the i-th spreader contacts an ignorant, the ignorant becomes 0-th spreader and the i-th spreader becomes $(i + 1)$-th spreader;
- when the $(k - 1)$-th spreader contacts an ignorant, the ignorant becomes 0-th spreader and the $(k - 1)$-th spreader becomes stifler;
- when a spreader of any class contacts another spreader of any group, both spreaders become stiflers;
- when a spreader of any class contacts a stifler, the spreader becomes stifler.

Also for this model we assume that a denial occurs according to a Poisson process of parameter ξ.
We denote by $X(t), Y_i(t)\,(i = 0, 1, \ldots, k - 1)$ and $Z(t)$ the normalized mean size of ignorants, i-th spreaders $(i = 0, 1, \ldots, k - 1)$ and stiflers at time t, respectively and with $Y(t) = \sum_{i=0}^{k-1} Y_i(t)$ the normalized mean size of spreaders at time t.
Conditions $X(0) = 1 - \frac{1}{N}$, $Y_0(0) = \frac{1}{N}$, $Z(0) = 0$, $Y_i(0) = 0$ $(1 \le i \le k - 1)$ and the normalizing condition $X(t) + Y(t) + Z(t) = 1$ $(\forall t \ge 0)$ holds. Assuming that N is sufficiently large (so we can approximate $Y_i(t)\left[Y_i(t) - \frac{1}{N}\right] \simeq Y_i^2(t)$ for $i = 0, 1, \ldots, k - 1$), the rumor spreading mechanism is described by the following

equations:

$$\begin{cases} \dfrac{dX(t)}{dt} = -\lambda X(t)Y(t) + \xi\Big[1 - \dfrac{1}{N}\Big] - \xi X(t) \\ \\ \dfrac{dY_0(t)}{dt} = \lambda X(t)Y(t) - \lambda Y_0(t) - \xi\Big[Y_0(t) - \dfrac{1}{N}\Big] \\ \\ \dfrac{dY_i(t)}{dt} = \lambda X(t)Y_{i-1}(t) - \lambda Y_i(t) - \xi Y_i(t), \qquad (i = 1, 2, \ldots, k-1) \\ \\ \dfrac{dZ(t)}{dt} = \lambda Y(t)\Big[1 - X(t)\Big] + \lambda X(t)Y_{k-1}(t) - \xi Z(t). \end{cases} \tag{3}$$

Setting $\rho = \xi/\lambda > 0$, $X = \lim_{t\to\infty} X(t)$, $Y_i = \lim_{t\to\infty} Y(t)$ $(1 \leq i \leq k-1)$, $Y = \sum_{i=0}^{k} Y_i$ and $Z = \lim_{t\to\infty} Z(t)$, recalling the normalizing condition and assuming N sufficiently large (so $1 - 1/N \cong 1$), from (3) one obtains

$$\begin{cases} -XY + \rho(1 - X) = 0 \\ XY - Y_0 - \rho\, Y_0 = 0 \\ XY_{i-1} - Y_i - \rho\, Y_i = 0 \qquad (i = 0, 1, \ldots, k-1). \end{cases} \tag{4}$$

By solving system (4), we have that the steady-state density of ignorants satisfies the following relations:

$$\begin{cases} X^2 - (A+1)X + A = 0 \qquad (k = 1) \\ \\ X^{k+1} + (A-1)\displaystyle\sum_{j=0}^{k-2} A^j(1-A)X^{k-j} - A^{k-1}(A+1)X + A^k = 0 \qquad (k \geq 2) \end{cases} \tag{5}$$

with $A = \rho + 1 > 1$.

For $k = 1$, solutions of (5) are 1 and A. Since we are interested into solutions less or equal than 1, we conclude that $X = 1$ is the unique acceptable solution. Hence, if $k = 1$ and N is sufficiently large, the rumor does not spread.

Now, we focus on the case $k \geq 2$; note that we can re-write equation (5) (for $k \geq 2$) as $\tilde{f}_k(X) = (X-1)f_k(X) = 0$, where

$$f_k(x) = x^k + Ax^{k-1} + A^2x^{k-2} + \ldots + A^{k-1}x - A^k. \tag{6}$$

Hence, one solution of (5), for $k \geq 2$, is $X = 1$ and the remaining solutions coincide with the zeros of the polynomial $f_k(X)$. These zeros are not computable explicitly, but we can determine the range in which the solution of our interest is. Indeed,

equation $f_k(x) = 0$ has a unique real solution in the interval $(0, A)$, because of $f_k(0) = -A^k < 0$, $f_k(A) = (k-1)A^k > 0$ and $f_k(x)$ is a continuous increasing function respect to x being $f'_k(x) > 0$ (for details see [45]).
Let x_k be the unique real solution of $f_k(x) = 0$ in the interval $(0, A)$. We write $x_k = d_k A$, with $0 < d_k < 1$.
By recalling that $A > 1$, for $x < A$ one has:

$$\begin{aligned} f_k(x) - f_{k+1}(x) &> \sum_{i=0}^{k-1} x^{k-i} A^i - \sum_{i=1}^{k} x^{k+1-i} A^i - x^{k+1} \\ &= (1-A)\, x\, \frac{x^k - A^k}{x - A} - x^{k+1} > \frac{x^{k+1}}{x-A}\,(1-x) \\ &> \frac{x^{k+1}}{x-A}\,(1-A) > 0. \end{aligned}$$

Hence, since $\{f_k(x)\}_{k\geq 2}$ is a decreasing succession, $\{x_k\}_{k\geq 2}$ is decreasing and consequently $\{d_k\}_{k\geq 2}$ is decreasing too.
Note that $f_2(x) = 0$ if and only if $x^2 + Ax - A^2 = 0$, that is $x = A\,(\sqrt{5}-1)/2$; hence, $d_2 = (\sqrt{5}-1)/2$.
Moreover, because $\lim_{k\to\infty} f_k(d_k A) = 0$ if, and only if, $\sum_{j=1}^{\infty} d_\infty^j - 1 = 0$, we have $d_\infty = 0.5$. From this last observation and recalling that $\{x_k\}_{k\geq 2}$ is decreasing, we conclude that the percentage of ignorants is always greater than 50% because $x_k = d_k\, A > d_\infty\, A = (\rho+1)/2 > 1/2$.
Since our interest is on the root less than 1, note that for $k \geq 2$, in order to $f_k(x) = 0$ has always a unique real root less than 1, we have to request $x_k = d_k(1+\rho) < 1$, i.e. $0 < \rho < \frac{1}{d_k} - 1$. Hence, being $\{d_k\}_{k\geq 2}$ a decreasing succession, if $\rho < 1/d_2 - 1 = d_2$, then the polynomial $f_k(x)$ has a unique real zero less than 1.
In conclusion, for large population one has:

- if $k = 1$, the rumor does not spread asymptotically,
- if $k \geq 2$ and $\rho = \frac{\xi}{\lambda} < (\sqrt{5}-1)/2 = 0.61803$, the percentage of ignorants is less than 1; in particular, X is solution of $f_k(x) = 0$, with $f_k(x)$ given in (6).

In Table 2 we list the proportion of ignorants for Model B with $N = 1000$ and various choices of ρ and k. Note that the values of X decrease as k increases because the rumor has more chance to spread. Moreover, as ρ increases, X grows to 1 and, for $\rho \geq 1$, the rumor does not spread at all. Fixed $\rho > 0$, the values for $k = 100$ in Table 2 coincide with the corresponding values of Model A, listed in Table 1 with $N = 1000$. In particular, one has that for $k = 6$ the percentage of ignorants reaches the same values obtained for $k \geq 7$, if we consider only two decimal digits.
From Table 2, one can observe that to spread as much as possible the rumor, it

is advisable to choice $k \geq 6$ and $\rho \leq 0.1$. In these cases just shy of 50% of the population knows the rumor.

ρ	$k=2$	$k=3$	$k=4$	$k=5$	$k=6$	$k=7$	$k=10$	$k=100$
0.01	0.62	0.54	0.52	0.51	0.50	0.50	0.50	0.50
0.02	0.63	0.55	0.52	0.51	0.51	0.51	0.51	0.51
0.04	0.64	0.56	0.53	0.52	0.52	0.52	0.52	0.52
0.06	0.65	0.57	0.54	0.53	0.53	0.53	0.53	0.53
0.08	0.66	0.58	0.56	0.54	0.54	0.54	0.54	0.54
0.10	0.67	0.59	0.57	0.55	0.55	0.55	0.55	0.55
0.30	0.80	0.70	0.67	0.66	0.65	0.65	0.65	0.65
0.50	0.92	0.81	0.77	0.76	0.75	0.75	0.75	0.75
0.70	1	0.92	0.88	0.86	0.85	0.85	0.85	0.85
0.90	1	1	0.98	0.96	0.95	0.95	0.95	0.95
1.00	1	1	1	1	1	1	1	1

Table 2: For Model B the values of X are listed for some choices of ρ and k.

0.2 Time non-homogeneous adaptive queue with catastrophes

Let $\{N(t),\, t \geq t_0\}$ be a non-homogeneous continuous Markov chain with jumps, representing a queueing system in the presence of catastrophes. We assume that catastrophes occur according to a time-non-homogeneous Poisson process. The state space for $N(t)$ is $S = 0, 1, 2, \ldots$. We assume that $N(t)$ is regulated from transitions that occur according to the following scheme:

- $n \to n+1$ with rate $\alpha_n(t)$, for $n = 0, 1, \ldots$,
- $n \to n-1$ with rate $\beta_n(t)$, for $n = 2, 3, \ldots$,
- $1 \to 0$ with rate $\beta_1(t) + \xi(t)$,
- $n \to 0$ with rate $\xi(t)$, for $n = 2, 3, \ldots$,

where $\alpha_n(t) > 0$, $\beta_n(t) > 0$ and $\xi(t) \geq 0$ are bounded and continuous functions of the time.

For the process $N(t)$ it is interesting to study some statistical characteristics as the transition probabilities, the related moments and the distribution of the random variable FVT to zero state.

The transition probabilities $p_{j,n}(t|t_0) = P\{N(t) = n \,|\, N(t_0) = j\}$, for $j, n \in S$ and $t > t_0 \geq 0$, satisfy the following system of forward equations:

$$\frac{d}{dt} p_{j,0}(t|t_0) = -[\alpha_0(t) + \xi(t)]\, p_{j,0}(t|t_0) + \beta_1(t)\, p_{j,1}(t|t_0) + \xi(t),$$

$$\frac{d}{dt}p_{j,n}(t|t_0) = -[\alpha_n(t) + \beta_n(t) + \xi(t)]\, p_{j,n}(t|t_0) + \alpha_{n-1}(t)\, p_{j,n-1}(t|t_0) \qquad (7)$$
$$+\beta_{n+1}(t)\, p_{j,n+1}(t|t_0) \qquad (n = 1, 2, \ldots)$$

with initial condition $\lim_{t\downarrow t_0} p_{j,n}(t|t_0) = \delta_{j,n}$.
We denote by $\{\widetilde{N}(t),\, t \geq t_0\}$ the time non-homogeneous continuous Markov chain obtained from $N(t)$ by removing the possibility of catastrophes, i.e. when $\xi(t) \downarrow 0$ for $t \geq t_0$. Hence, the transition probabilities $\widetilde{p}_{j,n}(t|t_0) = P\{\widetilde{N}(t) = n|\widetilde{N}(t_0) = j\}$ $(j, n \in S)$ satisfy the system of forward equations obtained from (7) by taking $\xi(t) \downarrow 0$ for $t \geq t_0$, with initial conditions $\lim_{t\to t_0} \widetilde{p}_{j,n}(t|t_0) = \delta_{j,n}$.

We restrict our attention to non-explosive processes $\widetilde{N}(t)$, i.e. we suppose $\sum_{n=0}^{+\infty} \widetilde{p}_{j,n}(t|t_0) = 1$, $j \in S, t \geq t_0$, and we assume that

$$\lim_{t\to+\infty} \int_{t_0}^{t} \xi(u)\, du = +\infty. \qquad (8)$$

The probabilities $p_{j,n}(t|t_0)$ can be expressed in terms of the probabilities $\widetilde{p}_{j,n}(t|t_0)$ of the process $\widetilde{N}(t)$. Indeed, conditioning on the age of the catastrophe process, for $j, n \in S$ and $t > t_0$ one has (see, for instance, [28], [32]):

$$p_{j,n}(t|t_0) = \varphi(t|t_0)\, \widetilde{p}_{j,n}(t|t_0) + \int_{t_0}^{t} \xi(\tau)\, \varphi(t|\tau)\, \widetilde{p}_{0,n}(t|\tau)\, d\tau, \qquad (9)$$

where we set

$$\varphi(t|t_0) = \exp\left\{-\int_{t_0}^{t} \xi(u)\, du\right\} \qquad (t \geq t_0). \qquad (10)$$

Furthermore, due to (9), the moments of the process $N(t)$ and those of $\widetilde{N}(t)$ are related. Indeed, let

$$M_\ell(t|j, t_0) = E[N^\ell(t)|N(t_0) = j] = \sum_{n=1}^{+\infty} n^\ell\, p_{j,n}(t|t_0),$$
$$\widetilde{M_\ell}(t|j, t_0) = E[\widetilde{N}^\ell(t)|N(t_0) = j] = \sum_{n=1}^{+\infty} n^\ell\, \widetilde{p}_{j,n}(t|t_0),$$

be the ℓth-order moments of the processes $\widetilde{N}(t)$ and $N(t)$, respectively; from (9), for $\ell = 1, 2, \ldots$ one obtains:

$$M_\ell(t|j, t_0) = \varphi(t|t_0)\, \widetilde{M_\ell}(t|j, t_0) + \int_{t_0}^{t} \xi(\tau)\, \varphi(t|\tau)\, \widetilde{M_\ell}(t|0, \tau)\, d\tau.$$

Let us now consider the FVT of $N(t)$ to 0 starting from the initial state j:

$$\mathcal{T}_{j,0}(t_0) = \inf\{t \geq t_0 : N(t) = 0\}, \qquad N(t_0) = j,$$

and we denote by $g_{j,0}(t|t_0) = dP\{T_{j,0}(t_0) \leq t\}/dt$ its pdf. For $j = 1, 2, \ldots$ and $t \geq t_0$, one has (see, for instance, [28])

$$g_{j,0}(t|t_0) = \varphi(t|t_0)\, \widetilde{g}_{j,0}(t|t_0) + \xi(t)\, \varphi(t|t_0) \Big[1 - \int_{t_0}^{t} \widetilde{g}_{j,0}(\tau|t_0)\, d\tau\Big], \tag{11}$$

where $\widetilde{g}_{j,0}(t|t_0)$ is the pdf of $\widetilde{\mathcal{T}}_{j,0}(t_0) = \inf\{t \geq t_0 : \widetilde{N}(t) = 0\}$, with $\widetilde{N}(t_0) = j$, describing the FPT pdf from j to 0 for the process $\widetilde{N}(t)$. By virtue of (8), from (11) we obtain $\int_{t_0}^{+\infty} g_{j,0}(\tau|t_0)\, d\tau = 1$, implying that the FVT of $N(t)$ to 0 occurs with probability 1, whereas for $\widetilde{N}(t)$ such an event may have probability less than 1.

In the following, we assume that catastrophes occur according to a Poisson process characterized by a bounded and periodic intensity function $\xi(t)$, such that $\xi(t + k\,Q) = \xi(t)$ $(k = 1, 2, \ldots)$. We denote by

$$\widehat{\xi} = \frac{1}{Q} \int_0^Q \xi(u)\, du \tag{12}$$

the average catastrophe rate in the period Q. Due to the periodicity of $\xi(t)$, we have

$$\int_t^{t+k\,Q} \xi(u)\, du = k \int_t^{t+Q} \xi(u)\, du = k\, Q\, \widehat{\xi} \qquad (k = 1, 2, \ldots). \tag{13}$$

Let

$$q_n(t) = \lim_{k \to +\infty} p_{j,n}(t + k\,Q|t_0) \qquad (n = 0, 1, 2 \ldots)$$

be the quasi-stationary distribution for the process $N(t)$. When $\widetilde{N}(t)$ is a time-homogeneous process, the process $N(t)$, subject to catastrophes of periodic intensity function $\xi(t)$, admits a quasi-stationary distribution, as shown in the following proposition.

Proposition 1. *Let $\widetilde{N}(t)$ be a time-homogeneous process, with arrival rates $\alpha_n(t) = \alpha_n$ $(n = 0, 1, \ldots)$ and departure rates $\beta_n(t) = \beta_n$ $(n = 1, 2, \ldots)$. If $\xi(t)$ is a bounded periodic function of period Q, then*

$$q_n(t) = \int_0^{+\infty} \xi(t - u)\, \varphi(t|t - u)\, \widetilde{p}_{0,n}(u)\, du \qquad (n = 0, 1, 2, \ldots), \tag{14}$$

where $\widetilde{p}_{j,n}(t) = \widetilde{p}_{j,n}(t|0)$.

Proof. Since $\widetilde{N}(t)$ is time-homogeneous, one has $\widetilde{p}_{j,n}(t|\tau) = \widetilde{p}_{j,n}(t - \tau|0)$, so that

from (9) one obtains:

$$p_{j,n}(t|t_0) = \varphi(t|t_0)\widetilde{p}_{j,n}(t-t_0) + \int_0^{t-t_0} \xi(t-u) \exp\Big\{-\int_0^u \xi(t-y)\,dy\Big\}\,\widetilde{p}_{0,n}(u)\,du. \quad (15)$$

Therefore, changing t into $t + k\,Q$ in (15) and recalling the periodicity of $\xi(t)$, it results:

$$\begin{aligned} p_{j,n}(t + k\,Q|t_0) &= e^{-k\,Q\,\widehat{\xi}}\,\varphi(t|t_0)\,\widetilde{p}_{j,n}(t + k\,Q - t_0) \\ &\quad + \int_0^{t+k\,Q-t_0} \xi(t-u)\,\exp\Big\{-\int_0^u \xi(t-y)\,dy\Big\}\,\widetilde{p}_{0,n}(u)\,du \end{aligned} \quad (16)$$

with $\widehat{\xi}$ given in (12). From (16), taking the limit for $k \to +\infty$, equation (14) follows. □

Note that, since $\widetilde{N}(t)$ is a non-explosive process, from (14) one has:

$$\sum_{n=0}^{+\infty} q_n(t) = \int_0^{+\infty} \xi(t-u)\,\varphi(t|t-u)\,du = 1.$$

Furthermore, from (14), by virtue of periodicity of $\xi(t)$, one has:

$$\begin{aligned} q_n(t + k\,Q) &= \int_0^{+\infty} \xi(t + k\,Q - u)\,\exp\Big\{-\int_{t+k\,Q-u}^{t+k\,Q} \xi(x)\,dx\Big\}\,\widetilde{p}_{0,n}(u)\,du \\ &= \int_0^{+\infty} \xi(t-u)\,\exp\Big\{-\int_{t-u}^{t} \xi(y + k\,Q)\,dy\Big\}\,\widetilde{p}_{0,n}(u)\,du \\ &= \int_0^{+\infty} \xi(t-u)\,\varphi(t|t-u)\,\widetilde{p}_{0,n}(z)\,dz = q_n(t) \quad (n = 0, 1, 2, \ldots), \end{aligned}$$

so that $q_n(t)$ is a periodic function of period Q. Moreover, under the assumptions of Proposition 1, from (14) one obtains the asymptotic moments of $N(t)$:

$$\begin{aligned} m_\ell(t) &= \lim_{k\to+\infty} M_\ell(t + k\,Q|j, t_0) = \sum_{n=1}^{+\infty} n^\ell\,q_n(t) \\ &= \int_0^{+\infty} \xi(t-u)\,\varphi(t|t-u)\,\widetilde{M}_\ell(u|0,0)\,dz \qquad (\ell = 1, 2, \ldots). \end{aligned} \quad (17)$$

From (17) follows that if $\widetilde{M}_\ell(t|0,0)$ is a bounded function for all t, hence the asymptotic moment $m_\ell(t)$ is certainly a bounded periodic function.

Now we analyze the influence of periodicity of $\xi(t)$ on FVT pdf of the process $N(t)$. To this aim we denote by $\widehat{N}(t)$ the continuous-time Markov chain with arrival rates $\alpha_n(t)$ and departure rates $\beta_n(t)$ subject to catastrophes that occur with exponential distribution of constant rate $\widehat{\xi}$ defined in (12). Furthermore, we denote

by $\widehat{g}_{j,0}(t|t_0)$ the FVT pdf from j to 0 for the process $\widehat{N}(t)$.

Proposition 2. *Let $\widetilde{N}(t)$ be an inhomogeneous process, with arrival rates $\alpha_n(t)$ $(n = 0, 1, \ldots)$ and departure rates $\beta_n(t)$ $(n = 1, 2, \ldots)$. If $\xi(t)$ is a bounded periodic function of period Q, then*

$$g_{j,0}(t + k\,Q|t_0) = \frac{\widetilde{g}_{j,0}(t + k\,Q|t_0) + \xi(t)\,\left[1 - \int_{t_0}^{t+k\,Q} \widetilde{g}_{j,0}(\tau|t_0)\,d\tau\right]}{\widetilde{g}_{j,0}(t + k\,Q|t_0) + \widehat{\xi}\,\left[1 - \int_{t_0}^{t+k\,Q} \widetilde{g}_{j,0}(\tau|t_0)\,d\tau\right]} \times \gamma(t|t_0)\,\widehat{g}_{j,0}(t + k\,Q|t_0), \tag{18}$$

where

$$\gamma(t|t_0) = \varphi(t|t_0)\,e^{\widehat{\xi}\,(t-t_0)}. \tag{19}$$

Proof. From (11), with $\xi(t) = \widehat{\xi}$, for the process $\widehat{N}(t)$ one has

$$\widehat{g}_{j,0}(t|t_0) = e^{-\widehat{\xi}\,(t-t_0)}\,\widetilde{g}_{j,0}(t|t_0) + \widehat{\xi}\,e^{-\widehat{\xi}\,(t-t_0)}\,\Big[1 - \int_{t_0}^{t} \widetilde{g}_{j,0}(\tau|t_0)\,d\tau\Big],$$

so that, changing t into $t + k\,Q$ and recalling (12) and (13), one obtains:

$$e^{-k\,Q\,\widehat{\xi}} = \frac{\widehat{g}_{j,0}(t + k\,Q|t_0)\,e^{\widehat{\xi}\,(t-t_0)}}{\widetilde{g}_{j,0}(t + k\,Q|t_0) + \widehat{\xi}\,\left[1 - \int_{t_0}^{t+k\,Q} \widetilde{g}_{j,0}(\tau|t_0)\,d\tau\right]}. \tag{20}$$

Similarly, for the process $N(t)$, changing t into $t + k\,Q$ into (11), it results

$$g_{j,0}(t + kQ|t_0) = e^{-kQ\,\widehat{\xi}}\,\varphi(t|t_0)\,\Big\{\widetilde{g}_{j,0}(t + kQ|t_0) + \xi(t)\Big[1 - \int_{t_0}^{t+k\,Q} \widetilde{g}_{j,0}(\tau|t_0)\,d\tau\Big]\Big\},$$

from which, by virtue of (19) and (20), equation (18) immediately follows. □

Proposition 2 allows to study the behavior of $g_{j,0}(t|t_0)$ in the intervals in which the function $\xi(t)$ exceeds, equals or is less than its average $\widehat{\xi}$ in a period, as expressed in the following

Remark 1. *Under the assumption of Proposition 2, for $t \geq t_0$ one has:*

$$g_{j,0}(t|t_0) \begin{cases} > \gamma(t|t_0)\,\widehat{g}_{j,0}(t|t_0), & \xi(t) > \widehat{\xi} \\ = \gamma(t|t_0)\,\widehat{g}_{j,0}(t|t_0), & \xi(t) = \widehat{\xi} \\ < \gamma(t|t_0)\,\widehat{g}_{j,0}(t|t_0), & \xi(t) < \widehat{\xi} \end{cases}$$

Proof. For all $t \geq 0$ such that $\xi(t + k\,Q) = \widehat{\xi}$, from (18) we obtain that

$$g_{j,0}(t + k\,Q|t_0) = \gamma(t + k\,t|t_0)\,\widehat{g}_{j,0}(t + k\,Q|t_0),$$

so $g_{j,0}(t|t_0)$ intersects the curve $\gamma(t|t_0)\,\widehat{g}_{j,0}(t|t_0)$ when $\xi(t) = \widehat{\xi}$. Similarly, from (18) it follows that $g_{j,0}(t|t_0)$ exceeds [is below] the curve $\gamma(t|t_0)\,\widehat{g}_{j,0}(t|t_0)$ when $\xi(t) > \widehat{\xi}$ [$\xi(t) < \widehat{\xi}$].

□

Proposition 2 also shows that choosing the periodic function $\xi(t)$ in such a way that $\xi(t_0) = \widehat{\xi}$, one has:

$$g_{j,0}(t_0 + k\,Q|t_0) = \widehat{g}_{j,0}(t_0 + k\,Q|t_0) \qquad (k = 1, 2, \ldots), \tag{21}$$

so that the FVT density with catastrophe periodic function $\xi(t)$ intersects the FVT pdf with constant catastrophe rate $\widehat{\xi}$, given in (12), at multiples of the period.

Now we study the $M/M/1$ process to provide an application in the context of queueing systems; other examples, such as the non stationary birth-death-immigration process and the queueing system $M(t)/M(t)/1$, $M(t)/M(t)/\infty$, are provided in the paper [43].
We consider the time-homogeneous $M/M/1$ model $\widetilde{N}(t)$ with arrival and departure rates

$$\alpha_n(t) = \alpha \quad (n = 0, 1, \ldots), \qquad \beta_n(t) = \beta \quad (n = 1, 2, \ldots).$$

The transition probabilities of $\widetilde{N}(t)$ are (cf. [88]):

$$\begin{aligned}\widetilde{p}_{j,n}(t|t_0) = e^{-(\alpha+\beta)(t-t_0)} \Big\{ &\Big(\frac{\alpha}{\beta}\Big)^{(n-j)/2} I_{n-j}[2\sqrt{\alpha\beta}\,(t-t_0)] \\ &+\Big(\frac{\alpha}{\beta}\Big)^{(n-j-1)/2} I_{n+j+1}[2\sqrt{\alpha\beta}\,(t-t_0)] \\ &+\Big(1-\frac{\alpha}{\beta}\Big)\Big(\frac{\alpha}{\beta}\Big)^{n} \sum_{k=n+j+2}^{+\infty} \Big(\frac{\alpha}{\beta}\Big)^{-k/2} I_k[2\sqrt{\alpha\beta}\,(t-t_0)]\Big\},\end{aligned}$$

where

$$I_\nu(z) = \sum_{m=0}^{\infty} \frac{(z/2)^{\nu+2m}}{m!\,(m+\nu))!} \qquad (\nu > 0)$$

denotes the Bessel function modified of first kind. Furthermore, the first two moments of $\widetilde{N}(t)$ are given by

$$\begin{aligned}\widetilde{M}_1(t|j, t_0) &= j + (\alpha - \beta)\,(t - t_0) + \beta \int_{t_0}^{t} \widetilde{p}_0(\tau|t_0)\,d\tau \\ \widetilde{M}_2(t|j, t_0) &= j^2 + (\alpha + \beta)\,(t - t_0) - \beta \int_{t_0}^{t} \widetilde{p}_0(\tau|t_0)\,d\tau \\ &\quad +2\,(\alpha - \beta) \int_{t_0}^{t} \widetilde{M}_1(\tau|j, t_0)\,d\tau.\end{aligned}$$

For the process $\widetilde{N}(t)$, the FVT pdf from j to zero is (cf., for instance, [28])

$$\widetilde{g}_{j,0}(t|t_0) = \frac{j}{(t-t_0)}\left(\frac{\beta}{\alpha}\right)^{j/2} e^{-(\alpha+\beta)\,(t-t_0)}\, I_j[2\sqrt{\alpha\,\beta}\,(t-t_0)] \tag{22}$$

for $t \geq t_0$ and $j = 1, 2, \ldots$. From (22) it follows that the first visit to zero starting from j is a sure event as $\alpha \leq \beta$, whereas it occurs with probability $P(\widetilde{\mathcal{T}}_{j,0} < +\infty) = (\beta/\alpha)^j$ when $\alpha > \beta$.

Let $N(t)$ be the process $M/M/1$ in the presence of catastrophes with periodic intensity function $\xi(t)$ of period Q. Since $\widetilde{N}(t)$ is a time-homogeneous process, the expressions of the asymptotic distribution and of the related moments of $N(t)$ are given in (14) and (17), respectively. Furthermore, making use of (22) in (11), one obtains the FVT pdf of $N(t)$ from j to zero:

$$\begin{aligned} g_{j,0}(t|t_0) = \left(\frac{\alpha}{\beta}\right)^{-j/2} e^{-(\alpha+\beta)\,(t-t_0)}\varphi(t|t_0)\Big\{\frac{j}{t-t_0}\, I_j[2\,\sqrt{\alpha\,\beta}\,(t-t_0)] \\ +\xi(t)\sum_{k=1}^{+\infty}\left(\frac{\alpha}{\beta}\right)^{k/2}\Big(I_{k-j}[2\,\sqrt{\alpha\,\beta}\,(t-t_0)] - I_{k+j}[2\,\sqrt{\alpha\,\beta}\,(t-t_0)]\Big)\Big\}, \end{aligned} \tag{23}$$

for $j = 1, 2, \ldots$ with $\varphi(t|t_0)$ given in (10). In particular, taking $j = 1$ in (23) and recalling that $z\,[I_{\nu-1}(z) - I_{\nu+1}(z)] = 2\,\nu\, I_\nu(z)$, one has

$$\begin{aligned} g_{1,0}(t|t_0) = \frac{\varphi(t|t_0)}{\alpha(t-t_0)}\, e^{-(\alpha+\beta)(t-t_0)}\Big\{\sqrt{\alpha\,\beta}\, I_1[2\,\sqrt{\alpha\,\beta}\,(t-t_0)] \\ +\xi(t)\sum_{k=1}^{+\infty} k\Big(\frac{\alpha}{\beta}\Big)^{k/2} I_k[2\,\sqrt{\alpha\,\beta}\,(t-t_0)]\Big\} \qquad (t \geq t_0). \end{aligned}$$

We also consider the process $\widehat{N}(t)$, with arrival rate α and departure rate β subject to catastrophes that occur according to a Poisson process with constant rate $\widehat{\xi}$, given in (12), and we denote by $\widehat{g}_{j,0}(t|t_0)$ the FVT pdf from j to zero. The function $\widehat{g}_{j,0}(t|t_0)$ can be obtained from (23) by setting $\xi(t) = \widehat{\xi}$ and $\varphi(t|t_0) = e^{-\widehat{\xi}(t-t_0)}$. In particular, if $\xi(t_0) = \widehat{\xi}$ relation (21) holds.

In Figure 1 we consider the periodic intensity function $\xi(t)$ given by

$$\xi(t) = D + \Big[1 - \cos\Big(\frac{2\pi\, t}{Q_1}\Big)\Big]\,\Big[A + B\,\sin\Big(\frac{2\pi\, t}{Q_1}\Big) + C\,\cos\Big(\frac{2\pi\, t}{Q_1}\Big)\Big], \tag{24}$$

with $A = 0.05$, $B = 0.04$, $C = 0.1$, $D = 0.25$, $Q_1 = 1$, and we compare $\widetilde{g}_{j,0}(t|0)$ for the process $M/M/1$ without catastrophes (dot-dashed curve), $\widehat{g}_{j,0}(t|0)$ (dashed curve) for the process $\widehat{N}(t)$ and $g_{j,0}(t|0)$ (solid curve) for the process $N(t)$. Figure 1 shows that $\widetilde{g}_{j,0}(t|0)$ is very flat when $\alpha > \beta$ with respect to the case in which $\alpha < \beta$.

Differently, in the presence of catastrophes, the discrepancy between analogous FVT densities is reduced. We note that the FVT pdf $g_{j,0}(t|0)$ is strongly influenced by the shape and the periodicity of $\xi(t)$. Furthermore, since $\xi(0) = \widehat{\xi} = 0.25$ and $Q_1 = 1$, by virtue of (21), it follows that $g_{j,0}(k|0) = \widehat{g}_{j,0}(k|0)$ $(k = 1, 2, \ldots)$, as evidenced in Figure 1.

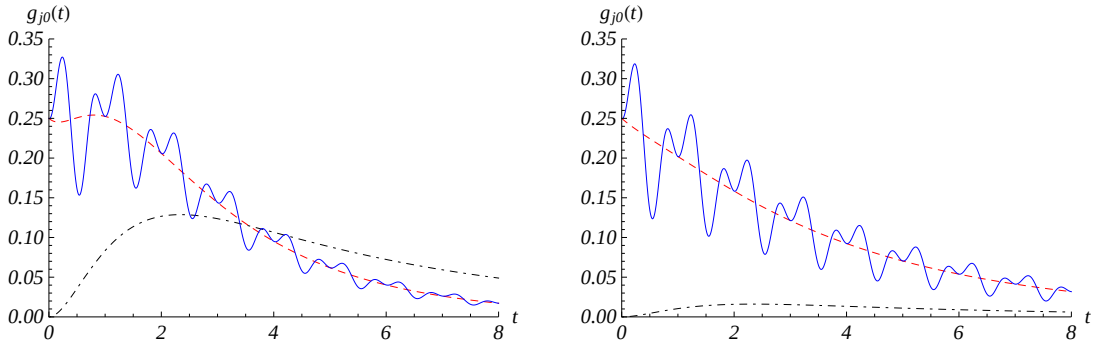

(a) $\alpha = 0.4$, $\beta = 0.8$, $j = 3$ (b) $\alpha = 0.8$, $\beta = 0.4$, $j = 3$

Figure 1: $\widetilde{g}_{j,0}(t|0)$ for the process $M/M/1$ without catastrophes (dot-dashed curve), $\widehat{g}_{j,0}(t|0)$ (dashed curve) for the process $\widehat{N}(t)$ and $g_{j,0}(t|0)$ (solid curve) for the process $N(t)$ are plotted with $\xi(t)$ given in (24).

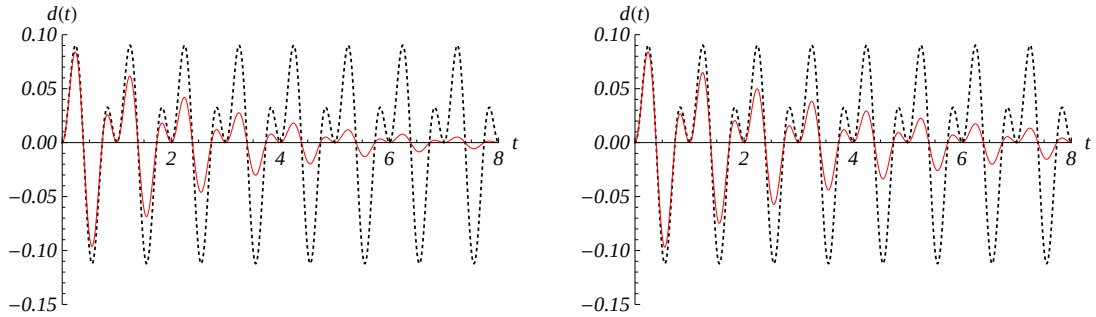

(a) $\alpha = 0.4$, $\beta = 0.8$, $j = 3$ (b) $\alpha = 0.8$, $\beta = 0.4$, $j = 3$

Figure 2: $\xi(t) - \widehat{\xi}$ (dotted curve) and $d(t|0)$ (solid curve) are plotted for the cases of Figure 1.

For $t \geq t_0$, we now consider the function

$$d(t|t_0) = g_{j,0}(t|t_0) - \varphi(t|t_0)\, e^{\widehat{\xi}\,(t-t_0)}\, \widehat{g}_{j,0}(t|t_0),$$

with $\varphi(t|t_0)$ defined in (10). In Figure 2 we plot the function $d(t) = d(t|0)$ (solid curve) and the function $\xi(t) - \widehat{\xi}$ (dotted curve) for the same cases of Figure 1. According to Remark 1, Figure 2 shows that $d(t) > 0$ when $\xi(t) - \widehat{\xi} > 0$ and $d(t) < 0$ when $\xi(t) - \widehat{\xi} < 0$.

Chapter 1

Stochastic diffusion processes with random jumps

1.1 Stochastic diffusion processes

Many physical, biological, economic and social phenomena are either well approximated or reasonably modeled by diffusion processes. These include examples from molecular motions of enumerable particles subject to interactions, security price fluctuations in a perfect market, some communication systems with noise, neurophysiological activity with disturbances, variations of population growth, changes in species numbers subject to competition and other community relationships, gene substitutions in evolutionary development, etc. In the following, we point out the most significant aspects of stochastic diffusion processes such as the probability density function, its moments and the FPT problem (cf. [51], [74]).

1.1.1 The probability density function and its moments

Definition 1. *A continuous time parameter stochastic process which has the (strong) Markov property and for which the sample paths $X(t)$ are (almost always) continuous functions of t is called a diffusion process.*

Let $\{X(t),\ t \geq t_0\}$ be a stochastic diffusion process defined in the *diffusion interval* $J \equiv (r_1, r_2)$, with $-\infty \leq r_1 < r_2 \leq +\infty$ and r_i called *boundary*. For all $\tau < t$ and $x, y \in I$ we define:

$$F(x,t|y,\tau) = P\{X(t) < x | X(\tau) < y\}$$
$$f(x,t|y,\tau) = \frac{\partial}{\partial x} F(x,t|y,\tau)$$

the transition distribution and the transition pdf of $X(t)$, respectively.

The pdf $f(x,t|y,\tau)$ of $X(t)$ satisfies the following integral relation, called *Chapman-Kolmogorov equation*:

$$f(x,t|y,\tau) = \int_{r_1}^{r_2} f(x,t|z,u) f(z,u|y,\tau) dz$$

for all $x, y \in J$ and $\tau < u < t$. On the other hand, one can study the process $X(t)$ via the so called *diffusion equations approach*. In particular, it is well-known that the transition pdf $f(x,t|y,\tau)$ satisfies the Fokker-Planck and the Kolmogorov equations:

$$\begin{cases} \frac{\partial f(x,t|y,\tau)}{\partial t} = -\frac{\partial}{\partial x}[A_1(x,t) f(x,t|y,\tau)] + \frac{1}{2}\frac{\partial^2}{\partial x^2}[A_2(x,t) f(x,t|y,\tau)], \\ \\ \frac{\partial f(x,t|y,\tau)}{\partial \tau} + A_1(y,\tau)\frac{\partial f(x,t|y,\tau)}{\partial y} + \frac{1}{2} A_2(y,t)\frac{\partial^2 f(x,t|y,\tau)}{\partial y^2} = 0, \end{cases} \tag{1.1}$$

respectively. The functions $A_1(x,t)$ and $A_2(x,t)$ are the *drift* and *infinitesimal variance* of the process and they are defined as follows:

$$\begin{aligned} A_i(x,t) &= \lim_{\Delta t \to 0} \frac{1}{\Delta t} E\left\{ [X(t+\Delta t) - X(t)]^i | X(t) = x \right\} \\ &= \lim_{\Delta t \to 0} \frac{1}{\Delta t} \int_{\mathbb{R}} (z-x)^i f(z, t+\Delta t | x, t) dz, \qquad (i = 1, 2). \end{aligned}$$

The diffusion equations (1.1) are used to determine $f(x,t|y,\tau)$ by using the following initial conditions:

$$\lim_{t \to \tau} f(x,t|y,\tau) = \lim_{\tau \to t} f(x,t|y,\tau) = \delta(x-y). \tag{1.2}$$

They mean that at the initial time the probability mass is completely concentrated at the initial state y. Nonetheless, the initial conditions are not always sufficient to determine uniquely the transition pdf, therefore boundary conditions may have to be considered.

The n-th moment of the process $X(t)$ is given by

$$\mu^{(n)}(t|y,\tau) = \int_{x \in J} x^n f(x,t|y,\tau)\, dx;$$

in particular, $E[X(t)|X(\tau) = y] = \mu^{(1)}(t|y,\tau) = \mu(t|y,\tau)$ is the mean of the process $X(t)$ and $Var[X(t)|X(\tau) = y] = \mu^{(2)}(t|y,\tau) - [\mu(t|y,\tau)]^2$ is the variance of $X(t)$.

Now we focus on *time homogeneous* diffusion processes:

Definition 2. *If for all $x \in I$ the drift $A_1(x,t) \equiv A_1(x)$ and the infinitesimal variance $A_2(x,t) \equiv A_2(x) > 0$ are continuous functions, the diffusion process $X(t)$*

is time homogeneous.

If $X(t)$ is time homogeneous, one has

$$f(x,t|y,\tau) = f(x,t-\tau|y,0) \equiv f(x,t-\tau|y),$$

and the diffusion equations (1.1) become

$$\begin{cases} \frac{\partial f(x,t|y)}{\partial t} = -\frac{\partial}{\partial x}[A_1(x)f(x,t|y)] + \frac{1}{2}\frac{\partial^2}{\partial x^2}[A_2(x)f(x,t|y)], \\ \\ \frac{\partial f(x,t|y)}{\partial t} = A_1(y)\frac{\partial f(x,t|y)}{\partial y} + \frac{1}{2}A_2(y)\frac{\partial^2 f(x,t|y)}{\partial y^2}. \end{cases} \tag{1.3}$$

Feller solved the integration problem for diffusion equations (1.3) (cf. [34], [35]) by introducing an original classification of the behavior of the process near the boundaries r_1 and r_2. Denoting by r_i $(i = 1, 2)$ the general boundary, the following classification holds.

Definition 3. *The boundary r_i $(i = 1, 2)$ is said inaccessible or unattainable if $X(t)$ never attains in finite time the state r_i with positive probability. Otherwise, r_i is said to be accessible or attainable.*

Accessible boundaries are divided into *regular* and *exit*, whereas inaccessible boundaries are *entrance* or *natural*. In particular:

1. r_i accessible

   - *regular*: it is a boundary crossed from the process in both directions, that is, $X(t)$ can enter or leave a regular boundary. For a full characterization of the process, the behavior at the boundary must be specified. This can range from full absorption to full reflection.
   - *exit*: if r_i is an exit boundary, starting at r_i the process cannot reach any interior state $x \in J$ in finite time, no matter how near to r_i is x.

2. r_i inaccessible

   - *entrance*: it cannot be reached from the interior of the state space, while it is possible to consider a process that starts right there. Such a process quickly moves to the interior never to return to the entrance boundary.
   - *natural*: the process $X(t)$ can neither reach a natural boundary in finite mean time nor be originated there.

Due to this classification, if one knows the nature of the diffusion interval's boundaries, one can decide what kind of boundary condition, if any, have to be associated

with the diffusion equation in order to determine the transition pdf of the process. Moreover it is possible to establish the nature of the boundaries without having to know preliminarly the transition pdf of the process. Indeed, as proved by Feller, the classification of the boundaries depends only on certain integrability properties of the coefficient $A_1(x)$ and $A_2(x)$ of the diffusion equations. More specifically, for all x and y $(x < y)$ inside the diffusion interval $J = (r_1, r_2)$, let introduce the following functions:

$$
\begin{aligned}
h(x) &= \exp\left\{-2\int^x \frac{A_1(\xi)}{A_2(\xi)}d\xi\right\} \quad (scale\ function)\\
s(x) &= \frac{2}{A_2(x)h(x)} \quad (speed\ density)\\
H[x,y] &= \int_x^y h(\xi)d\xi \quad (scale\ measure)\\
S[x,y] &= \int_x^y s(\xi)d\xi \quad (speed\ measure).
\end{aligned}
$$

The relevant integrals for the boundaries classification are:

$$
\begin{aligned}
&H(r_1) \equiv H(r_1,x] = \lim_{a\to r_1} H[a,x], \quad H(r_2) \equiv H[x,r_2) = \lim_{b\to r_2} H[x,b],\\
&S(r_1) \equiv S(r_1,x] = \lim_{a\to r_1} S[a,x], \quad S(r_2) \equiv S[x,r_2) = \lim_{b\to r_2} S[x,b],\\
&U(r_1) \equiv U(r_1,x] = \lim_{a\to r_1} \int_a^x h(u)S[u,x]du,\\
&U(r_2) \equiv U[x,r_2) = \lim_{b\to r_2} \int_x^b h(u)S[x,u]du,\\
&V(r_1) \equiv V(r_1,x] = \lim_{a\to r_1} \int_a^x s(u)H[u,x]du,\\
&V(r_2) \equiv V[x,r_2) = \lim_{b\to r_2} \int_x^b s(u)H[x,u]du.
\end{aligned}
$$

In Table 1.1, Feller's criteria for such boundary classification are summarized. The asterisk $*$ indicates the minimal sufficient conditions for establishing the nature of the boundary r_i. For example, to establish that a boundary r_i is entrance, it suffices to verify that $H(r_i) = \infty$ and $U(r_i) < \infty$. Note that when both boundaries are natural, the initial conditions (1.2) alone uniquely determines the transition pdf as the solution of the diffusion equations (1.3). In the other cases, we must consider boundary conditions to solve (1.3) with (1.2). The most useful boundary conditions are the following:

1. *total reflection at* r_i when r_i is an exit boundary: by this one means that there is no probability flow at the boundary. Therefore, the appropriate boundary conditions are:

Table 1.1: Feller's criteria for boundary classification.

$H(r_i)$	$S(r_i)$	$U(r_i)$	$V(r_i)$	classification of boundary r_i
$<\infty*$	$<\infty*$	$<\infty$	$<\infty$	regular (attracting, attainable)
$<\infty$	$=\infty*$	$<\infty*$	$=\infty$	exit (absorbing, attracting, attainable)
$<\infty*$	$=\infty*$	$=\infty*$	$=\infty$	natural (attracting, unattainable)
$=\infty*$	$<\infty*$	$=\infty$	$=\infty*$	natural (nonattracting, unattainable)
$=\infty*$	$=\infty*$	$=\infty$	$=\infty*$	natural (nonattracting, unattainable)
$=\infty*$	$<\infty$	$=\infty$	$<\infty*$	entrance (nonattracting, unattainable)

- for the Fokker-Planck equation

$$\lim_{x\to r_i}\left\{\frac{\partial}{\partial x}\left[\frac{A_2(x)}{2}f(x,t|y)\right]-A_1(x)f(x,t|y)\right\}=0,$$

- for the Kolmogorov equation

$$\lim_{y\to r_i} h^{-1}(y)\frac{\partial}{\partial y}f(x,t|y)=0.$$

2. *total absorption at* r_i when r_i is an entrance boundary:

- for the Fokker-Planck equation the condition is

$$\lim_{x\to r_i}[A_2(x)h(x)f(x,t|x_0)]=0,$$

- for the Kolmogorov equation the condition is

$$\lim_{x_0\to r_i} f(x,t|x_0)=0.$$

Sometimes the transition pdf of a time-homogeneous process admits a limit for $t\to\infty$. This limit is a pdf $W(x)$, called *stationary* density (or *steady-state* density), that does not depend on the initial state y. One can determine this density in the following way.
From the Fokker-Planck equation one can easily prove that $W(x)$ satisfies

$$\frac{1}{2}\frac{d^2}{dx^2}[A_2(x)W(x)]-\frac{d}{dx}[A_1(x)W(x)]=0. \tag{1.4}$$

Equation (1.4) can be written as:

$$\frac{1}{2}\frac{d}{dx}[A_2(x)W(x)]-[A_1(x)W(x)]=\frac{c_1}{2},$$

with c_1 an arbitrary constant. From this last equation one has

$$W(x) = \frac{1}{h(x)A_2(x)} \left[c_2 + c_1 \int^x h(u)du \right],$$

where $h(x)$ is the scale function and the constants c_1 and c_2 are determinated such that $W(x) > 0$ and $\int_{r_1}^{r_2} W(x)dx = 1$. When this is possible, a stationary density exists.
Note that, for a lot of diffusion processes, one has $c_1 = 0$ to assure $W(x) > 0$. Specifically, if $S(r_i) < \infty \, (i = 1, 2)$, then the steady-state density exists and is given by

$$W(x) = \frac{1}{h(x)A_2(x)} c_2. \tag{1.5}$$

Moreover, by using the condition $\int_{r_1}^{r_2} W(x)dx = 1$, the following expression of c_2 holds:

$$c_2 = \left[\int_{r_1}^{r_2} \frac{1}{h(x)A_2(x)} dx \right]^{-1}.$$

Hence, if $c_1 = 0$ and $c_2 > 0$, $W(x)$ exists and is given by (1.5).

1.1.2 The first passage time problem

In many physical and biological problems, a prime concern is the time at which a process *first enters or crosses* a particular state. Indeed, also for processes analyzed in Chapter 2 and Chapter 3, the knowledge concerning the FPT random variable is fundamental. Specifically, in Chapter 2 we consider cancer population growth and we use the mean FPT to propose a strategy in order to keep the cancer mass under a control threshold during an intermittent treatment. In Chapter 3, we study the neuronal activity for which the firing pdf is modeled by FPT pdf of the stochastic process invoked to mimic the membrane potential time course.
In the following, we focus on the FTP problem for a diffusion process in the presence of one threshold and we consider time dependent and constant thresholds.

Let $\{X(t); t > \tau \geq 0\}$ be a time-homogeneous stochastic diffusion process defined in the interval $J \equiv (r_1, r_2)$, where r_1, r_2 are natural boundaries.

A time depending threshold

Let $S(t)$ a continuous function, called *threshold* or *boundary*. The first passage time random variable is defined as follows:

$$T_y(\tau) = \begin{cases} \inf_{t \geq \tau} \{t : \ X(t) > S(t)\}, & X(\tau) = y < S(t) \\ \inf_{t \geq \tau} \{t : \ X(t) < S(t)\}, & X(\tau) = y > S(t). \end{cases} \tag{1.6}$$

The pdf $g\left[S(t),t|y,\tau\right]$ of the random variable $T_y(\tau)$ is defined as

$$g\left[S(t),t|y,\tau\right]=\frac{\partial}{\partial t}P(T_y(\tau)<t).$$

Note that the sample paths of $X(t)$ are continuous functions, so any sample path that reaches a state $x>S(t)$ $[x<S(t)]$, after starting at time τ from $y<S(\tau)$ $[y>S(\tau)]$, must cross $S(\theta)$ for the first time at some intermediate instant θ $(\tau<\theta<t)$. Hence the following relation holds:

$$f(x,t|y,\tau)=\int_{\tau}^{t}g\left[S(\theta),\theta|y,\tau\right]f\left[x,t|S(\theta),\theta\right]d\theta, \tag{1.7}$$

for $x\leq S(t)$ and $y>S(\tau)$ or $x\geq S(t)$ and $y<S(\tau)$.
Equation (1.7) is a first-kind Volterra integral equation in the unknown function $g[S(t),t|y,\tau]$. It is characterized by the kernel $f[x,t|S(\theta),\theta]$ that exhibits a singularity of the type $1/\sqrt{t-\theta}$ as $\theta\uparrow t$. Hence, efficient numerical methods must be used to determine $g[S(t),t|y,\tau]$ from (1.7).
The idea is to remove the singularity of the kernel of the equation (1.7) by changing the equation itself. In the following the essential results of the procedure are shown (cf. [15], [38], [74]).
Given $S(t)\in C^1[t_0,\infty)$, the FPT pdf $g[S(t),t|y,\tau]$ satisfies the following second-kind Volterra integral equation

$$g[S(t),t|y,\tau]=\rho\left\{-2\Psi\left[S(t),t|y,\tau\right]+2\int_{\tau}^{t}g[S(\theta),\theta|y,\tau]\Psi[S(t),t|S(\theta),\theta]d\theta\right\} \tag{1.8}$$

with $y\neq S(\tau)$, where

$$\rho=sgn[S(\tau)-y]=\begin{cases}1, & y<S(t)\\ -1, & y>S(t)\end{cases}$$

and

$$\Psi[S(t),t|z,\theta]=\frac{d}{dt}F[S(t),t|z,\theta]+k(t)f[S(t),t|z,\theta],$$

with

$$F[x,t|z,\theta]=P\left[X(t)<x|X(\theta)=z\right].$$

In particular

$$\begin{aligned}\Psi[S(t),t|z,\theta] &= \left\{S^{'}(t)-A_1[S(t)]+\frac{1}{2}A_2^{'}[S(t)]+k(t)\right\}f[S(t),t|z,\theta]+\\ &+\frac{1}{2}A_2[S(t)]\frac{\partial}{\partial x}f(x,t|z,\theta)|_{x=S(t)},\end{aligned} \tag{1.9}$$

with $S'(t) = \frac{dS(t)}{dt}$, $A_2'[S(t)] = \frac{dA_2(x)}{dx}|_{x=S(t)}$ and $k(t)$ an arbitrary continuous function. By choosing a specific function $k(t)$, it is possible to remove the singularity of the kernel. Indeed, if $S(t) \in C^2[t_0, \infty)$, one has

$$\lim_{\theta \to t} \Psi[S(t), t|S(\theta), \theta] = 0 \tag{1.10}$$

if, and only if,

$$k(t) = \frac{1}{2}\left\{A_1[S(t)] - \frac{A_2'[S(t)]}{4} - S'(t)\right\}. \tag{1.11}$$

Hence, choosing $k(t)$ as in (1.11), the kernel of the equation (1.7) becomes non singular so that a simple numerical procedure can be used. Indeed, denoting by $h > 0$ the integration step and setting $t = \tau + kh,\ k = 1, 2, ...,$ equation (1.8) becomes:

$$\begin{aligned} g[S(\tau + kh), \tau + kh|y, \tau] &= \rho\{-2\Psi[S(\tau + kh), \tau + kh|y, \tau] \\ &+2\int_{\tau}^{\tau+kh} g[S(\theta), \theta|y, \tau]\Psi[S(\tau + kh), \tau + kh|S(\theta), \theta]d\theta\}. \end{aligned} \tag{1.12}$$

Note that by taking $k(t)$ as in (1.11), condition (1.10) is satisfied. Hence, from equation (1.12), using a composite trapezium rule, one obtains the following approximate solution $\check{g}$ to g:

$$\check{g}[S(\tau + h), \tau + h|y, \tau] = -2\Psi[S(\tau + h), \tau + h|y, \tau],$$

and for $k = 2, 3, \ldots$

$$\begin{aligned} \check{g}[S(\tau + kh), \tau + kh|y, \tau] &= \rho\left\{-2\,\Psi[S(\tau + kh), \tau + kh|y, \tau]\right. \\ &+2h\sum_{j=1}^{k-1} \check{g}[S(\tau + jh), \tau + jh|y, \tau] \\ &\left.\times\Psi[S(\tau + kh), \tau + kh|S(\tau + jh), \tau + jh]\right\}. \end{aligned} \tag{1.13}$$

A constant threshold

Let focus on the FPT problem through a constant threshold S; the random variable $T_y(\tau)$ is defined as in (1.6) with $S(t) = S$. In this case equation (1.7) becomes

$$f(x, t|y) = \int_0^t g(S, \theta|y) f(x, t - \theta|S)d\theta, \tag{1.14}$$

for $x \leq S$ and $y > S$ or $x \geq S$ and $y < S$. An analytic approach to the solution of equation (1.14) is based on the Laplace transform (LT).

Let

$$g_\lambda(S|y) = \int_0^{+\infty} e^{-\lambda t} g(S,t|y)dt$$

$$f_\lambda(S|y) = \int_0^{+\infty} e^{-\lambda t} f(S,t|y)dt$$

be the LT with respect to t of the functions g and f, respectively. Since a convolution integral appears on the right-side of (1.14), passing to the LT one obtains:

$$g_\lambda(S|y) = \frac{f_\lambda(x|y)}{f_\lambda(x|S)}. \tag{1.15}$$

If the transition pdf of $X(t)$ is known and if its LT can be calculated, the right-hand-side of (1.15) can be determined. If the inverse LT of the function $g_\lambda(S|y)$ can be calculated, one can determine $g(S,t|y)$; otherwise, the function $g_\lambda(S|y)$ can be used to get other information on the FPT. Specifically, we can determine the FPT probability $P(S|y) = \int_0^\infty g(S,t|y)dt = g_\lambda(S|y)|_{\lambda=0}$. Moreover, if $P(S|y) = 1$ the moments of $T_y(\tau)$ are given by

$$t_n(S|y) = \int_0^\infty t^n g(S,t|y)dt = (-1)^n \frac{d^n g_\lambda(S|y)}{d\lambda^n}|_{\lambda=0},\ n = 1,2,\ldots.$$

Note that, if $y < S$ and $H(r_1) = \infty$, the probability $P(S|y) \equiv t_0(S|y) = 1$ and the moments $t_n(S|y)$ can be iteratively calculated in the following way

$$t_n(S|y) = n\int_y^S dz h(z) \int_{r_1}^z s(u)t_{n-1}(S|u)du,\ \ n = 1,2,\ldots. \tag{1.16}$$

If, instead, $y > S$ and $H(r_2) = \infty$, one has $P(S|y) \equiv t_0(S|y) = 1$ and

$$t_n(S|y) = n\int_S^y dz h(z) \int_z^{r_2} s(u)t_{n-1}(S|u)du,\ \ n = 1,2,\ldots. \tag{1.17}$$

As proved by Siegert (cf. [78]), when the process $X(t)$ admits of the steady-state density, the FPT probability $P(S|y)$ is unity and relations (1.16) and (1.17) hold.

1.1.3 The asymptotic behavior of the FPT density

Let assume that $X(t)$ admits of the steady-state density pdf $W(x)$. In the following the boundary r_1 is denoted by r if $\rho = -1$, while $r \equiv r_2$ for $\rho = 1$.

We analyze the following two cases (cf. [39], [74]): *Case (i)* the threshold possesses an asymptote; *Case (ii)* the threshold is asymptotically periodic.

Case (i) Let assume that the threshold $S(t)$ possesses an asymptote S, i.e.

$$\lim_{t\to\infty} S(t) = S, \qquad S \in J. \tag{1.18}$$

For all $y \in J$ we consider the function:

$$R(S) = -2\rho \lim_{t\to\infty} \Psi[S(t), t|y, \tau] = -\rho \left[A_1(S) - \frac{A_2'(S)}{4} \right] W(S),$$

where $\Psi[S(t), t|y, \tau]$ is defined in (1.9) and $W(x)$ is the stationary density of the process.
If $S(t)$ is bounded such that (1.18) holds in $[0, \infty)$ and if, for $0 \le \theta < t$,

$$\begin{aligned}
&\lim_{S\to r} R(S) = 0 \\
&\lim_{S\to r} \left\{ -2\rho [R(S)]^{-1} \Psi \left[S\left(\frac{t}{R(S)}\right) - \frac{t}{R(S)} \, |y] \right\} = 1 \\
&\lim_{S\to r} \left\{ -2\rho [R(S)]^{-1} \Psi \left[S\left(\frac{t}{R(S)}\right) - \frac{t}{R(S)} \, \middle| S\left(\frac{\theta}{R(S)}\right) - \frac{\theta}{R(S)} \right] \right\} = 1
\end{aligned}$$

then,

$$\lim_{S\to r} \left\{ \frac{1}{R(S)} g \left[\frac{t}{R(S)} \, |y] \right\} = e^{-t}. \right.$$

Last relation leads to the following asymptotic result, for $S \to r$:

$$g(t|y) \approx R(S) \exp\left\{ -R(S) t \right\}.$$

If $\lim_{S\to r} R(S) = 0$ and if

$$\begin{aligned}
\lim_{S\to r} \quad & \left[A_1(S) - \frac{A_2'(S)}{4} \right]^{-2} \\
& \times \left\{ A_2(S) \left[A_1'(S) - \frac{A_2''(S)}{4} \right] - \frac{A_2'(S)}{2} \left[A_1(S) - \frac{A_2'(S)}{4} \right] \right\} = 0,
\end{aligned}$$

then the mean FPT has the following asymptotic representation

$$t_1(S|y) \approx [R(S)]^{-1}.$$

Case (ii) Let assume that the threshold $S(t)$ is asymptotically periodic, i.e.

$$\lim_{n\to\infty} S(t + nT) = V(t), \tag{1.19}$$

with $V(t)$ a periodic function of period T. For all $y \in J$ we consider the function

$$\begin{aligned} R[V(t)] &= -2\rho \lim_{t\to\infty} \Psi[S(t), t|y, \tau] \\ &= -\rho \left\{ V'(t) + A_1[V(t)] - \frac{A_2'[V(t)]}{4} \right\} W[V(t)], \end{aligned}$$

where $\Psi[S(t), t|y, \tau]$ is defined in (1.9) and $W(x)$ is the stationary density of the process.
Note that if $S(t)$ is a bounded function such that (1.19) holds as $t \in [0, \infty)$, setting

$$S = \frac{1}{T}\int_0^T V(\tau)d\tau, \qquad \gamma = \frac{1}{T}\int_0^T R[V(\tau)]d\tau,$$

one can define a non-negative monotonically increasing function $\varphi(t)$ which is solution of

$$\int_0^{\varphi(t)} R[V(\tau)]d\tau = \gamma t$$

and such that

$$\varphi(t + nT) = \varphi(t) + nT \qquad (n = 0, 1, \ldots).$$

Furthermore, if there exists $S^* \in J$ such that $R[V(t)] > 0$ for $\rho(S - S^*) > 0$ and if

$$\begin{aligned} &\lim_{S\to r} R\left\{ V\left[\varphi\left(\frac{t}{\gamma} \right) \right] \right\} = 0 \\ &\lim_{S\to r} \frac{-2\rho\Psi\left\{ S\left[\varphi\left(\frac{t}{\gamma} \right) \right], \varphi\left(\frac{t}{\gamma} \right) |y \right\}}{R\left\{ V\left[\varphi\left(\frac{t}{\gamma} \right) \right] \right\}} = 1 \\ &\lim_{S\to r} \frac{-2\rho\Psi\left\{ S\left[\varphi\left(\frac{t}{\gamma} \right) \right], \varphi\left(\frac{t}{\gamma} \right) \middle| S\left[\varphi\left(\frac{\theta}{\gamma} \right) \right], \varphi\left(\frac{\theta}{\gamma} \right) \right\}}{R\left\{ V\left[\varphi\left(\frac{t}{\gamma} \right) \right] \right\}} = 1 \end{aligned}$$

one has:

$$\lim_{S\to r} \left\{ \left[\frac{d}{dt}\varphi\left(\frac{t}{\gamma} \right) \right] g\left[\varphi\left(\frac{t}{\gamma} \right) |y \right] \right\} = e^{-t}.$$

This last relation shows that for $S \to r$ the following asymptotic result holds

$$g(t|y) \approx R[V(t)] \exp\left\{ -\int_0^t R[V(\theta)]d\theta \right\}.$$

1.1.4 Example: the Wiener process

The Wiener process is a diffusion process $\{X(t), t \geq 0\}$ defined in the diffusion interval $J \equiv (-\infty, \infty)$, with drift and infinitesimal variance

$$A_1(x) = \mu, \quad A_2(x) = \sigma^2,$$

respectively, where $\mu \in \mathbb{R}$ and $\sigma > 0$. Since $A_1(x)$ and $A_2(x)$ do not depend on t, $X(t)$ is time-homogeneous. When $\mu = 0$ and $\sigma^2 = 1$ the Wiener process is called *standard*.
From the Feller's classification, it follows that $r_i = \pm\infty$ are natural. In particular:

if $\mu < 0$, r_1 is attracting and r_2 is nonattracting,

if $\mu > 0$, r_1 is nonattracting and r_2 is attracting,

if $\mu = 0$, both boundaries are nonattracting.

For this process, one can prove that the transition pdf is

$$f(x, t|y) = \frac{1}{\sqrt{2\pi\sigma^2 t}} \exp\left\{-\frac{(x - y - \mu t)^2}{2\sigma^2 t}\right\}. \tag{1.20}$$

Moreover the mean and the variance of $X(t)$ are

$$\begin{aligned} E[X(t)|X(0) = y] &= y + \mu\, t, \\ Var[X(t)|X(0) = y] &= \sigma^2\, t, \end{aligned} \tag{1.21}$$

respectively. The Wiener process does not have the steady-state density and the FPT pdf through a constant threshold $S \neq y$ is

$$g(S, t|y) = \frac{|S - y|}{\sqrt{2\pi\sigma^2 t^3}} \exp\left\{-\frac{(S - y - \mu t)^2}{2\sigma^2 t}\right\}. \tag{1.22}$$

1.2 Stochastic diffusion processes with random jumps

Now we consider stochastic diffusion processes subject to jumps. We call *catastrophe*, *jump* or *return* the random event that transforms the state of the process in a certain value from which the process can re-start, and we call *inter-jump interval* the time interval elapsing between two consecutive jumps.
In [25], [26], [28], [29] some general results for the transient and steady-state pdf's of diffusion processes in the presence of catastrophes have been obtained. However,

in all these works the effect of a catastrophe is to reset the process to a fixed and particular point for the process, the process re-start following the same behavior of before and the inter-jump intervals are identically distributed following the exponential law.

Whereas, we suppose that catastrophes occur at time interval following a general distribution and the return points are randomly chosen. Moreover, we consider the possibility that, after each jump, the process can evolve with a different dynamics respect to the previous processes; we also suppose that the inter-jump intervals and the return points are not identically distributed.

In the following, we construct the process with jumps, we analyze the pdf and its moments, the FPT problem and we perform the Wiener process with catastrophes as example.

Let $\left\{\tilde{X}_k(t),\, t \geq t_0 \geq 0\right\}$ be a diffusion stochastic process defined in the diffusion interval J_k, for $k = 0, 1, \ldots$. We construct the stochastic process with random catastrophes $X(t)$ as follows. Starting from the initial state $\rho_0 = y$ at time t_0, the process $X(t)$ evolves according to the process $\tilde{X}_0(t)$ until a random catastrophe occurs shifting process to a random state ρ_1. From here, $X(t)$ re-starts according to $\tilde{X}_1(t)$ until another catastrophe occurs resetting the process to ρ_2. In general, the effect of the k-th catastrophe ($k = 1, 2, \ldots$) is to transform the state of $X(t)$ in a certain level ρ_k, randomly chosen according to a pdf $\phi_k(x)$. Then, the process evolves like $\tilde{X}_k(t)$, until a new catastrophe occurs.

The process $X(t)$ consists of independent cycles $\mathcal{I}_1, \mathcal{I}_2$ ..., whose durations are

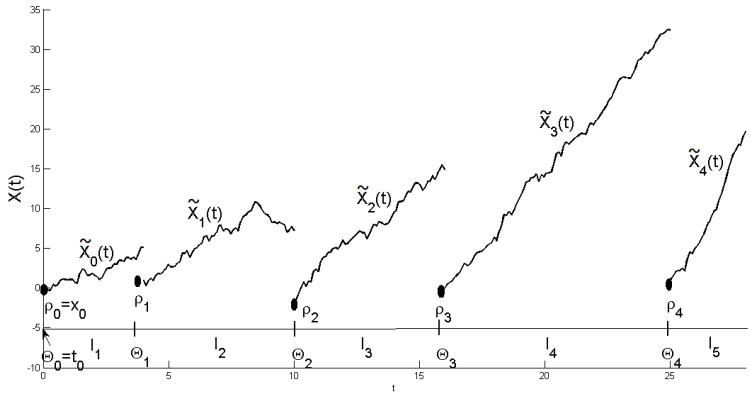

Figure 1.1: The notation for a process with jumps.

described by the independent random variables $I_1,\ I_2, \ldots$, that represent the time intervals between two consecutive catastrophes. The random variable I_k is described by the pdf $\psi_k(\cdot)$ ($k = 1, 2, \ldots$).

Moreover, we denote by $\Theta_1, \Theta_2, \ldots$ the times in which the jumps occur and we set

$\Theta_0 = t_0$. Let $\xi_k(\tau)$ be the pdf of the random variable Θ_k, $k = 1, 2, \ldots$, if the initial time of observation is t_0. The variables I_k and Θ_k are related, indeed it results: $\Theta_1 = I_1$, and for $k > 1$ one has $\Theta_k = I_1 + I_2 + \ldots I_k$.

We summarize the notation as follows and we represent it in Figure 1.1:

- $\mathcal{I}_0$ is the interval starting at t_0 and finishing when the first jump occurs; while, $\mathcal{I}_k$ is the time elapsing between the k-th and the $(k+1)$-th jump, for $k \geq 1$;
- I_k is the duration of the k-th inter-jump interval, for $k \geq 1$;
- $\Theta_0 = t_0$ and the k-th jump occurs at $\Theta_k = I_1 + I_2 + \ldots I_k$, for $k \geq 1$;
- $\rho_0 = y$ and ρ_k is the return point in correspondence to the k-th jump, for $k \geq 1$;
- $\tilde{X}_k(t)$ is a stochastic diffusion process which starts from ρ_k at the time Θ_k and it lasts until the time Θ_{k+1}.

In the following, given two random variables X and Y, we write $X \equiv Y$ if they are identically distributed; whereas, given two stochastic processes $X(t)$ and $Y(t)$, we write $X(t) \equiv Y(t)$ if they are characterized by same drift and infinitesimal variance. In the remaining part of this chapter, we analyze the pdf of the process with jumps, its moments and the FPT problem. Note that, these characteristics will be expressed in terms of the same characteristics of the involved processes without jumps. Finally, we consider the Wiener process with jumps.

1.2.1 The probability density function and its moments

Let $\tilde{f}_k(x, t|x_0, t_0) = \frac{\partial}{\partial x}\mathrm{P}\left[\tilde{X}_k(t) < x | \tilde{X}_k(t_0) = y\right]$ be the pdf of the process $\tilde{X}_k(t)$.

To obtain the pdf $f(x, t|y, t_0)$ of $X(t)$ we note the following.

Starting from ρ_0 at time t_0, the process reaches x at time t if one, and only one, of the successive events occur:

- there are not jumps between t_0 and t: this probability is expressed by $1 - P(0 < I_1 < t - t_0) = 1 - \int_0^{t-t_0} \psi_1(s)\, ds$, so that the pdf of $X(t)$ is equal to the pdf of $\tilde{X}_0(t)$;
- k jumps have occurred between t_0 and t, for $k = 1, 2, \ldots$.
  The k-th jump occurs at time τ $(t_0 < \tau < t)$ with intensity $\xi_k(\tau)$ (i.e. $\xi_k(\tau)d\tau \approx P(\tau < \Theta_k < \tau + d\tau)$); then the process starts from ρ_k at time τ and evolves according to $\tilde{X}_k(t)$ to reach the state x at time t. In particular, we want that the last jump occurs in τ, so the duration of the k-th

interjump interval, starting at τ , has to stop before t: this is expressed by $1 - P(0 < I_k < t - \tau) = 1 - \int_0^{t-\tau} \psi_k(s)\, ds$.

Therefore

Remark 2. *The pdf of the process $X(t)$ is:*

$$f(x,t|\rho_0,t_0) = \left(1 - \int_0^{t-t_0} \psi_1(s)\, ds\right) \tilde{f}_0(x,t|\rho_0,t_0) + \sum_{k=1}^{\infty} \int_{t_0}^{t} \xi_k(\tau) \left(1 - \int_0^{t-\tau} \psi_k(s) ds\right) \left(\int_{z\in J_k} \phi_k(z)\, \tilde{f}_k(x,t|z,\tau)\, dz\right) d\tau, \qquad (1.23)$$

and its moments $\mu^{(n)}(t|y,\tau)$ are:

$$\mu^{(n)}(t|\rho_0,t_0) = \left(1 - \int_0^{t-t_0} \psi_1(s)\, ds\right) \tilde{\mu}_0^{(n)}(t|\rho_0,t_0) + \sum_{k=1}^{\infty} \int_{t_0}^{t} \xi_k(\tau) \left(1 - \int_0^{t-\tau} \psi_k(s) ds\right) \left(\int_{z\in J_k} \phi_k(z)\, \tilde{\mu}_k^{(n)}(t|z,\tau)\, dz\right) d\tau, \qquad (1.24)$$

where $\tilde{\mu}_k^{(n)}(t|y,\tau)$ are the moments of $\tilde{X}_k(t)$.

From Remark 2 one obtains:

Remark 3. *If the return points are fixed states $\rho_1, \rho_2, \ldots$, the expression (1.23) becomes*

$$f(x,t|\rho_0,t_0) = \left(1 - \int_0^{t-t_0} \psi_1(s)\, ds\right) \tilde{f}_0(x,t|\rho_0,t_0) + \sum_{k=1}^{\infty} \int_{t_0}^{t} \xi_k(\tau) \left(1 - \int_0^{t-\tau} \psi_k(s) ds\right) \tilde{f}_k(x,t|\rho_k,\tau) d\tau. \qquad (1.25)$$

In the following, for clarity, we suppose that the return points are fixed states.

Now, we show two examples in which deterministic and exponentially distributed inter-jump intervals are considered.

Deterministic inter-jumps

We set $\tau_0 = t_0 = 0$ and jumps occur in the time instants $\tau_1, \tau_2, \ldots, \tau_N$. The resulting process $X(t)$ consists of a combination of processes $\tilde{X}_k(t)$:

$$X(t) = \sum_{k=0}^{N} \tilde{X}_k(t) \mathbf{1}_{(\tau_k,\tau_{k+1})}(t), \qquad \tilde{X}_k(\tau_k) = \rho_k$$

where $\tau_{N+1} = \infty$ and $\mathbf{1}_{(\tau_k,\tau_{k+1})}(t) = \begin{cases} 1, & t \in (\tau_k, \tau_{k+1}) \\ 0, & t \notin (\tau_k, \tau_{k+1}) \end{cases}$.
The random variable I_k is described by the degenerate pdf $\psi_k(t) = \delta\left[t - (\tau_k - \tau_{k-1})\right]$, where $\delta(\cdot)$ is the Dirac delta-function. In this case Θ_k is a degenerate random variable, indeed $\Theta_k = \tau_k$ almost surely (a.s.) and consequently $\xi_k(t) = \delta(t - \tau_k)$. Note that, denoting by

$$H(x) = \int_{-\infty}^{x} \delta(u)\, du = \begin{cases} 0, & x < 0 \\ 1, & x > 0, \end{cases}$$

the Heaviside unit step function, one obtains $\int_a^b \delta(s - \tau_k) ds = H(b - a - \tau_k)$. Hence, from (1.25) one has:

$$\begin{aligned} f(x,t|\rho_0,0) &= \left[1 - H\left(t - \tau_1\right)\right] \tilde{f}_0(x,t|\rho_0,0) \\ &+ \sum_{k=1}^{N} \int_0^t \delta\left(\tau - \tau_k\right) \left[1 - H\left(t - \tau - (\tau_k - \tau_{k-1})\right]\right. \tilde{f}_k(x,t|\rho_k,\tau) d\tau \\ &= \left[1 - H\left(t - \tau_1\right)\right] \tilde{f}_0(x,t|\rho_0,0) \\ &+ \sum_{k=1}^{N} H\left(t - \tau_k\right) \left[1 - H\left(t - \tau_k - (\tau_k - \tau_{k-1})\right)\right] \tilde{f}_k\left(x,t|\rho_k,\tau_k\right). \end{aligned}$$

Taking into consideration the definition of the Heaviside unit step function, one has

$$\begin{aligned} f(x,t|\rho_0,0) &= \sum_{k=0}^{N} \tilde{f}_k\left(x,t|\rho_k,\tau_k\right) \mathbf{1}_{(\tau_k,\tau_{k+1})}(t) \\ &= \begin{cases} \tilde{f}(x,t|\rho_0,0), & t \in \mathcal{I}_1 \\ \\ \tilde{f}(x,t|\rho_k,\tau_k), & t \in \mathcal{I}_{k+1} \quad (k = 1,2,\ldots,N). \end{cases} \end{aligned} \tag{1.26}$$

and the moments are

$$\mu^{(n)}(t|\rho_0,0) = \sum_{k=0}^{N} \tilde{\mu}^{(n)}\left(t|\rho_k,\tau_k\right) \mathbf{1}_{(\tau_k,\tau_{k+1})}(t). \tag{1.27}$$

Exponentially distributed inter-jumps

We assume that $\tilde{X}_k(t) \equiv \tilde{X}(t)$, $\rho_k = \rho$ (for all k) and that I_k are identically distributed with $\psi_k(s) \equiv \psi(s) = \xi e^{-\xi s}$, for $k \geq 1$. In this case Θ_k is the sum of k exponentially distributed random variables so that $\xi_k(\tau) = \frac{\xi^k \tau^{k-1} e^{-\xi\tau}}{(k-1)!}$ is an Erlang

distribution with parameters (k, ξ). From (1.25) one has:

$$\begin{aligned} f(x,t|\rho,t_0) = \quad & e^{-\xi(t-t_0)}\tilde{f}(x,t|\rho,t_0) + \sum_{k=1}^{\infty}\int_{t_0}^{t}\frac{\xi^k\tau^{k-1}}{(k-1)!}e^{-\xi t}\tilde{f}(x,t|,\tau)d\tau \\ = \quad & e^{-\xi(t-t_0)}\tilde{f}(x,t|\rho,t_0) + \int_{t_0}^{t}\sum_{k=1}^{\infty}\frac{(\xi\tau)^{k-1}}{(k-1)!}\xi e^{-\xi t}\tilde{f}(x,t|\rho,\tau)d\tau \end{aligned}$$

Since $\sum_{k=1}^{\infty}\frac{(\xi\tau)^{k-1}}{(k-1)!} = e^{\xi\tau}$, one has that the pdf of $X(t)$ is

$$f(x,t|\rho,t_0) = e^{-\xi(t-t_0)}\tilde{f}(x,t|\rho,t_0) + \xi\int_{t_0}^{t}e^{-\xi(t-\tau)}\tilde{f}(x,t|\rho,\tau)d\tau; \tag{1.28}$$

and its moments are

$$\mu^{(n)}(t|\rho,t_0) = e^{-\xi(t-t_0)}\tilde{\mu}^{(n)}(t|\rho,t_0) + \xi\int_{t_0}^{t}e^{-\xi(t-\tau)}\tilde{\mu}^{(n)}(t|\rho,\tau)d\tau. \tag{1.29}$$

1.2.2 The first passage time problem

In this section we focus on the FPT problem for the process $X(t)$ through a constant threshold S.

Let

$$T_{\rho_0}(t_0) = \inf\{t \geq t_0 :\, X(t) > S\}, \qquad X(t_0) = \rho_0 < S$$

be the FPT random variable of $X(t)$ through S and let $g(S,t|\rho_0,t_0)$ be its pdf.
For $k = 0, 1, \ldots$, let

$$\tilde{T}^k_{\rho}(\theta) = \inf\{t \geq \theta :\, \tilde{X}_k(t) > S\}, \qquad \tilde{X}_k(\theta) = \rho < S$$

be the FPT random variable through S of the process $\tilde{X}_k(t)$, which starts from ρ at the time θ, and let $\tilde{g}_k(S,t|\rho,\theta)$ be its pdf.
We obtain an expression for g as follows. Starting from ρ_0 at time t_0, the process reaches the threshold S for the first time at t if one, and only one, of the successive events occurs:

- there are not jumps between t_0 and t, so that $X(t) \equiv \tilde{X}_0(t)$ and $g(S,t|\rho_0,t_0) = \tilde{g}_0(S,t|\rho_0,t_0)$;
- k jumps occur ($k \geq 1$); the k-th jump occurs in $\tau \in [0,t]$ and S is not crossed before τ. Recalling that $\tilde{X}_k(t)$ is defined in the time interval $\mathcal{I}_{k+1} = [\Theta_k, \Theta_{k+1}]$ and making use of the independence of cycles $\mathcal{I}_1, \mathcal{I}_2 \ \ldots$, the probability that none of the processes $\tilde{X}_0, \tilde{X}_1, \ldots, \tilde{X}_{k-1}$ cross S before τ is given by $\prod_{j=0}^{k-1}\Big[1 - P(\tilde{T}^j_{\rho_j}(\Theta_j) < \Theta_{j+1})\Big]$.

Therefore one has:

Remark 4. *The FPT pdf of $X(t)$ through S is*

$$\begin{aligned} g(S,t|\rho_0,t_0) &= \left(1-\int_0^{t-t_0}\psi(s)\,ds\right)\tilde{g}_0(S,t|\rho_0,t_0) \\ &+ \sum_{k=1}^{\infty}\int_{t_0}^{t}\xi_k(\tau)\left(1-\int_0^{t-\tau}\psi(s)ds\right)\tilde{g}_k(S,t|\rho_k,\tau)\,d\tau \\ &\times \left\{\prod_{j=0}^{k-1}\left[1-P(\tilde{T}^j_{\rho_j}(\Theta_j)<\Theta_{j+1})\right]\right\}. \end{aligned} \tag{1.30}$$

Deterministic inter-jumps

We set $\tau_0 = t_0$ and we suppose that jumps occur at times τ_k, $k = 1, 2, \ldots$. Since $\Theta_k \equiv \tau_k$, one has $1 - P(\tilde{T}^k_{\rho_k}(\tau_k) < \tau_{k+1}) = 1 - \int_{\tau_k}^{\tau_{k+1}} \tilde{g}_k(S,\tau|\rho_k,\tau_k)d\tau$; so, following the procedure to obtain (1.26), from (1.30), one has:

$$g(S,t|\rho_0,t_0) = \begin{cases} \tilde{g}_0(S,t|\rho_0,t_0), & t\in\mathcal{I}_1 \\ \displaystyle\prod_{j=0}^{k-1}\left[1-\int_{\tau_j}^{\tau_{j+1}}\tilde{g}_j(S,\tau|\rho_i,\tau_j)d\tau\right]\tilde{g}_k\left(S,t|\rho_k,\tau_k\right), & t\in\mathcal{I}_k, \end{cases} \tag{1.31}$$

with $k = 2, 3, \ldots$.

We note that, if the processes $\tilde{X}_k(t)$ are time homogeneous and $t_0 = 0$, the expression (1.31) becomes

$$\begin{aligned} &g(S,t|\rho_0) = \\ &= \begin{cases} \tilde{g}_0(S,t|\rho_0), & t\in\mathcal{I}_1 \\ \displaystyle\prod_{j=0}^{k-1}\left[1-\int_0^{\tau_{j+1}-\tau_j}\tilde{g}_j(S,\tau|\rho_j)d\tau\right]\tilde{g}_k\left(S,t-\tau_k|\rho_k\right), & t\in\mathcal{I}_k. \end{cases} \end{aligned} \tag{1.32}$$

In particular, if $I_k \equiv I$ are characterized by the same amplitude $A > 0$, $\rho_k = \rho$, $\tilde{X}_k \equiv \tilde{X}$ and denoting $\tilde{g}_k(S,t|\rho_0)$ with $\tilde{g}(S,t|\rho_0)$, the expression (1.32) becomes

$$g(S,t|\rho) =$$

$$= \begin{cases} \tilde{g}(S,t|\rho), & t \in \mathcal{I}_1 \\ \prod_{j=0}^{k-1}\left[1-\int_0^A \tilde{g}(S,\tau|\rho)d\tau\right] = \left[1-\int_0^A \tilde{g}(S,\tau|\rho)d\tau\right]^k, & t \in \mathcal{I}_k. \end{cases}$$

Exponentially distributed inter-jumps

We suppose $\rho_k = \rho$, $I_k \equiv I$ exponentially distributed with mean $1/\xi$ and the processes $\tilde{X}_k(t) \equiv \tilde{X}(t)$ are time homogeneous ($\tilde{T}_\rho^k(\Theta) \equiv \tilde{T}_\rho(\Theta)$).
Noting that $P(\tilde{T}_{\rho_j}^j(\Theta_j) < \Theta_{j+1}) = P(\tilde{T}_{\rho_j}^j(0) < I_{j+1}) = P(\tilde{T}_\rho(0) < I)$, the expression (1.30) becomes:

$$\begin{aligned} g(S,t-t_0|\rho) \quad &= \\ &= e^{-\xi(t-t_0)}\tilde{g}(S,t-t_0|\rho) \\ &+ \int_0^{t-t_0}\sum_{k=1}^{\infty}\frac{(\xi\tau)^{k-1}e^{-\xi\tau}}{(k-1)!}\xi e^{-\xi(t-\tau)}\tilde{g}(S,t-\tau|\rho)d\tau \times \left\{\prod_{j=0}^{k-1}\left[1-P(\tilde{T}_\rho(0)<I)\right]\right\} \\ &= e^{-\xi(t-t_0)}\tilde{g}(S,t-t_0|\rho) + \int_0^{t-t_0}\sum_{k=1}^{\infty}\frac{\left(\xi\tau\left[1-P(\tilde{T}_\rho(0)<I)\right]\right)^{k-1}}{(k-1)!} \\ &\times\xi e^{-\xi t}\tilde{g}(S,t-\tau|\rho)d\tau\left[1-P(\tilde{T}_\rho(0)<I)\right] \\ &= e^{-\xi(t-t_0)}\tilde{g}(x,t-t_0|\rho) \\ &+\xi\left[1-P(\tilde{T}_\rho(0)<I)\right]e^{-\xi t}\int_0^{t-t_0} e^{\xi\tau\left[1-P(\tilde{T}_\rho(0)<I)\right]}\tilde{g}(S,t-\tau|\rho)d\tau. \end{aligned} \tag{1.33}$$

1.2.3 Example: Wiener process with jumps

Let $\tilde{X}_k(t)$ be the Wiener diffusion processes with drift $A_1^k = \mu_k$ and infinitesimal variance $A_2^k = \sigma_k^2$. Let $X(t)$ be the process with jumps constructed as described in Paragraph 1.2.

Wiener process with deterministic jumps

We suppose that $\tau_0 = t_0 = 0$, $\tau_1, \tau_2, \ldots, \tau_N$ are the instants in which jumps occur and $\mathcal{I}_k = [\tau_{k-1}, \tau_k]$, $k = 2, 3, \ldots, N$ with $\mathcal{I}_{N+1} = [\tau_N, \tau_{N+1}]$ and $\tau_{N+1} = \infty$.
From (1.26), by taking into account (1.20), the pdf of $X(t)$ is

$$f(x,t|\rho_0) = \sum_{k=0}^{N}\frac{1}{\sqrt{2\pi\sigma^2(t-\tau_k)}}\exp\left\{-\frac{[x-\rho_k-\mu_k(t-\tau_k)]^2}{2{\sigma_k}^2(t-\tau_k)}\right\}\mathbf{1}_{(\tau_k,\tau_{k+1})}(t).$$

From (1.27) and (1.21), the mean of $X(t)$ is

$$E[X(t)|\rho_0] = \sum_{k=0}^{N} [\rho_k + \mu_k(t - \tau_k)] \ \mathbf{1}_{(\tau_k, \tau_{k+1})}(t).$$

In Figure 1.2 a sample path of the Wiener process $X(t)$ with deterministic catastrophes' instants $(4, 8, 13, 17, 20, 22)$ is plotted. The red line is a sample path of $\tilde{X}_0(t)$. The coefficients are $\mu_k = 0.5$ (on the left), $\mu_k = 0.5 + k$ (on the right) and the infinitesimal variance is $\sigma_k^2 = 2$, for all k. The return points are $\rho_k = 0$ on the left and $\rho_k = -k$ on the right. In Figure 1.3 and Figure 1.4 the pdf $f(1, t|0, 0)$ and the mean $E[X(t)|0, 0]$ of $X(t)$ are shown, respectively, with the same choices of Figure 1.2.

Regarding the FPT pdf, since the Wiener processes $\tilde{X}_k(t)$ are time homogeneous,

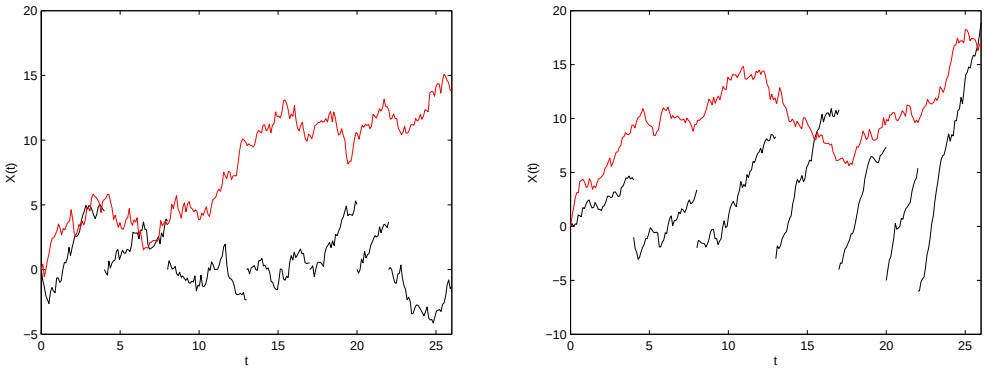

Figure 1.2: A sample path of the process $X(t)$ (black line) for $x_0 = 0$, and deterministic catastrophes' instants $(4, 8, 13, 17, 20, 22)$. The coefficients are $\mu_k = 0.5$ (on the left), $\mu_i = 0.5 + i$ (on the right) and the infinitesimal variance is $\sigma_k^2 = 2$. The return points are $\rho_i = 0$ on the left and $\rho_i = -i$, $i = 0, 1, \ldots$ on the right. The red line is a sample path of the process $\tilde{X}_0(t)$.

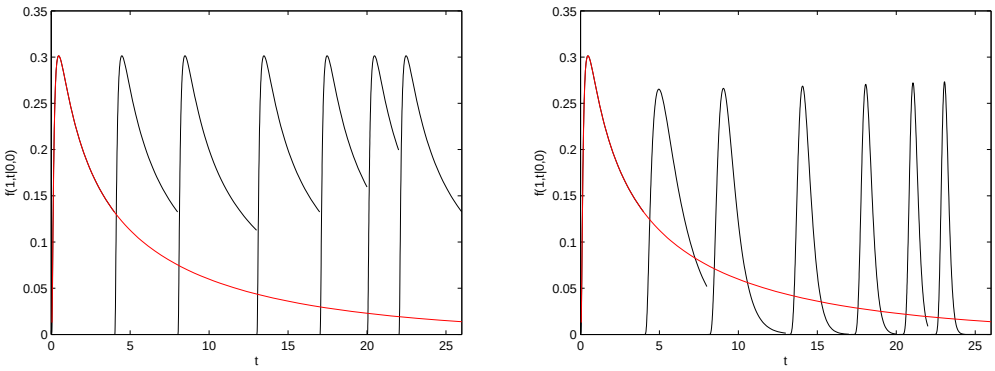

Figure 1.3: The pdf $f(1, t|0, 0)$ (black line) and the pdf $\tilde{f}_0(1, t|0, 0)$ (red line) with deterministic jumps, for the same choices of Figure 1.2.

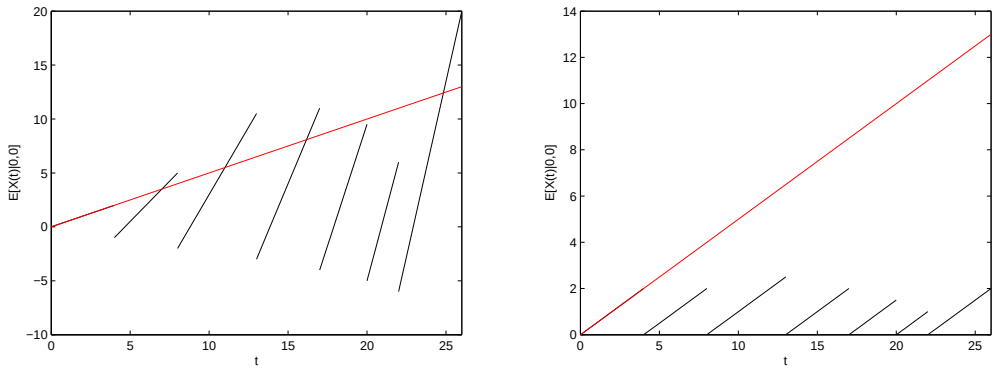

Figure 1.4: The mean $E[X(t)|0,0]$ (black line) and $E[\tilde{X}_0(t)|0,0]$ (red line) with deterministic jumps, for the same choices of Figure 1.2.

the expression of $g(S,t|\rho_0)$ is given by (1.32) where $\tilde{g}_k(S,\tau|\rho_k)$ is defined in (1.22), so, for $\rho_k < S$ and $k \geq 1$, one has:

$$
\begin{aligned}
& g(S,t|\rho_0) = \\
& = \begin{cases}
\frac{(S-\rho_0)}{\sqrt{2\pi\sigma_0^2 t^3}} \exp\left\{-\frac{(S-\rho_0-\mu_0 t)^2}{2\sigma_0^2 t}\right\}, & t \in \mathcal{I}_1 \\
\prod_{j=0}^{k-1}\left[1 - \int_0^{\tau_{j+1}-\tau_j} \frac{(S-\rho_j)}{\sqrt{2\pi\sigma_j^2\tau^3}} \exp\left\{-\frac{(S-\rho_j-\mu_j\tau)^2}{2\sigma_j^2\tau}\right\} d\tau\right] & \\
\times \frac{(S-\rho_k)}{\sqrt{2\pi\sigma_k^2(t-\tau_k)^3}} \exp\left\{-\frac{[S-\rho_k-\mu_k(t-\tau_k)]^2}{2\sigma_k^2(t-\tau_k)}\right\}, & t \in \mathcal{I}_k
\end{cases}
\end{aligned}
$$

where

$$
\begin{aligned}
& \int_0^{\tau_{j+1}-\tau_j} \frac{(S-\rho_j)}{\sqrt{2\pi\sigma_j^2\tau^3}} \exp\left\{-\frac{(S-\rho_j-\mu_j\tau)^2}{2\sigma_j^2\tau}\right\} d\tau \\
& \qquad = \frac{1}{2} Erfc\left[\frac{S-\rho_j+\mu_j(\tau_{j+1}-\tau_j)}{\sqrt{2(\tau_{j+1}-\tau_j)\sigma_j^2}}\right] \\
& \qquad + \frac{1}{2}\exp\left\{-\frac{2\mu_j(S-\rho_j)}{\sigma_j^2}\right\} Erfc\left[\frac{S-\rho_j-\mu_j(\tau_{j+1}-\tau_j)}{\sqrt{2(\tau_{j+1}-\tau_j)\sigma_j^2}}\right],
\end{aligned}
$$

with $Erfc = (2/\sqrt{\pi})\int_x^\infty e^{-t^2} dt$ the complementary error function.
In Figure 1.5 the FPT pdfs' $g(5,t|0)$ (black line) and $\tilde{g}_0(5,t|0)$ (red line) are plotted for the same choices of Figure 1.2.

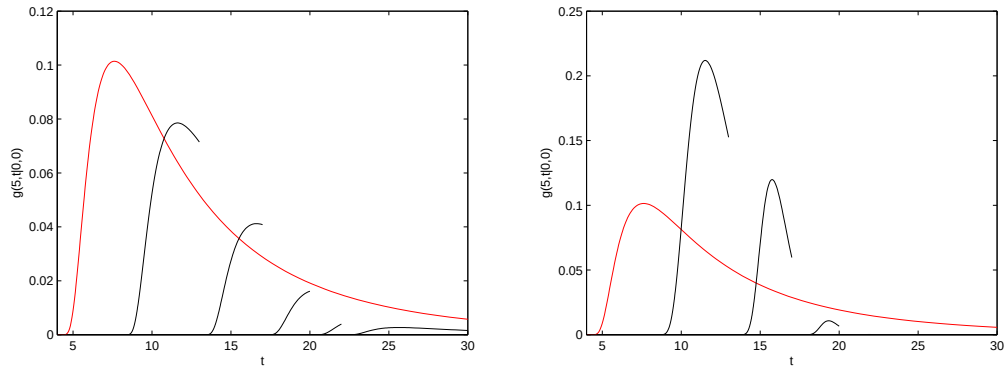

Figure 1.5: FPT pdfs' $g(5,t|0)$ (black line) and $\tilde{g}_0(5,t|0)$ (red line), with deterministic jumps, are plotted for the same choices of Figure 1.2.

Wiener process with exponentially distributed jumps

We assume that $\tilde{X}_k \equiv \tilde{X}$, $\rho_k = \rho$ and $\psi_k(s) \equiv \psi(s) = \xi e^{-\xi s}$. The expression (1.28) holds, where $f(x,t|\rho)$ is defined in (1.20), so one has for $t_0 = 0$:

$$\begin{aligned} f(x,t|\rho) &= \frac{e^{-\xi t}}{\sqrt{2\pi\sigma^2 t}} \exp\left\{-\frac{(x-\rho-\mu t)^2}{2\sigma^2 t}\right\} \\ &\quad +\xi \int_0^t \frac{e^{-\xi(t-\tau)}}{\sqrt{2\pi\sigma^2(t-\tau)}} \exp\left\{-\frac{[x-\rho-\mu(t-\tau)]^2}{2\sigma^2(t-\tau)}\right\} d\tau \end{aligned}$$

where

$$\begin{aligned} &\int_0^t \frac{e^{-\xi(t-\tau)}}{\sqrt{2\pi\sigma^2(t-\tau)}} \exp\left\{-\frac{[x-\rho-\mu(t-\tau)]^2}{2\sigma^2(t-\tau)}\right\} d\tau = \\ &\qquad \frac{e^{(x-\rho)(\mu-\sqrt{\mu^2+2\sigma^2\xi})}}{2\sqrt{\mu^2+2\sigma^2\xi}} \times \left[Erfc\left(\frac{x-\rho-t\sqrt{\mu^2+2\sigma^2\xi}}{\sqrt{2t\sigma^2}}\right)\right. \\ &\qquad \left. -e^{\frac{2(x-\rho)\sqrt{\mu^2+2\sigma^2\xi}}{\sigma^2}} Erfc\left(\frac{x-\rho+t\sqrt{\mu^2+2\sigma^2\xi}}{\sqrt{2\theta\sigma^2}}\right)\right]. \end{aligned}$$

Moreover, the mean of $X(t)$ has the expression given in (1.29) for $n = 1$, with $\tilde{\mu}^{(1)}(t|\rho)$ defined in (1.21); so it results, for $t_0 = 0$:

$$E[X(t)|X(0) = \rho] = e^{-\xi t}(\rho + \mu t) + \xi \int_0^t e^{-\xi(t-\tau)}[\rho + \mu(t-\tau)]d\tau$$

with

$$\int_0^t e^{-\xi(t-\tau)}[\rho + \mu(t-\tau)]d\tau = \frac{\rho}{\xi} + \frac{\mu}{\xi^2} - e^{-\xi t}\left[-\frac{\rho}{\xi} + \frac{\mu}{\xi^2} + \frac{\mu t}{\xi}\right].$$

On the left of Figure 1.6 the pdf's $f(1,t|0,0)$ (black line) and $\tilde{f}_0(1,t|0,0)$ (red line) for $\rho_k = 0$ $(k = 0,1,\ldots)$ and exponentially distributed inter-jumps with $1/\xi = 4$ are

plotted. Each $X_k(t)$ is a Wiener diffusion process with drift $A_1 = \mu$ and infinitesimal variance $A_2 = \sigma^2$, where $\mu = 0.5$ and $\sigma^2 = 2$. On the right of Figure 1.6 the mean $E[X(t)|0,0]$ (black line) and $E[\tilde{X}_0(t)|0,0]$ (red line) are plotted for the same choices of the left side.

The FPT pdf is given in (1.33), where $\tilde{g}_j(S,\tau|\rho)$ is defined in (1.22); so one has, for $t_0 = 0$,

$$g(S,t|\rho) = e^{-\xi t}\frac{S-\rho}{\sqrt{2\pi\sigma^2 t^3}}\exp\left\{-\frac{(S-\rho-\mu t)^2}{2\sigma^2 t}\right\} + \xi\left[1 - P(\tilde{T}_\rho(0) < I)\right]e^{-\xi t}$$
$$\times \int_0^t e^{\xi\tau\left[1-P(\tilde{T}_\rho(0)<I)\right]}\frac{S-\rho}{\sqrt{2\pi\sigma^2(t-\tau)^3}}\exp\left\{-\frac{(S-\rho-\mu(t-\tau))^2}{2\sigma^2(t\tau)}\right\}d\tau,$$

with

$$P(\tilde{T}_\rho(0) < I) = \int_0^\infty d\theta\xi e^{-\xi\theta}\int_0^\theta \frac{S-\rho}{\sqrt{2\pi\sigma^2 v^3}}e^{-\frac{(S-\rho-\mu v)^2}{2\sigma^2 v}}dv$$
$$= \int_0^\infty d\theta\xi e^{-\xi\theta}\left\{-\frac{1}{2}Erfc\left[\frac{\rho-S+\mu\theta}{\sqrt{2\sigma^2\theta}}\right] - \frac{1}{2}Erfc\left[\frac{\rho-S-\mu\theta}{\sqrt{2\sigma^2\theta}}\right]\right\}$$
$$= -\frac{1}{2}\xi\left\{L_\xi\left[Erfc\left(\frac{\rho-S+\mu\theta}{\sqrt{2\sigma^2\theta}}\right)\right] + L_\xi\left[Erfc\left(\frac{\rho-S-\mu\theta}{\sqrt{2\sigma^2\theta}}\right)\right]\right\},$$

where $L_\xi[k(\theta)] = \int_0^\infty e^{-\xi\theta}k(\theta)d\theta$ is the Laplace Transform. In this case, the closed form for $g(S,t|\rho)$ is not found.

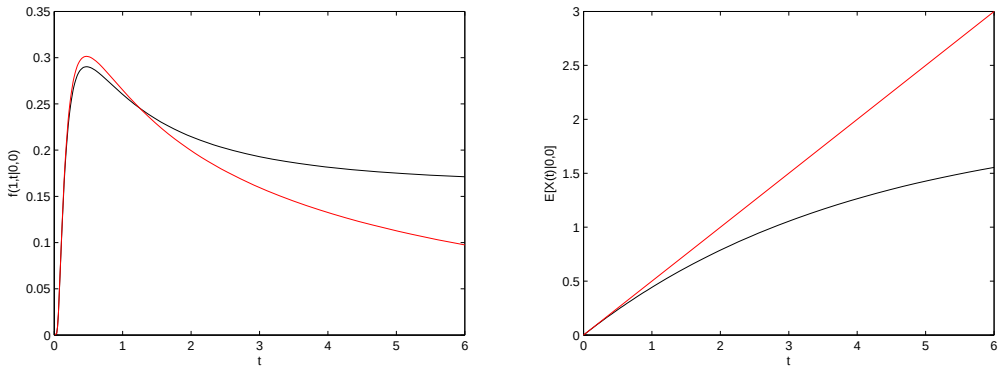

Figure 1.6: On the left the pdf's $f(1,t|0,0)$ (black line) and $\tilde{f}_0(1,t|0,0)$ (red line) for $\rho_k = 0$ $(k = 0,1,\ldots)$ and exponentially distributed inter-jumps with mean 4. Each $X_k(t)$ is a Wiener diffusion process with drift $A_1 = \mu$ and infinitesimal variance $A_2 = \sigma^2$, where $\mu = 0.5$ and $\sigma^2 = 2$. On the right the mean $E[X(t)|0,0]$ (black line) and $E[\tilde{X}_0(t)|0,0]$ (red line) are plotted for the same choices of the left side.

Chapter 2

A Gompertz model with jumps for an intermittent treatment in cancer growth

Tumor is one of the main causes of death in the modern society so, in least decades, a lot of attempts have been made to describe the tumor dynamic. From the mathematical point of view, the studies in this direction have also affected the construction and the analysis of some models aimed at predicting the evolution of the disease under particular conditions or under the influence of specific therapies. Most of these models are based on the assumption that the growth curve is exponential type (see, for instance, [36] for historical development of tumor growth laws). These models describe the increase of the tumor size over time via differential equations. Since the exponential curve seems unable to explain tumor growth in the longer term, different models have been formulated for describing the tumor dynamic. More accurate models are characterized by the presence of an inflection point. This point determines a sigmoidal shape whose limit value, called *carrying capacity*, is imposed by some environmental limitation such as nutrients. In particular, the law of Gompertz plays an important role in the dynamic of solid tumor because in several contexts it seems to fit experimental data in a reasonable precise way (cf., for example, [66] and [86]). Specifically, the Gompertz equation has proven to be a useful tool to describe human cancer evolution. For example, in [17], [49], [69], [79], [80], Gomperztian model of breast cancer growth have been formulated and analyzed. In [64] the problem of optimal chemotherapy is considered based on the Gompertz cancer model. In [65] fourteen deterministic mathematical models have been studied to describe the tumor growth in vivo. In that context, the authors show how the Gompertz model best fits data from colon carcinoma. The Gompertz law has been also used to describe the interaction between the cancer and the immunological system. In

this direction, in [5], [23], [24], models that include the principal characteristics of the T-cell-metiated reaction against cancer was proposed. Moreover, in [54] it has been considered also the dynamics between proliferating and quiescent cells that form the tumor mass.

However, often some discrepancies exist between clinical data and theoretical predictions, due to more or less intense environmental fluctuations depending on various factors that are not measurable or are not known. So, to take into consideration such environmental fluctuations, generally associated with the dynamics of real systems, the notion of growth in random environment has been formulated. Various contributions which follow the stochastic approach are present in literature. In [61] and [62], the proposed models take account of both cell fission and mortality. In [1] the growth of tumor size under the effect of therapies that modify the growth rates of the phenomenon has been studied. In [4] a stochastic Gompertz model is used to describe the evolution of a solid tumor treated with a time-dependent therapy able to modify the birth rate of the cancer cells. Since then, various other models have been formulated to include interesting parameters of the phenomenon. Specifically, in [6] the interactions between proliferating and quiescent cells have been analyzed under the effect of two kinds of therapies: non-specific cycle drugs (that can damage tumor cells in any phase of the cellular cycle) and specific cycle drugs (that act on tumor cells only in a fixed phase of their cycle). In [9], the authors have studied the growth of tumor size under the effect of anti-proliferative and/or pro-apoptotic therapies that modify both growth rates of the phenomenon.

Recently, some models have been proposed to describe the tumor dynamic under the effect of therapies that reduce an intrinsic factor of the tumor worsening at predefined levels. In particular, in [50] and [83] models of prostate tumor growth under intermittent hormone therapy have been studied. The models are categorized into a hybrid dynamical system because switching between on-treatment and off-treatment intervals are considered in addition to continuous dynamics of tumor growth.

In the following we consider the tumor size as the intrinsic factor to control.

In order to describe the effect of a therapeutic program that produces an intermittent suppression of the intrinsic factor, we consider a Gompertz process with jumps. Each jump represents the effect of a therapeutic application and it shifts the process to a certain return value which, in general, we can assume random.
We consider a process with jumps $X(t)$ such that in the k-th inter-jump interval is defined by a Gompertz diffusion process $\tilde{X}_k(t)$. In this context the process $X(t)$ consists of recurring cycles whose durations are described by random variables which

represent the time elapsing between successive applications of the therapy.
In the following, we construct $X(t)$ and we perform a particular case for which $\tilde{X}_k(t) \equiv \tilde{X}(t)$, $I_{k+1} \equiv I$, $\rho_{k+1} = \rho$ (for all $k \geq 0$) and we study the transition pdf, the average state of the system (representing the mean size of the tumor) and the number of therapeutic applications to be carried out in time intervals of fixed amplitude. In particular, we consider two probability distributions for the inter-jump intervals and for each of these we consider three distributions for the random variable describing the return point. Note that we consider ρ as a random point because we want to take into account that the therapy would not be precise.
After this firs step, we introduce a more realistic model. Specifically:

- the therapeutic program has a deterministic scheduling, so that jumps occur in fixed and conveniently chosen time instants;
- the return points ρ_1, $\rho_2, \ldots$ are deterministic; we consider only deterministic points because we will show that in this case there is not a loss of generality;
- when a therapy is applied there is a selection event in which only the most aggressive clones survive; for example, this perspective could be applied to targeted drugs that have a much lower toxicity for the patient.

The obtained process $X(t)$ is composed of independent cycles that can be of variable deterministic durations if the inter-jump intervals are not constant; moreover, after each jump, the process starts with a gradually increased growth rate, depending on the number of applications made. Hence, each therapeutic application involves a reduction of the tumor mass, but it also implies an increase of the growth speed. This raises the problem of finding a compromise between these two aspects. We analyze the deterministic and the stochastic process with jumps and we propose two possible schedulings to control the cancer growth.
In Scheduling 1 we assume that inter-jump intervals have equal size. This study could be useful when one is forced to apply the therapy at equidistant times. In this case, we show interesting properties which are useful for the choice of the most appropriate application times, fixed the toxicity of the therapy.
In Scheduling 2 we suggest to apply the therapy just before the cancer mass reaches the control threshold and we provide information on how to choose the application times so that the cancer size remains bounded during the treatment.
Finally, we compare the deterministic and the stochastic approaches, and we provide a comparison between the two proposed scheduling.

2.1 The Gompertz model

The deterministic model of tumor growth is based on the Gompertz growth model. The Gompertz curve is the function $\tilde{x}(t)$ solution of

$$\frac{d\tilde{x}}{dt} = \alpha\tilde{x} - \beta\tilde{x}\log\tilde{x}, \tag{2.1}$$

with the initial condition

$$\tilde{x}(0) = \rho_0. \tag{2.2}$$

In this context, $\tilde{x}(t)$ represents the cancer size at time t and $\rho_0 > 0$ expresses the size at the initial time, considering 0 as the moment in which the disease was diagnosed. We suppose that $\tilde{x}(t)$ is a continuous and differentiable function. Parameters α and β, representing the growth and decrease rate respectively, are used as controller parameters and they are measured in the inverse of the unit time chosen; they depend on the evolution of different types of cancer.

Let $\tilde{x}_k(t)$ the Gompertz curve with $\alpha = \alpha_k$ and $\beta = \beta_k$ for $k \geq 0$; it is solution of (2.1) with the initial condition $\tilde{x}_k(0) = \rho_k$, that is, the Gompertz curve $\tilde{x}_k(t)$ is given by:

$$\tilde{x}_k(t) = \exp\left\{\frac{\alpha_k}{\beta_k} + \left(\ln\rho_k - \frac{\alpha_k}{\beta_k}\right)e^{-\beta_k t}\right\}. \tag{2.3}$$

The function (2.3) is a sigmoidal curve and it is limited by the environmental capacity given by

$$C_k = \lim_{t\to+\infty}\tilde{x}_k(t) = e^{\frac{\alpha_k}{\beta_k}}, \tag{2.4}$$

which represents the maximum tumor density that an organism can tolerate. The Gompertz curve (2.3) is a growing curve in $\left[0, e^{\frac{\alpha_k}{\beta_k}}\right)$, it has upwards concavity up to the inflection point f such that $\tilde{x}_k(f) = e^{\frac{\alpha_k}{\beta_k}-1}$, then the function continues to grow with downwards concavity; in our context, f is the point where the tumor mass reaches the maximum growth speed. Moreover, the Gompertz law has an exponential trend around the origin: this is in agreement with the studies of tumor growth which shows that for small tumor sizes the growth velocity is such as to not make the immune system effectively, and this means that the tumor, initially, grows faster.

As already mentioned, there is often a discrepancy between the clinical data and the theoretical predictions, this is due to more or less intense environmental fluctuations, as happens for all biological systems. Ignoring these oscillations may lead to wrong predictions which, in many cases, cause inadequate therapy. Then, we consider the growth in random environment following a standard procedure (cf., for example, [67] and [73]), starting from equation (2.1).

For $\tau > 0$, equation

$$\tilde{x}_{(n+1)\tau} - \tilde{x}_{n\tau} = (\alpha\tau - \beta\tau \log \tilde{x}_{n\tau})\tilde{x}_{n\tau}, \quad n = 0, 1, 2, \ldots \tag{2.5}$$

approximates (2.1) and (2.2) holds for $n = 0$.
Now we make an assumption about the randomness of the environment. Suppose that in $[n\tau, (n+1)\tau)$ $(n = 0, 1, \ldots)$ the intrinsic variation of the population size is the average value of a sequence of independent and identically distributed Bernoulli random variables $Z_0, Z_\tau, Z_{2\tau}, \ldots$ characterized by the following probability distribution

$$\begin{array}{l} P\left(Z_{n\tau} = \sigma\sqrt{\tau}\right) = \frac{1}{2} + \frac{a\sqrt{\tau}}{2\sigma}, \;\; n = 0, 1, \ldots \\ P\left(Z_{n\tau} = -\sigma\sqrt{\tau}\right) = \frac{1}{2} - \frac{a\sqrt{\tau}}{2\sigma}, \;\; n = 0, 1, \ldots \end{array} \tag{2.6}$$

where $\sigma > 0$ is a constant, measuring the width of environment fluctuations.
The mean and higher moments of $Z_{n\tau}$ are:

$$E\left(Z_{n\tau}\right) = \alpha\tau, \quad E\left(Z_{n\tau}^2\right) = \sigma^2\tau, \quad E\left(Z_{n\tau}^{2+k}\right) = o(\tau), \; k = 1, 2, ...$$

Taking into consideration (2.6), equation (2.5) in a random environment is

$$\tilde{X}_{(n+1)\tau} - \tilde{X}_{n\tau} = \left(\alpha\tau - \beta\tau \log \tilde{X}_{n\tau}\right) \tilde{X}_{n\tau}, \; n = 0, 1, 2, ... \tag{2.7}$$

where $\tilde{X}_{n\tau}$ is a stochastic process.
The initial condition implies that the population size at the initial instant $t_0 = 0$ must be ρ_0, that is $P\left(\tilde{X}_0 = \rho_0\right) = 1$. It is not difficult to prove that the moments of the increment process $\tilde{X}_{(n+1)\tau} - \tilde{X}_{n\tau}$ conditional upon $\tilde{X}_{n\tau} = x$ are:

$$E\left[\tilde{X}_{(n+1)\tau} - \tilde{X}_{n\tau} | \tilde{X}_{n\tau} = x\right] = (\alpha - \beta \log x)x\tau,$$

$$E\left[\left(\tilde{X}_{(n+1)\tau} - \tilde{X}_{n\tau}\right)^2 | \tilde{X}_{n\tau} = x\right] = \sigma^2 x^2 \tau + o(\tau),$$

$$E\left[\left(\tilde{X}_{(n+1)\tau} - \tilde{X}_{n\tau}\right)^{2+k} | \tilde{X}_{n\tau} = x\right] = o(\tau), \; (k = 1, 2, \ldots).$$

Dividing both members by τ and taking the limit as τ goes to zero, from (2.7) one has that $\tilde{X}_{n\tau}$ converges to a time homogeneous stochastic diffusion process $\tilde{X}(t)$ with drift and infinitesimal variance

$$\begin{array}{l} A_1(x) = ax + \beta x \log x, \\ A_2(x) = \sigma^2 x^2, \end{array}$$

respectively. The diffusion interval is $J \equiv (0, +\infty)$, whose boundaries are natural, non-attracting and non-attainable.

Let $\tilde{X}_k(t)$ $(k \geq 0)$ the Gompertz process characterized by drift and infinitesimal variance

$$A_1^{(k)}(x) = (\alpha_k - \beta_k \ln x)x, \qquad A_2^{(k)}(x) = \sigma_k^2 x^2, \tag{2.8}$$

respectively and diffusion interval $J_k \equiv (0, +\infty)$. It is also described by the following stochastic differential equation

$$d\tilde{X}_k(t) = [\alpha_k - \beta_k \log \tilde{X}_k(t)]\, \tilde{X}_k(t)\, dt + \sigma_k\, \tilde{X}_k(t)\, dB(t)$$

where $B(t)$ is a standard Wiener process. Some sample paths of the processes $\tilde{X}_k(t)$ are plotted in Figure 2.1 for $k = 0, 1, \ldots, 5$, from the bottom to the top. Parameters are $\rho_0 = 0.1$, $\sigma_k = \sigma = 0.01$ for both the figures, while on the left $\beta_k = \beta = 0.3$, $\alpha_k = 4.5 + 0.1k$ and on the right $\alpha_k = \alpha = 5$, $\beta_k = 1 - 0.1k$. Of course, for increasing values of α the sample paths are higher, while for increasing values of β the sample paths decrease.

Because the boundaries are natural, the initial condition $P(\tilde{X}_k(\tau_k) = \rho_k)$ leads

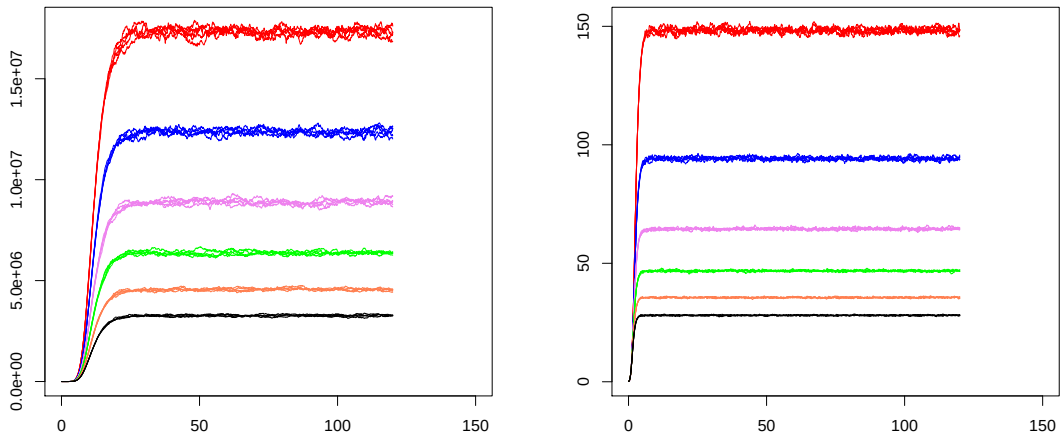

Figure 2.1: Some sample paths of the processes $\tilde{X}_k(t)$, from the bottom to the top, are plotted for $k = 0, 1, \ldots, 5$. Parameters are $\rho_0 = 0.1$, $\sigma_k = \sigma = 0.01$ for both the figures, while on the left $\beta_k = \beta = 0.3$, $\alpha_k = 4.5 + 0.1k$ and on the right $\alpha_k = \alpha = 5$, $\beta_k = 1.5 - 0.1k$.

to the unique solution of the Fokker-Planck equation (the first expression of (1.3)), which describes the pdf of the process. Note that the study of $\tilde{X}_k(t)$ can be performed via an Ornstein-Uhlenbeck process, with transformation coordinates $z =$

$\log x$, $z_0 = \log \rho_0$ (cf. for example [4]). Hence, the process $\tilde{X}_k(t)$ is characterized by the lognormal transition pdf:

$$\tilde{f}_k(x,t|\rho_k,\tau_k) = \frac{1}{x\sqrt{2\pi V_k^2(t|\tau_k)}} \exp\left\{-\frac{[\ln x - M_k(t|\ln\rho_k,\tau_k)]^2}{2V_k^2(t|\tau_k)}\right\}, \tag{2.9}$$

where

$$\begin{cases} M_k(t|y,\tau) = y\, e^{-\beta_k(t-\tau)} - \frac{\sigma_k^2/2-\alpha_k}{\beta_k}(1-e^{-\beta_k(t-\tau)}) \\ \\ V_k^2(t|\tau) = \frac{\sigma_k^2}{2\beta_k}\left(1-e^{-2\beta_k(t-\tau)}\right), \end{cases} \tag{2.10}$$

whereas, the moments are given by

$$\tilde{\mu}_k^{(n)}(t|\rho_k,\tau_k) = \exp\left\{nM_k(t|\ln\rho_k,\tau_k) + \frac{n^2}{2}V_k^2(t|\tau_k)\right\}. \tag{2.11}$$

Since $\tilde{X}_k(t)$ is a time homogeneous process, one has $\tilde{f}_k(x,t|\rho_k,\tau_k) = \tilde{f}_k(x,t-\tau_k|\rho_k)$, $\tilde{\mu}_k^{(n)}(t|\rho_k,\tau_k) = \tilde{\mu}_k^{(n)}(t-\tau_k|\rho_k)$, $M_k(t|y,\tau) = M_k(t-\tau|y)$ and $V_k^2(t|\tau) = V_k^2(t-\tau)$. Moreover, the process always admits the steady-state lognormal density:

$$\tilde{w}_k(x) = \sqrt{\frac{\beta_k}{\sigma_k^2\pi}}\frac{1}{x}\exp\left\{-\left[\sqrt{\frac{\beta_k}{\sigma_k^2}}\log x - \frac{1}{2}\sqrt{\frac{\sigma_k^2}{\beta_k}}\left(\frac{2\alpha_k}{\sigma_k^2}-1\right)\right]^2\right\}.$$

Now we remark some aspects regarding the FPT of $\tilde{X}_k(t)$ through a constant boundary S. Let

$$\tilde{T}_{\rho_k}^k(\tau) = \inf\{t \geq \tau : \tilde{X}_k(t) > S\}, \qquad \tilde{X}_k(\tau) = \rho_k < S$$

be the random variable FPT of $\tilde{X}_k(t)$ through the threshold S and let $\tilde{g}_k(S,t|\rho_k,\tau)$ be its pdf. For $S > \rho_k$, we recall that the density $\tilde{g}_k$ is solution of the following second kind Volterra integral equation (cf., for example, [15] and [38])

$$\tilde{g}_k(S,t|\rho,\tau) = -2\Psi_k(S,t|\rho,\tau) + 2\int_\tau^t \tilde{g}_k(S,u|\rho,\tau)\Psi_k(S,t|S,u)\,du, \tag{2.12}$$

where

$$\begin{aligned} \Psi_k(S,t|z,u) &= -\frac{S}{2}\left[\left(\alpha_k - \beta_k\ln S - \frac{3\sigma_k^2}{2}\right)\tilde{f}_k(S,t|z,u)\right. \\ &\qquad \left. -\sigma_k^2 S\frac{\partial\tilde{f}_k(x,t|z,u)}{\partial x}\Big|_{x=S}\right]. \end{aligned} \tag{2.13}$$

Note that $\tilde{T}_\rho^k(\tau) = \tau + \tilde{T}_\rho^k(t_0)$, where $\tilde{T}_\rho^k(t_0)$ is the FPT of the process $\tilde{X}_k(t)$ translated

to the initial time t_0. Therefore, one has

$$E[\tilde{T}_\rho^k(\tau)] = \tau + E[\tilde{T}_\rho^k(t_0)].$$

Moreover, following [74], we can prove that $\tilde{T}_\rho^k(t_0)$ is an honest random variable and its mean can be evaluate by means of

$$E[\tilde{T}_\rho^k(t_0)] = \int_\rho^S dz\, h_k(z) \int_{t_0}^z du\, s_k(u), \tag{2.14}$$

where

$$h_k(x) = x^{-2\alpha_k/\sigma_k^2} \exp\Big\{\frac{\beta_k}{\sigma_k^2} \ln^2 x\Big\}, \qquad s_k(x) = \frac{2}{A_2^{(k)}(x) h_k(x)},$$

are the scale function and speed density of $\tilde{X}_k(t)$, respectively.
Moreover, we recall that the function $\tilde{g}_k(S, t|\rho, \tau)$ can be approximated with the function $\check{g}_k(S, t|\rho, \tau)$ via the following numerical algorithm (cf. [15] and [38]):

$$\begin{aligned}
&\check{g}_k(S, \tau + h|\rho, \tau) = -2\Psi_k(S, \tau + h|\rho, \tau) \\
&\check{g}_k(S, \tau + i\,h|\rho, \tau) = -2\Psi_k(S, \tau + i\,h|\rho, \tau) \\
&\quad +2h \sum_{r=1}^{i-1} \check{g}_k(S, \tau + r\,h|\rho, \tau)\Psi_k(S, \tau + i\,h|S, \tau + r\,h) \quad (i = 2, 3, \ldots)
\end{aligned} \tag{2.15}$$

where h represents the integration step and Ψ_k is given in (2.13).

2.2 The Gompertz model with jumps

In order to analyze the effect of a therapeutic program that provides intermittent suppression of cancer cells, we suppose that the growth process is influenced by jumps, producing instantaneous changes of the system state. We define the process with jumps $X(t)$ as showed in the first chapter. More precisely, $X(t)$, starting from $X(t_0) = \tilde{X}_0(t_0) = \rho_0$, evolves as $\tilde{X}_0(t)$ as long as a jump occurs shifting the process in a state $\rho_1 > 0$ randomly chosen according to the pdf $\phi_1(x)$; from here, after a random time interval, $X(t)$ evolves with the same dynamics of $\tilde{X}_1(t)$ as long as another jump occurs, representing a new application of the therapy, which leads $X(t)$ in ρ_2, and so on. The process $X(t)$ consists of recurring cycles $\mathcal{I}_1, \mathcal{I}_2, \ldots$ whose duration are described by independent and identically distributed random variables $I_1, I_2, \ldots$, described by pdf's $\psi_1(\cdot), \psi_2(\cdot), \ldots$, which represent the time intervals between successive applications of the therapy. Moreover, we denote by $\Theta_1, \Theta_2, \ldots$ the times in which jumps occur.
The transition pdf $f(x, t|\rho_0, t_0)$ of $X(t)$ is given in (1.23), and the expression of the

moments $\mu^{(n)}(t|y,\tau)$ follows from (1.24).

In the following we give a simple example of $X(t)$ focusing on the moments of the process.

2.2.1 A special case

We assume that $t_0 = 0$, $\tilde{X}_k \equiv \tilde{X}$ ($\alpha_k = \alpha$, $\beta_k = \beta$, $\sigma_k = \sigma$), $I_{k+1} \equiv I$ (ψ is the pdf of I) and $\rho_{k+1} \equiv \rho$ (ϕ is the pdf of ρ) for $k \geq 0$. In this case, the expression of moments $\mu^{(n)}(t|y,\tau)$, from (1.24), is:

$$\mu^{(n)}(t|\rho) = \left(1 - \int_0^t \psi(s)\, ds\right) \tilde{\mu}^{(n)}(t|\rho) + \sum_{i=1}^{\infty} \int_0^t \xi_i(\tau) \left(1 - \int_0^{t-\tau} \psi(s) ds\right) \left(\int_{z\in J} \phi(z)\, \tilde{\mu}^{(n)}(x, t-\tau|z)\, dz\right) d\tau,$$

where $\tilde{\mu}^{(n)}$ are the moments of $\tilde{X}(t)$ and they are defined in (2.11).
In the following we consider two kinds of intermittent therapeutic treatments defined in terms of the pdf's characterizing the random variables I. In particular, we assume that the function ψ is a degenerate pdf (constant intermittence) and an exponential pdf (exponential intermittence). Furthermore, for all specified ψ, we assume three pdf's for the random variable ρ: degenerate, uniform and bounded bi-exponential. In the first case we suppose that the therapy is so precise that the process jumps exactly in the chosen point; otherwise the therapy shifts the cancer mass in an interval with central point ρ without any preferences (uniform distribution) or favoring the central points of the interval (bounded bi-exponential distribution).
Moreover, we consider the stochastic process N_t representing the number of therapeutic treatments to be applied until a fixed time t.

Therapeutic treatment with constant intermittence

We assume that the duration between two consecutive therapeutic treatments is $1/\xi$, ($\xi > 0$), so that I is described by the degenerate pdf $\psi(t) = \delta\left(t - \frac{1}{\xi}\right)$, where $\delta(\cdot)$ is the Dirac delta-function; $\Theta_k = k/\xi$ almost surely. Let N_t the number of treatments to be applied until the time t, one has that

$$N_t = \sum_{k=1}^{\infty} H\left(t - \frac{k}{\xi}\right),$$

where $H(x)$ denotes the Heaviside unit step function. Note that the last jump before t occurs at N_t/ξ.

The moments of $X(t)$ can be obtained as the moments (1.27), but with a random return point:

$$\mu^{(n)}(t|\rho_0) = \begin{cases} \tilde{\mu}^{(n)}(t|\rho_0), & t < 1/\xi \\ \\ \int_0^\infty \phi(z)\tilde{\mu}^{(n)}\left(t - \frac{N_t}{\xi}|z\right) dz, & t > 1/\xi. \end{cases}$$

where $\tilde{\mu}^{(n)}(t|y)$ is defined in (2.11).

Case a): $\phi(z)$ degenerate
We suppose that $\phi(z) = \delta(z - \rho)$ is a degenerate distribution in ρ. In this case the moments of $X(t)$ are:

$$\mu^{(n)}(t|\rho_0) = \begin{cases} \tilde{\mu}^{(n)}(t|\rho_0), & t < 1/\xi \\ \\ \tilde{\mu}^{(n)}\left(t - \frac{N_t}{\xi}|\rho\right), & t > 1/\xi. \end{cases}$$

Case b): $\phi(z)$ uniform
We consider $\phi(z) = \frac{1}{2l}$ for $z \in [\rho - l,\, \rho + l]$. In this case we have:

$$\mu^{(n)}(t|\rho_0) = \begin{cases} \tilde{\mu}^{(n)}(t|\rho_0), & t < 1/\xi \\ \\ \frac{1}{2l}\int_{\rho-l}^{\rho+l} \tilde{\mu}^{(n)}\left(t - \frac{N_t}{\xi}|z\right) dz, & t > 1/\xi. \end{cases}$$

Taking into consideration the expressions of M_k and V_k^2 given in (2.10), the explicit form of the involved integral is:

$$\begin{aligned} \int_{\rho-l}^{\rho+l} \tilde{\mu}^{(n)}\left(t - \frac{N_t}{\xi}|z\right) dz = \\ = \exp\left\{\frac{n^2}{2}\sigma^2(1 - e^{-2\beta(t-k/\xi)}) - n\frac{\sigma^2/2 - \alpha}{\beta}\left(1 - e^{-\beta(t-k|\xi)}\right)\right\} \\ \times \int_{\rho-l}^{\rho+l} n \exp\left\{e^{-\beta(t-k/\xi)} \log z\right\} dz, \end{aligned}$$

where,

$$\begin{aligned} \int_{\rho-l}^{\rho+l} \exp\left\{e^{-\beta(t-k/\xi)} \log z\right\} dz &= \int_{\log(\rho-l)}^{\log(\rho+l)} \exp\left\{u\left(ne^{-\beta(t-k/\xi)} + 1\right)\right\} du \\ &= \frac{1}{n\left(e^{-\beta(t-k/\xi)} + 1\right)}\left[\exp\left\{\left(ne^{-\beta(t-k/\xi)} + 1\right)\log(\rho + l)\right\}\right. \end{aligned}$$

$$- \exp\left\{\left(ne^{-\beta(t-k/\xi)}+1\right)\log(\rho-l)\right\}\Big].$$

Hence, one has:

$$\mu^{(n)}(t|\rho_0)$$
$$= \begin{cases} \tilde{\mu}^{(n)}(t|\rho_0), & t < 1/\xi \\ \\ \frac{1}{2l}\exp\left\{\frac{n^2}{2}\sigma^2(1-e^{-2\beta(t-k/\xi)}) - n\frac{\sigma^2/2-\alpha}{\beta}(1-e^{-\beta(t-k/\xi)})\right\} & \\ \\ \times\frac{1}{n(e^{-\beta(t-k/\xi)}+1)}\left[(\rho+l)^{ne^{-\beta(t-k/\xi)}+1} - (\rho-l)^{ne^{-\beta(t-k/\xi)}+1}\right], & t > 1/\xi \end{cases}$$

Case c): $\phi(z)$ bounded bi-exponential
We suppose $\phi(\cdot)$ a bounded bi-exponential distribution in $[\rho-l,\ \rho+l]$ with parameter λ, that is $\phi(z) = \frac{1}{2(1-e^{\lambda l})}e^{-\lambda|z-\rho|}$ for $z \in (\rho-l,\ \rho+l)$. The moments of $X(t)$ result:

$$\mu^{(n)}(t|\rho_0) = \begin{cases} \tilde{\mu}^{(n)}(t|\rho_0), & t < 1/\xi \\ \\ \frac{1}{2(1-e^{\lambda l})}\int_{\rho-l}^{\rho+l} e^{-\lambda|z-\rho|}\tilde{\mu}^{(n)}\left(t-\frac{N(t)}{\xi}|z\right)dz, & t > 1/\xi. \end{cases}$$

Therapeutic treatment with exponential intermittence

We assume that I is described by the exponential pdf $\psi(x) = \xi e^{-\xi x}$, for $x > 0$. In this case, N_t is a Poisson process of parameter ξ.
The expression of moments of $X(t)$ are given in (1.29), but with a random return point:

$$\mu^{(n)}(t|\rho_0) = e^{-\xi t}\tilde{\mu}^{(n)}(t|\rho_0) + \xi\int_0^t e^{-\xi(t-\tau)}\left(\int_0^\infty \phi(z)\tilde{\mu}^{(n)}(t-\tau|z)dz\right)d\tau.$$

Case a): $\phi(z)$ degenerate
The moments of $X(t)$ are given by

$$\mu^{(n)}(t|\rho_0) = e^{-\xi t}\tilde{\mu}^{(n)}(t|\rho_0) + \xi\int_0^t e^{-\xi(t-\tau)}\tilde{\mu}^{(n)}(t-\tau|\rho)d\tau.$$

Case b): $\phi(z)$ uniform
For $\phi(z) = \frac{1}{2l}$ for $z \in [\rho-l,\ \rho+l]$ one has:

$$\mu^{(n)}(t|\rho_0) = e^{-\xi t}\tilde{\mu}^{(n)}(t|\rho_0) + \frac{\xi}{2l}\int_0^t d\tau e^{-\xi(t-\tau)}\int_{\rho-l}^{\rho+l}\tilde{\mu}^{(n)}(t-\tau|z)\phi(z)dz.$$

Case c): $\phi(z)$ bounded bi-exponential
We assume that $\phi(z) = \frac{1}{2(1-e^{\lambda l})} e^{-\lambda|z-\rho|}$ for $z \in (\rho - l,\, \rho + l)$. In this case

$$\mu^{(n)}(t|\rho_0) \;=\; e^{-\xi t}\tilde{\mu}^{(n)}(t|\rho_0) + \frac{\lambda\xi}{2(1-e^{\lambda l})} \int_0^t d\tau e^{-\xi(t-\tau)} \int_{\rho-l}^{\rho+l} e^{-\lambda|z-\rho|}\tilde{\mu}^{(n)}(t-\tau|z)\phi(z)dz.$$

Numerical results

We compare the means of the process $X(t)$ in correspondence to two therapeutic protocols for three considered return point distributions. In Figure 2.2 the means of $X(t)$ are shown for $\alpha = 1,\ \beta = 0.5,\ \sigma = 1,\ \rho_0 = 0.1$ and $\rho = 0.5$ in correspondence to deterministic (on the left) and exponential (on the right) protocol. For both therapeutic treatments three different return point distributions are compared: degenerate pdf (blue curve), uniform pdf with $l = 0.4$ (red curve) and bi-exponential pdf for $l = 0.4$ and $\lambda = 1$ (magenta curve). Note that, although the red and magenta curves are below the blue curve, they are comparable, so we can study only the degenerate case without loss of generality (since this happens also for other choices of parameters).

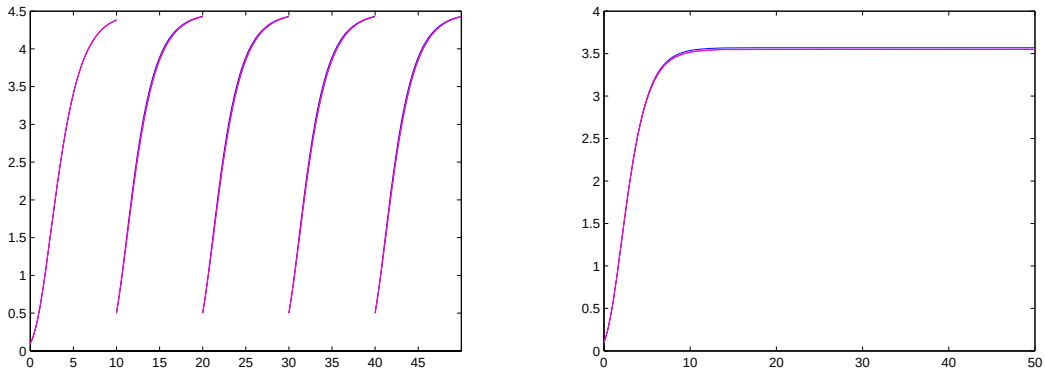

Figure 2.2: The means of $X(t)$ are shown for $\alpha = 1,\ \beta = 0.5,\ \sigma = 1,\ \rho_0 = 0.1$ and $\rho = 0.5,\ \xi = 0.1$ in correspondence to a constant (on the left) and exponential (on the right) therapeutic protocols for the three different return distributions: degenerate (blue curve), uniform (red curve) and bi-exponential (magenta curve) for $l = 0.4$ and $\lambda = 1$.

Figures 2.3-2.6 show the mean of $X(t)$ for the constant (on the left) and exponential (on the right) intermittence in correspondence to degenerate distribution for $\alpha = 1,\ \beta = 0.5, \sigma = 1,\ \rho_0 = 0.1$ and $\rho = 0.5$ and $1/\xi = 10, 5, 4, 3$, respectively. The green line represents the carrying capacity $C = C_k = \exp\{\alpha/\beta\}$, given in (2.4), of

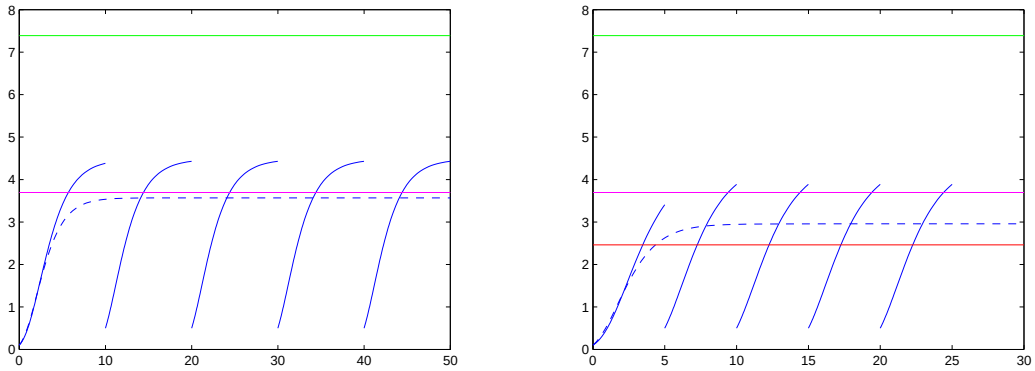

Figure 2.3: The means of $X(t)$ are shown for $\alpha = 1,\ \beta = 0.5, \sigma = 1,\ \rho_0 = 0.1$ and $\rho = 0.5$ in correspondence to a constant (on the left) and exponential (on the right) therapeutic protocols with $1/\xi = 10$ for degenerate return process.

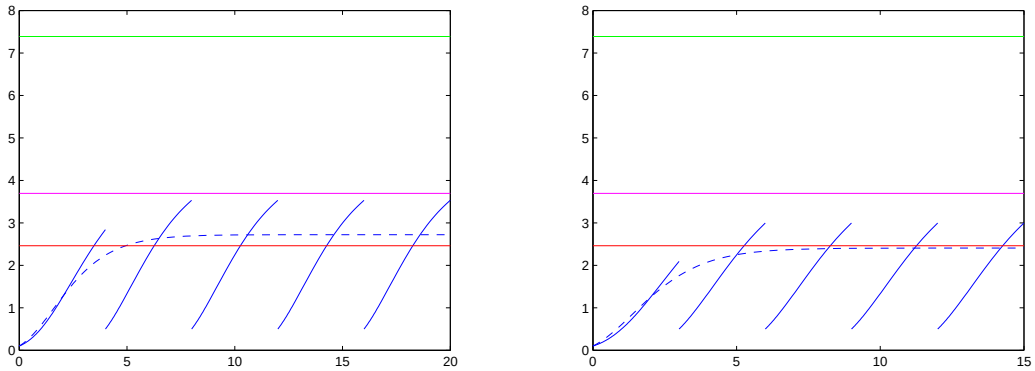

Figure 2.4: As in Figure 2.3 with $1/\xi = 5$.

the deterministic Gompertz curve $\tilde{x}_k(t)$, given in (2.3). In all cases we note that the mean of the process for the exponential distribution is less than the mean for the constant case. In particular, for $1/\xi = 10$ (cf. Figure 2.3), only for the exponential treatment the tumor size is kept under the level $C/2$. It is understandable because in the exponential case the probability of occurrence of more than one jump before of the time 10 is non-zero, while in the constant case it is equal to zero. The mean of the jump process decreases by reducing the frequency of treatments, however the better results are obtained for the exponential intermittences. In particular for $1/\xi = 3$ (cf. Figure 2.6) the exponential treatment reduces the tumor size below $C/3$.

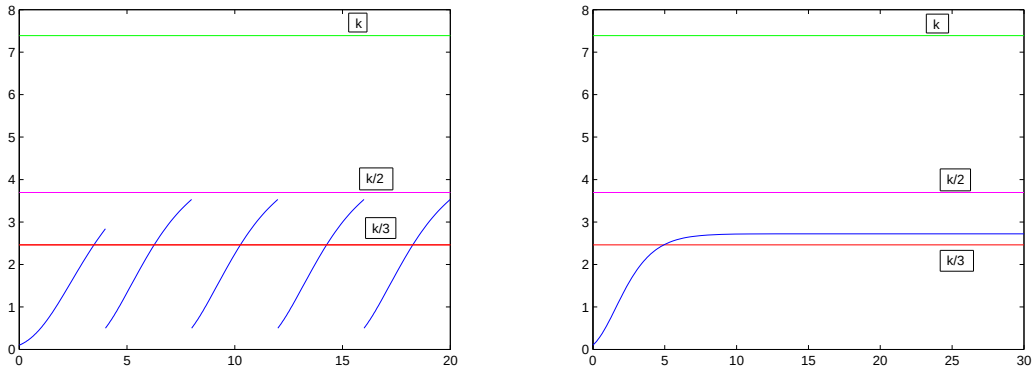

Figure 2.5: As in Figure 2.3 with $1/\xi = 4$.

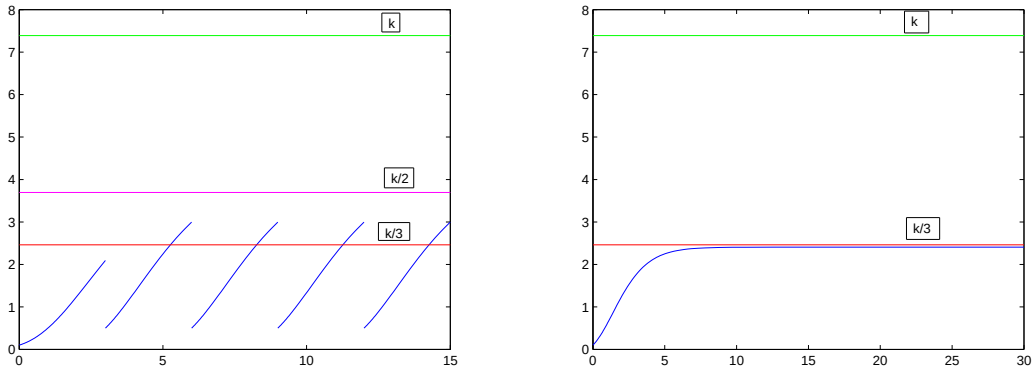

Figure 2.6: As in Figure 2.3 with $1/\xi = 3$.

2.3 The model with combined effects: reduction of tumor size and rise of growth rate

We want to take into account other effects that a therapy can cause. Firstly, therapeutic treatments weaken an ill organism. Moreover, when a therapy is applied, there is a selection event in which only the most aggressive clones survive. Hence, we assume that after a therapeutic application, the tumor size returns to a fixed value from which the evolution starts with an increased growth rate. For example, this perspective could be applied to targeted drugs that have a much lower toxicity for the patient.

Specifically, we assume that, after each jump, the process starts with a gradually increased growth rate, depending on the number of applications made. Hence, each therapeutic application involves a reduction in the tumor mass, but it also implies

an increase in the speed of growth. This raises the problem of finding a compromise between these two aspects.

We suppose that the therapeutic program consists of N therapeutic applications and the return state ρ is equal to the initial tumor mass. We denote by ζ_1 the time interval between the initial time and the first jump, ζ_k the amplitude of the k-th inter-jump interval ($2 \leq k \leq N$), $\tau_k = \zeta_1 + \zeta_2 + \ldots + \zeta_k$ ($1 \leq k \leq N$) the time instant in which the k-th jump occurs.

Let $x(t)$ $[X(t)]$ be the deterministic [stochastic] process describing the tumor size at the time t. Then, $x(t)$ $[X(t)]$ consists of independent cycles, each of one is described by the Gompertz law with different growth rates. In particular, starting from $\rho > 0$ at the time $t_0 = 0$, the process evolves according to the Gompertz law with parameters $\alpha_0 = \alpha$ and β, where $\alpha > 0$ and $\beta > 0$ are the natural growth parameters of the tumor cells in the absence of therapies. After a time ζ_1 a therapy is applied, whose effect is to reduce the tumor size to ρ_1 on one hand, and on the other hand to increase the growth rate. Thus proceeding, after the k-th application occurring at τ_k, the process evolves from the state ρ_k following the Gompertz law with growth parameter $\alpha_k > \alpha_{k-1}$, while parameter β remains the same of before.

The effectiveness of an intermittent treatment depends on the amplitude of the inter-jump intervals; of course the choice of ζ_k must comply with both the times that medical needs. Denoting by S a control threshold, we require that $x(t)[X(t)] < \mathrm{S}$ during the treatment. Hence, in the following we propose two possible therapeutic schedulings: inter-jump intervals with constant size and inter-jump intervals determined such that the therapy is applied just before the threshold's crossing of the process.

2.3.1 The deterministic model

Generally, assuming that the therapy is applied N times, the cancer size at time t can be described as follows:

$$x(t) = \sum_{k=0}^{N} \tilde{x}_k(t) \mathbf{1}_{[\tau_k, \tau_{k+1})}(t), \tag{2.16}$$

with $x(\tau_k^-) = \tilde{x}_{k-1}(\tau_k)$, $x(\tau_k) = \rho_k$, $\tau_0 = 0$, $\tau_{N+1} = \infty$, where $\tilde{x}_k(t)$ is given in (2.3) and its carrying capacity C_k is defined in (2.4). Note that, if $\rho < C_k$, $\tilde{x}_k(t)$ increases until C_k, being this value an upper bound, else $\tilde{x}_k(t)$ decrease until C_k. Here, we consider the case $\rho < C_k$.

2.3.2 The stochastic model

The corresponding stochastic process $X(t)$ of the deterministic one (2.16) is defined by:

$$X(t) = \sum_{k=0}^{N} \tilde{X}_k(t) \mathbf{1}_{[\tau_k, \tau_{k+1})}(t), \tag{2.17}$$

where $\tilde{X}_k(t)$ is characterized by drift and infinitesimal variance given in (2.8). The transition pdf of $\tilde{X}_k(t)$ and its moments are defined in (2.9) and (2.11) respectively. In order to show graphically the behavior of the process $X(t)$, several simulated sample-paths are plotted in Figure 2.7.

In the simulation analysis we assume that the rates are measured in years^{-1} and the tumor size is given by the tumor cell density. Specifically, following [71], we consider $\alpha = 6.46$ year^{-1}, $\beta = 0.314$ year^{-1}, $\tilde{X}_k(\tau_k) = \rho = 10^8$. Note that the value 10^8 is representative of a 0.1 gram tumor mass (namely the smallest diagnosable mass). In Figure 2.7, a sample path of $X(t)$ is plotted for $N = 5$ with $\alpha_k = \alpha + 0.1k$ ($k = 0, 1, \ldots, 5$), $\sigma = 0.1$ and different choices of inter-jump intervals. On the left of Figure 2.7 the instants of the therapeutic applications are (1, 3, 5.5, 7), in the center are (2, 6, 10, 13) and on the right we choose (2, 4, 6, 8, 10). The blue and red curves represent $X(t)$ and $\tilde{X}_0(t)$, respectively. Note that for this choice of parameters, during the treatment, the process $X(t)$ is below $\tilde{X}_0(t)$, corresponding to the natural evolution of the illness.

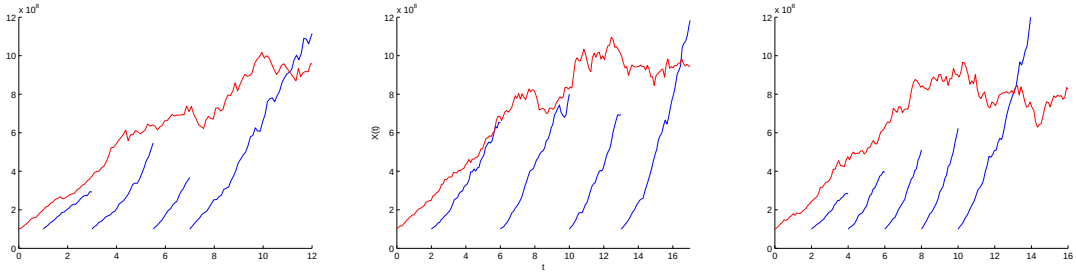

Figure 2.7: The sample-paths $X(t)$ are plotted for $\rho_k = \rho = 10^8$, $\alpha_k = 6.46 + 0.1k$, $\beta = 0.314$, $\sigma = 0.1$ and therapeutic application times (1, 3, 5.5, 7), (2, 6, 10, 13) and (2, 4, 6, 8, 10) from left to right. The red line represents $\tilde{X}_0(t)$.

We focus on the FPT problem for the process $X(t)$ through a constant threshold S because we are interested in keeping the cancer mass under S as long as possible. Since $X(t)$ is defined in terms of the single processes $\tilde{X}_k(t)$, we firstly recall some aspects about the FPT of $\tilde{X}_k(t)$ through S.

Let

$$\tilde{T}_\rho^k(\tau_k) = \inf\{t \geq \tau_k : \tilde{X}_k(t) > S\}, \qquad \tilde{X}_k(\tau_k) = \rho < S$$

be the random variable FPT of $\tilde{X}_k(t)$ through the threshold S and let the function

$\tilde{g}_k(S, t-\tau_k|\rho)$ be its pdf. For $S > \rho$, the density $\tilde{g}_k$ is solution of (2.12) and it can be approximated with the function $\check{g}_k$ via the numerical algorithm shown in (2.15). Moreover, we recall that $E[\tilde{T}_\rho^k(\tau_k)] = \tau_k + E[\tilde{T}_\rho^k(0)]$.
Let

$$T_{\rho_0}(0) = \inf\{t \geq 0 : X(t) > S\}, \qquad X(0) = \rho_0 < S$$

be the FPT of $X(t)$ through S and let $g(S, t|\rho_0)$ be its pdf. The expression of g follows from (1.32), that is:

$$g(S,t|\rho_0) = \begin{cases} \tilde{g}_0(S,t|\rho_0), & t \in \mathcal{I}_1 \\ \displaystyle\prod_{j=0}^{k-1}\left[1 - \int_0^{\tau_{j+1}-\tau_j} \tilde{g}_j(S, \tau-\tau_j|\rho_j)d\tau\right] \tilde{g}_k(S, t-\tau_k|\rho_k), & t \in \mathcal{I}_k, \end{cases}$$

where $\mathcal{I}_k = [\tau_k, \tau_{k+1})$ for $k \geq 0$.
Moreover, the mean of $T_\rho(0)$

$$E[T_\rho(0)] = \int_0^\infty t\, g(S,t|\rho)\, dt,$$

can be computed by using the numerical evaluation of $g(S, t|\rho)$.
In Figure 2.8 the FPT pdf of $X(t)$ is plotted for $\alpha_k = 6.46 + 0.1k$, $\beta = 0.314$, $\sigma = 0.1$, $S = 8 \cdot 10^8$, $\rho_k = \rho = 10^8$ and various choices of the application times: (1, 3, 5.5, 7), (2, 6, 10, 13) and (2, 4, 6, 8, 10) from left to right.

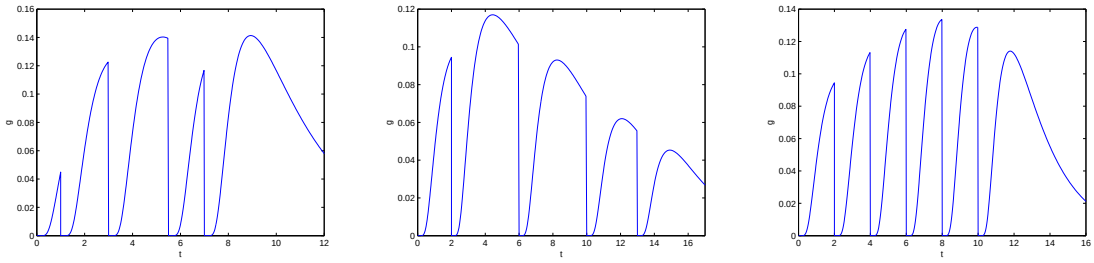

Figure 2.8: The FPT pdf of $X(t)$ for values $\alpha_k = 6.46 + 0.1k$, $\beta = 0.314$, $\sigma = 0.1$, $S = 8 \cdot 10^8$, $\rho_k = \rho = 10^8$ and therapeutic application times (1, 3, 5.5, 7), (2, 6, 10, 13) and (2, 4, 6, 8, 10) from left to right.

2.3.3 Scheduling 1

We assume that $\rho_{k+1} = \rho$ and the inter-jump intervals have equal size $\zeta_k = \zeta > 0$, for $k \geq 0$. Since $\tau_k = k\,\zeta$, (2.16) [(2.17)] becomes

$$x(t) = \sum_{k=0}^{N} \tilde{x}_k(t) 1_{\{k\zeta<t<(k+1)\zeta\}} \qquad \left[X(t) = \sum_{k=0}^{N} \tilde{X}_k(t) 1_{\{k\zeta<t<(k+1)\zeta\}} \right].$$

Moreover, we suppose that

$$\alpha_k = \alpha + k\gamma.$$

For each $k = 1, 2, \ldots, N$, the constant $\gamma > 0$ describes the toxicity of the drug. In this case, α_k depends on the number of applications and toxicity of the drug.

Deterministic approach

Let consider the couples $(\zeta k,\ \tilde{x}_{k-1}(\zeta k))$ for $k = 1, 2, \ldots$, where $\zeta\, k$ represents the time of the k-th therapeutic application and $\tilde{x}_{k-1}(\zeta k)$ is the corresponding cancer mass at this time. We note that $(\zeta k,\ \tilde{x}_{k-1}(\zeta k))$ is the maximum point of $\tilde{x}_{k-1}(t)$. Let $y(t)$ be the curve interpolating the points $(\xi k,\ \tilde{x}_{k-1}(\xi k))$ for $k = 1, 2, \ldots$. One has:

$$y(t)|_{t=k\,\zeta} = \tilde{x}_{k-1}(t)|_{t=k\,\zeta} = \tilde{x}_{t/\zeta-1}(k\,\zeta),$$

from which, recalling the expression of $\tilde{x}_k(t)$ in (2.3), one obtains

$$y(t) = \exp\left\{ \frac{\alpha + \left(\frac{t}{\zeta} - 1\right)\gamma}{\beta} + \left(\log\rho - \frac{\alpha + \left(\frac{t}{\zeta} - 1\right)\gamma}{\beta} \right) e^{-\beta\left[t - \left(\frac{t}{\zeta} - 1\right)\zeta\right]} \right\},$$

hence

$$y(t) = \exp\left\{ \frac{\alpha + \left(\frac{t}{\zeta} - 1\right)\gamma}{\beta} \left(1 - e^{-\beta\zeta}\right) \right\} \rho^{e^{-\beta\zeta}}, \qquad t \geq \zeta. \tag{2.18}$$

In this context, we consider $S > \rho$ as a threshold which represents a mortality or a control level characterizing the particular cancer and the patient's organism. The curve $y(t)$ is useful in order to understand where the tumor mass is in a certain instant or when it reaches a certain threshold. Indeed, an alarm time for the patient, whose illness is described by $x(t)$, is given by the intersection point t^* between S and the curve $y(t)$. For example, in Figure 2.9 the process $x(t)$ (black line), the curve $y(t)$ (red curve) and the threshold S (blue line) are plotted for $\alpha = 6.46$, $\beta = 0.314$, $\gamma = 0.5$, $\zeta = 0.25$, $\rho = 10^8$, $S = 8 \cdot 10^8$ and t^* is represented by the magenta circle.

We are interested in computing the time t^* by solving the equation $y(t) = S$. From

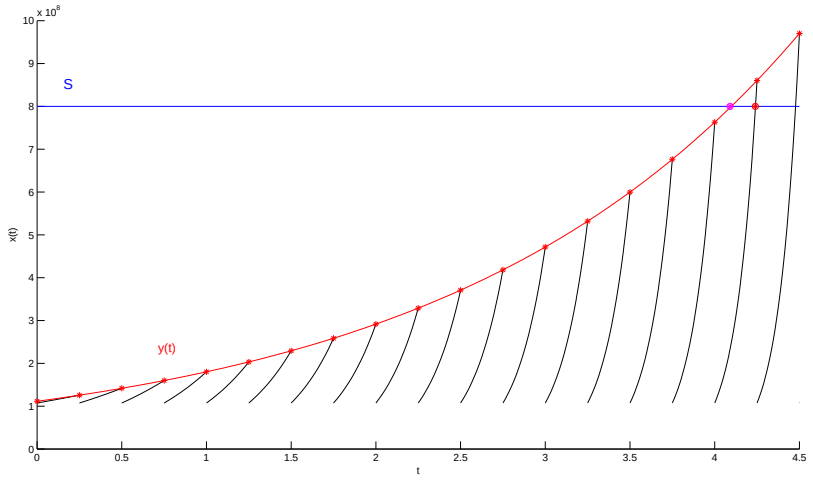

Figure 2.9: The process $x(t)$ (black lines), the curve $y(t)$ (red curve) and the threshold S (blue line) with $\alpha = 6.46, \beta = 0.314, \gamma = 0.5, \xi = 1/4, \rho = 1.074 \times 10^8, S = 8 \cdot 10^8$. The magenta circle is $y(t^*)$.

(2.18), one has:

$$\frac{\alpha + \left(\frac{t}{\zeta} - 1\right)\gamma}{\beta}\left(1 - e^{-\beta\zeta}\right) + \log \rho e^{-\beta\zeta} = \log S,$$

then

$$\frac{t}{\zeta} - 1 = -\frac{\alpha}{\gamma} + \frac{\beta}{\gamma\left(1 - e^{-\beta\zeta}\right)}\left(\log S - \log \rho e^{-\beta\zeta}\right),$$

so we obtain

$$t^* = \zeta\left[1 - \frac{\alpha}{\gamma} + \frac{\beta}{\gamma(1 - e^{-\beta\zeta})}\left(\log S - e^{-\beta\zeta}\log \rho\right)\right]. \tag{2.19}$$

Note that t^* is not the point in which the cancer mass reaches the threshold, but it gives an alarm: before the successive application of the therapy the cancer mass crosses S; i.e. if $t^* \in [(k-1)\,\zeta,\, k\,\zeta]$, then $\tilde{x}_k(t)$ crosses S. To know the time of such crossing $\bar{t}$, represented by the red circle in Figure 2.9, we will consider the intersection of the involved curve $\tilde{x}_k(t)$ with S.

First of all, our objective is to maximize t^*. Note that parameters α, β, S and ρ are fixed because they are specific of cancer or of patient's organism, hence we can analyze and, eventually, modify only the kind of therapy and the frequency of applications. In other words, we want to determine a strategy, i.e. a couple (γ, ζ), in order to delay the threshold's crossing.
We consider t^* as a function of γ and ζ. For each fixed ζ, t^* is decreasing with re-

spect to γ, that is, if the toxicity of the drug increases, the alarm time t^* decreases. Hence, if we are forced to use a fixed ζ, it is better to apply the most delicate possible therapies.
Instead, for each fixed γ it is not evident the monotony of t^* with respect to ζ, thus we need to pay more attention on the analytic form of t^* by using its derivative with respect to ζ. From (2.19), setting $r = \gamma - \alpha$, one has:

$$\begin{aligned}\frac{dt^*}{d\zeta} = \quad & r + \beta \log S + e^{-\beta t}\left[-2r - \beta \log S - \beta \log \rho + \zeta \beta^2 \log \frac{\rho}{S}\right] \\ & + e^{-2\beta\zeta}\left[r + \beta \log \rho\right],\end{aligned}$$

or, equivalently,

$$\begin{aligned}\frac{dt^*}{d\zeta} = \quad & (r + \beta \log S)\left(1 - e^{-\beta\zeta}\right) - (r + \beta \log \rho)\left(1 - e^{-\beta\zeta}\right) e^{-\beta\zeta} \\ & + \zeta \beta^2 e^{-\beta\zeta} \log \frac{\rho}{S}. \end{aligned} \tag{2.20}$$

Proposition 3. *If*

$$\gamma < \alpha - \beta \, \log S, \tag{2.21}$$

therefore the alarm time t^* is a decreasing function of ζ.

Proof. Recalling $\rho < S$, one has $\zeta \beta^2 e^{-\beta\zeta} \log \frac{\rho}{S} < 0$, hence, from (2.20) it follows:

$$\frac{dt^*}{d\zeta} < (r + \beta \log S)\left(1 - e^{-\beta\zeta}\right) - (r + \beta \log \rho)\left(1 - e^{-\beta\zeta}\right) e^{-\beta\zeta}. \tag{2.22}$$

Moreover, since $1 - e^{-\beta\zeta} > 0$, we have

$$|r + \beta \log S| > |r + \beta \log \rho| > |r + \beta \log \rho| \, e^{-\beta\zeta}. \tag{2.23}$$

From (2.22), if $r + \beta \log S < 0$, i.e. (2.21) holds, one has $r + \beta \log \rho < r + \beta \log S < 0$. So that, from (2.23), observing that $1 - e^{-\beta\zeta} > 0$, it results

$$(r + \beta \log S)\left(1 - e^{-\beta\zeta}\right) < (r + \beta \log \rho)\left(1 - e^{-\beta\zeta}\right) e^{-\beta\zeta} < 0.$$

Thus, if (2.21) holds, from (2.22) one has $\dfrac{dt^*}{d\zeta} < 0$, the thesis follows. □

We note that if (2.21) holds, one has $t^* \geq 0$ when $\zeta < \bar{\zeta}$, where $\bar{\zeta}$ is:

$$\bar{\zeta} = -\frac{1}{\beta} \, \log \frac{\alpha - \gamma - \beta \, \log S}{\alpha - \gamma - \beta \, \log \rho}; \tag{2.24}$$

From Proposition 1, if $\gamma < \alpha - \beta \log S$, we can conclude that t^* decreases with ζ; hence to have a longer crossing time it is better using the smallest plausible $\zeta < \bar{\zeta}$, that is, one should apply the therapies as frequently as possible.
However, (2.21) is only a sufficient condition and it would be interesting to analyze what happens in other cases. In particular, in the following, we determine conditions on γ such that t^* is an increasing function of ζ. To this purpose we consider the following lemma.

Lemma 1. *For all $x > 0$ the function*

$$G(x) = \frac{\beta \log \rho \left(1 - e^{-\beta x}\right) e^{-\beta x} - \beta \log S \left(1 - e^{-\beta x}\right) - \beta^2 x e^{-\beta x} \log \frac{\rho}{S}}{\left(1 - e^{-\beta x}\right)^2} \tag{2.25}$$

is decreasing.

Proof. The derivative of $G(x)$ with respect to x is:

$$\frac{dG(x)}{dx} = \frac{e^{-\beta x} \log \frac{S}{\rho}}{\left(1 - e^{-\beta x}\right)^2} \left(2 - \beta x \frac{1 + e^{-\beta x}}{1 - e^{-\beta x}}\right).$$

To study the sign of $\dfrac{dG(x)}{dx}$, we note that $\dfrac{e^{-\beta x} \log \frac{S}{\rho}}{\left(1 - e^{-\beta x}\right)^2} > 0$, so we need to pay more attention on the sign of the function $2 - \beta x \dfrac{1 + e^{-\beta x}}{1 - e^{-\beta x}}$ depending only on sign of the function

$$f(x) = 2 \left(1 - e^{-x}\right) - x \left(1 + e^{-x}\right),$$

which is smaller than zero for $x > 0$. Indeed, $f(x)$ is null for $x \to 0$ and it is a decreasing function because, making use of from Bernoulli's inequality $e^x > 1 + x$, one has:

$$\frac{df(x)}{dx} = (1 + x)e^{-x} - 1 < 0 \qquad x > 0.$$

Hence, the thesis follows. □

Proposition 4. *Let ζ_0 be the smallest plausible ζ. If*

$$\gamma > \alpha + G(\zeta_0), \tag{2.26}$$

therefore the alarm time t^* is a increasing function of ζ.

Proof. From (2.20), we have that $\dfrac{dt^*}{d\zeta} > 0$ if

$$\gamma > \alpha + G(\zeta).$$

Therefore, recalling that $G(\zeta)$ is decreasing respect to ζ, we obtain the thesis. □

When condition (2.26) is satisfied, t^* is an increasing function of ζ, so that it is better applying the treatment infrequently.
Once chosen ζ and γ in order to maximize the time t^*, we calculate the crossing time $\bar{t}$ of $x(t)$ through S to understand how long the cancer mass is below the threshold. To obtain the crossing time $\bar{t}$ we have to calculate k such that $(k-1)\,\zeta < t^* \leq k\,\zeta$ and then we have to solve the equation $\tilde{x}_k(t) = S$ in the variable t. In particular, taking into consideration the expression of t^* given in (2.19), one has $(k-1)\,\zeta < t^* \leq k\,\zeta$ for $k = \bar{k}$, with $\bar{k}$ given by:

$$\bar{k} = \left\lfloor 1 - \frac{\alpha}{\gamma} + \frac{\beta}{\gamma(1-e^{-\beta\zeta})}\left(\log S - e^{-\beta\zeta}\log\rho\right)\right\rfloor, \tag{2.27}$$

where $\lfloor x \rfloor$ is the largest integer not greater than x. Then, considering this particular $\bar{k}$, that represents the maximum number N of applications, we obtain $\bar{t}$ by solving $\tilde{x}_{\bar{k}}(t) = S$; that is the crossing time $\bar{t}$ is:

$$\bar{t} = -\frac{1}{\beta}\log\left[\frac{\log S - \frac{\alpha+\bar{k}\gamma}{\beta}}{\log\rho - \frac{\alpha+\bar{k}\gamma}{\beta}}\right] + \zeta\,\bar{k}. \tag{2.28}$$

Moreover, we require that at least one application is made, that is $N \geq 1$. To compute the value $\hat{\zeta}$ such that $N \geq 1$, we solve the inequality $\bar{k} \geq 1$ respect to ζ, so from (2.27) we obtain:

$$\zeta \leq -\frac{1}{\beta}\ln\left(\frac{\alpha - \beta\ln S}{\alpha - \beta\ln\rho}\right) = \hat{\zeta}. \tag{2.29}$$

In conclusion, fixed γ, we can decide what is better to do:

- one should apply the therapy as frequently as possible if (2.21) is verified, by choosing $\zeta <\min\left\{\bar{\zeta}, \hat{\zeta}\right\}$, with $\hat{\zeta}$ and $\bar{\zeta}$ given in (2.24) and (2.29) respectively;
- one should apply the therapy as infrequently as possible if (2.26) holds, by choosing $\zeta < \hat{\zeta}$, with $\hat{\zeta}$ given in (2.29).

Let be the parameters $\alpha = 6.46$, $\beta = 0.314$, $\rho = 10^8$ and $S = 6 \cdot 10^8$. In Table 2.1 we show the times t^*, the number of application N and the crossing time $\bar{t}$ for various values of ζ by choosing a therapy such that $\gamma = 0.1$ on the left table and $\gamma = 0.6$ on the right table.
For the first choice of $\gamma = 0.1$, one has $\gamma < \alpha - \beta\log S = 0.113294$, so our study suggests to apply the therapy as frequently as possible, with $\zeta <\min\{12.0021,\ 5.68812\}$. Results on the left of Table 2.1 support this, since longer times are obtained for more frequent applications ($\zeta = 1/12$). For the second choice of $\gamma = 0.6$, one has

$\gamma > \alpha + G(10^{-6}) = 0.404641$, so our study suggests to apply the therapy as infrequently as possible. The results on the right of Table 2.1 confirm this, since the longest time is obtained for the most infrequent application, that is $\zeta = 5.6$. We do not consider larger value of ζ because for $\zeta = 5.7$ one has $N = 0$.
Now we analyze values of γ such that $0.113294 = \alpha - \beta \log S < \gamma < \alpha + G(10^{-6}) = 0.404641$. Note that in these cases we do not have analytical results so only a numerical analysis can provide an efficient criterion to choose the application times. In Table 2.2 we consider the same parameters of Table 2.1 with $\gamma = 0.3$ (on the left) and $\gamma = 0.37$ (on the right). For the chosen parameters, from Table 2.2 one has that if $\gamma = 0.3$ it is better to apply the therapy as frequently as possible, whereas if $\gamma = 0.37$ it is better to apply the therapy infrequently.
Finally, we analyze what happens for different values of the threshold.
We consider $\gamma = 0.1$, $\zeta = 1/12$ and we compute the maximum number of application N and $\bar{t}$ in Table 2.3. Obviously, for decreasing values of S the values of N and $\bar{t}$ decrease.

$\gamma = \frac{1}{10}$	$\zeta = \frac{1}{12}$	$\zeta = \frac{1}{4}$	$\zeta = \frac{1}{2}$	$\zeta = 1$
t^*	17.67	17.19	16.48	15.11
N	212	68	32	15
$\bar{t}$	17.74	17.24	16.49	15.95

$\gamma = \frac{6}{10}$	$\zeta = 3$	$\zeta = 4$	$\zeta = 5$	$\zeta = 5.6$
t^*	4.23	4.78	5.28	5.63
N	1	1	1	1
$\bar{t}$	4.85	5.85	6.85	7.45

Table 2.1: The times t^*, the number of applications N and $\bar{t}$ are computed for the values $\alpha_k = 6.46 + \gamma k$, $\beta = 0.314$, $S = 6 \cdot 10^8$, $\rho = 10^8$, $\gamma = 0.1$ on the left, $\gamma = 0.6$ on the right and various choices of ζ.

$\gamma = 0.3$	$\zeta = \frac{1}{4}$	$\zeta = \frac{1}{2}$	$\zeta = 1$	$\zeta = 2$
t^*	5.89	5.82	5.70	5.53
N	23	11	5	2
$\bar{t}$	5.99	5.98	5.95	5.85

$\gamma = 0.37$	$\zeta = \frac{1}{4}$	$\zeta = \frac{1}{2}$	$\zeta = 1$	$\zeta = 2$
t^*	4.82	4.81	4.81	4.86
N	19	9	4	2
$\bar{t}$	4.99	4.98	4.96	5.61

Table 2.2: The times t^*, the number of applications N and $\bar{t}$ are computed for the same value of Table 2.1 with $\gamma = 0.3$ on the left, $\gamma = 0.37$ on the right and for various choices of ζ.

S	$6 \cdot 10^8$	$3 \cdot 10^8$	$1.5 \cdot 10^8$
$\bar{t}$	17.74	10.66	3.66
N	212	127	43

Table 2.3: The times $\bar{t}$ and the number of applications N are listed for $\gamma = 0.1$, $\zeta = 1/12$ and various values of S.

Stochastic approach

In the present context, we can numerically analyze the behavior of the cancer mass, but we need a new tool to understand how many applications can be done. We proceed as follows.
For $k = 0, 1, \ldots$:

- if $E[\tilde{T}_\rho^k(0)] > \zeta$ (that is, intuitively, $\tilde{X}_k < S$), then we apply the therapy at time $(k+1)\,\zeta$,
- else, if $E[\tilde{T}_\rho^k(0)] < \zeta$, the number of applications is $N = k$ and it results $E[T_{\rho_0}(0)] = k\,\zeta + E[\tilde{T}_\rho^k(0)]$.

Let fix the parameters $\alpha = 6.46$, $\beta = 0.314$, $\rho = 10^8$ and $S = 6 \cdot 10^8$. In Table 2.4 we list the number of application N and the mean FPT of $X(t)$ through S (denoted with $E[T]$) for various values of ζ with $\gamma = 0.1$, $\sigma = 0.1$ on the left table and $\sigma = 0.5$ on the right table. For $\sigma = 0.1$, the results are almost similar to ones obtained in the deterministic approach, since the chosen σ is small. In Figure 2.10 we plot the mean of $X(t)$ for the same parameters of Table 2.4 for $\sigma = 0.1$, with $\zeta = 1$ on the left and $\zeta = 1/2$ on the right. Whereas, with a bigger $\sigma = 0.5$ (on the right of Table 2.4), we note that the mean FPT times (denoted with $E[T]$) are bigger than ones obtained in the deterministic case and more applications are possible.
In Table 2.5 we list N and $E[T_{\rho_0}(0)] \equiv E[T]$ for $\gamma = 0.6$ with $\sigma = 0.1$ on the left table and $\sigma = 0.5$ on the right table. Also in this case, the mean FPT times for $\sigma = 0.5$ are bigger respect than $\sigma = 0.1$, but, since γ is big, no more that one application is possible .
However, the criterion used in the deterministic case to chose the most appropriate ζ is a very useful tool also in the stochastic environment.

	$\zeta = \frac{1}{12}$	$\zeta = \frac{1}{4}$	$\zeta = \frac{1}{2}$	$\zeta = 1$
N	212	68	32	15
$E[T]$	17.74	17.24	16.49	15.95

	$\zeta = \frac{1}{12}$	$\zeta = \frac{1}{4}$	$\zeta = \frac{1}{2}$	$\zeta = 1$
N	213	69	33	16
$E[T]$	17.83	17.49	17	16.95

Table 2.4: The number of applications N and $E[T_{\rho_0}(0)]$ (denoted by $E[T]$) are computed for $\alpha_k = 6.46 + \gamma k$, $\beta = 0.314$, $S = 6 \cdot 10^8$, $\rho = 10^8$, $\gamma = 0.1$, $\sigma = 0.1$ on the left, $\sigma = 0.5$ on the right and various choices of ζ.

	$\zeta = 3$	$\zeta = 4$	$\zeta = 5$	$\zeta = 5.6$
N	1	1	1	1
$E[T]$	4.85	5.85	6.85	7.45

	$\zeta = 3$	$\zeta = 4$	$\zeta = 5$	$\zeta = 5.6$
N	1	1	1	1
$E[T]$	5.02	6.02	7.02	7.62

Table 2.5: The number of applications N and $E[T_{\rho_0}(0)]$ (denoted by $E[T]$) are computed for the same parameters of Table 2.4 with $\gamma = 0.6$.

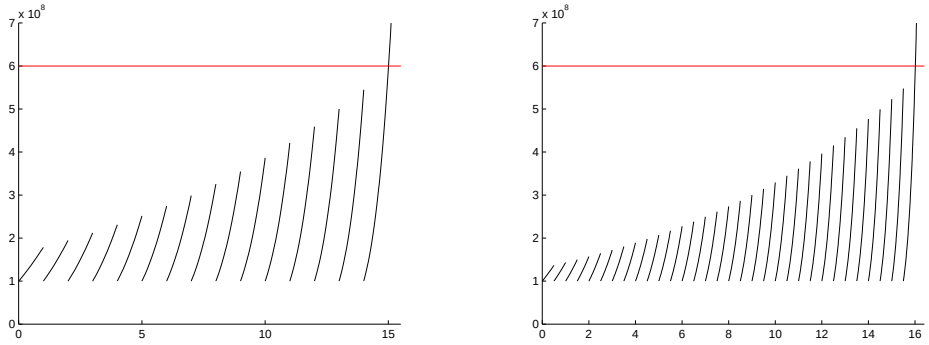

Figure 2.10: The mean of $X(t)$ for the same parameters of Table 2.4, with $\zeta = 1$ on the left and $\zeta = 1/2$ on the right. The line $S = 6 \cdot 10^8$ represents the threshold.

2.3.4 Scheduling 2

We propose to apply the therapy before $x(t)$ $[X(t)]$ reaches S. Hence, for $k \geq 0$ we choose $\zeta_{k+1} < \hat{t}_k$, where $\hat{t}_k$ is the solution of $\tilde{x}_k(t) = S$ in the deterministic model, while $\hat{t}_k = E[\tilde{T}^k_\rho(\tau_k)]$ is the FPT mean of $\tilde{X}_k(t)$ through S in the stochastic model. One could consider $\zeta_{k+1} = \hat{t}_k - A$ $(k \geq 0)$, where $A > 0$ is an arbitrary constant such that $\zeta_{k+1} > 0$, but this is not an objective choice because A is not related with the involved values. It is more plausible that $A = h\,\hat{t}_k$ is proportional to the crossing time or the FPT mean. Thus, we consider $\tau_{k+1} = \tau_k + \zeta_{k+1}$, for $k \geq 0$, with

$$\zeta_{k+1} = (1 - h)\,\hat{t}_k, \tag{2.30}$$

where $0 < h < 1$ is the percentage of reduction respect to $\hat{t}_k$. Hence, increasing values of h (that correspond to decreasing inter-jump intervals) are safer in terms of not passing the control threshold. Generally, the maximum number of applications N is chosen such that, for $k > 0$, one has $\tau_{k+1} - \tau_k > \theta$, where θ can be considered as the minimum waiting time between consecutive applications.

In the following, we consider fixed values of α_k, β_k, σ_k and S; we calculate $\hat{t}_k$ to determine $(\tau_1, \tau_2, \ldots, \tau_N)$ via the crossing times of $\tilde{x}_k(t)$ through S in the deterministic case and via the FPT times of $\tilde{X}_k(t)$ thought S in the stochastic model. Then, we compute the crossing time $\bar{t}_k$ given in (2.28) for the deterministic model, while, for the stochastic model we determine the mean FPT $E[T_{\rho_0}(0)] = \tau_N + E[\tilde{T}^N_{\rho_N}(0)]$ with $E[\tilde{T}^N_{\rho_N}(0)]$ given in (2.14).

Note that the proposed strategy allows to make predictions for any choice of the parameters and of the inter-jumps intervals. On the other hand, the choice of application times depends on the parameters involved in the model that can be estimated via the maximum likelihood method, as shown in [48].

However, to illustrate the proposed procedure, we assume that the parameters

are $\alpha_k = 6.46 + k\gamma$, $\beta = 0.314$, $\rho_k = \rho = 10^8$ (for all k) and we choose various values of γ and S. We consider three values for the inter-jump intervals and for the application times of the therapy for $k = 0, 1, \ldots, N-1$:

- Case (a): $h = 0.10, \quad \zeta^a_{k+1} = 90\%\, \hat{t}_k, \quad \tau^a_1 = \zeta^a_1, \quad \tau^a_{k+1} = \tau^a_k + \zeta^a_{k+1},$
- Case (b): $h = 0.05, \quad \zeta^b_{k+1} = 95\%\, \hat{t}_k, \quad \tau^b_1 = \zeta^b_1, \quad \tau^b_{k+1} = \tau^b_k + \zeta^b_{k+1},$
- Case (c): $h = 0.01, \quad \zeta^c_{k+1} = 99\%\, \hat{t}_k, \quad \tau^c_1 = \zeta^c_1, \quad \tau^c_{k+1} = \tau^c_k + \zeta^c_{k+1}.$

The maximum number of applications N is chosen such that $\zeta^a_{k+1} \geq 0.5$, so it is also $\zeta^b_{k+1} \geq 0.5$ and $\zeta^c_{k+1} \geq 0.5$.

Deterministic approach

For Case (a), Case (b) and Case (c), in Table 2.6 the value of $\hat{t}_k$ for $S = 6 \cdot 10^8$ and $\gamma = 0.1$ are listed in the second column; in the other columns we report the amplitude of inter-jump intervals (ζ_{k+1}), the application times (τ_{k+1}) and the corresponding crossing times $\bar{t}$ if the therapeutic program consists of $k+1$ applications. We note that $\bar{t}$ is always greater than $\hat{t}_0$ and it increases as the number of applications increases. The crossing times for Case (c) are greater respect to the other considered cases (cf. Table 2.6), so it is preferable waiting as long as before applying another therapy.

In Table 2.7 the analysis is realized for the same choices of Table 2.6 but assuming $\gamma = 0.6$. In this case, since γ is greater, the number of therapeutic applications and the crossing time of $x(t)$ are considerably lower than the previous case. However, as before, the best results are for Case (c).
In Table 2.8, in order to show as the control threshold influences the crossing time of $x(t)$, we propose the same analysis for $S = 3 \cdot 10^8$ and $\gamma = 0.1$; since the threshold is lower the mean FPT of $X(t)$ and the number of therapeutic applications decrease respect to the results of Table 2.6. Also for decreasing values of the threshold S, Case (c) gives bigger crossing time (cf. Table 2.8).

In conclusion, Case (c) gives always the best results, in particular the crossing time is larger for smaller values of γ and for higher control threshold.

Stochastic approach

For Case (a), Case (b) and Case (c), in Table 2.9 the means of $\tilde{T}^k_{\rho_0}(0)$ through $S = 6 \cdot 10^8$ and $\gamma = 0.1$ are listed in the second column; in the other columns we report the amplitude of inter-jump intervals (ζ_{k+1}), the application times (τ_{k+1}) and the corresponding mean of $T_{\rho_0}(0)$ if the therapeutic program consists of $k+1$ applications. We note that $E[T_{\rho_0}(0)]$ is always greater than $E[\tilde{T}^0_{\rho_0}(0)]$ and it increases as the number of the applications increases. In Figure 2.11, to summarize the results of Table 2.9, we plot the mean FPT of $X(t)$ when the therapy is applied 29 times. As shown in Figure 2.12, the strategy is effective for the considered values of h, indeed the mean of $X(t)$ (blue curve) is always below S (black line) and $E[\tilde{X}_0(t)|\tilde{X}_0(0) = \rho]$ (red curve) during the treatment. However, since the mean FPT of $X(t)$ for the Case (c) is greater respect to the other considered cases (cf. Table 2.9 and Figure 2.11), it is preferable waiting as long as before applying the therapy.
In Table 2.10 and in Figure 2.13, the analysis is realized for the same choices of Table 2.9 but assuming $\gamma = 0.6$. In this case, since γ is greater, the number of therapeutic applications and the mean FPT of $X(t)$ are considerably lower than the previous case. Also in this case the best results are for Case (c).
In Table 2.11 and in Figure 2.14, the same analysis for $S = 3 \cdot 10^8$ and $\gamma = 0.1$ is proposed; since the threshold is lower, the mean FPT of $X(t)$ and the number of therapeutic applications decrease respect to the results of Table 2.9.
Also for decreasing values of the threshold S, Case (c) gives larger mean FPT (cf. Table 2.11 and Figure 2.14).
In conclusion, Case (c) gives always the best results, in particular the mean FPT is larger for smaller values of γ and for higher control threshold.

We summarize the results regarding the mean FPT of $X(t)$ and of N associated to Case (c) for different values of γ (Figure 2.15) and S (Figure 2.16).
Specifically, from Figure 2.15 we note that the product $\gamma E[T_{\rho_0}(0)] \in (4, 8)$ increases as γ increases, whereas $\gamma N \in (2, 2.8)$ decreases as γ increases.
Moreover, as shown in Figure 2.16, the quantities $E[T_{\rho_0}(0)]/S \in (1.3{\cdot}10^{-8}, 1.83{\cdot}10^{-8})$ and $N/S \in (1.3 \cdot 10^{-8}, 1.83 \cdot 10^{-8})$ increase with S.

2.3.5 Comparison between the deterministic and the stochastic approach

To underline the effect of the stochasticity, we show the mean FPT considering various choice of σ for both the proposed scheduling. The results for $\sigma = 0$ correspond to the deterministic case. Moreover, we analyze the mean FPT of $X(t)$ for some choices of S and of γ.

In Figure 2.17, we show the means of $T_{\rho_0}(0)$ for Scheduling 1 with various choices of σ: on the left we consider $\gamma = 0.1$, $\zeta = 1.8\bar{3}$ and $S = 3 \cdot 10^8, 6 \cdot 10^8$, while on the right $S = 6 \cdot 10^8$ and for $\gamma = 0.1$, 0.5 we consider $\zeta = 1/12$, 5.6 respectively.
In Figure 2.18, we show the means of $T_{\rho_0}(0)$ for Scheduling 2 in Case (c) with various choices of σ and $N = 6$: on the left we consider $\gamma = 0.1$ and $S = 3 \cdot 10^8, 6 \cdot 10^8$, while on the right $S = 6 \cdot 10^8$ and $\gamma = 0.1$, 0.5.
We note that for both scheduling the mean FPT increases as σ increases even if the rise is slow for $\sigma \leq 0.5$. Indeed, the deterministic curve goes up to the carrying capacity while the sample paths of the stochastic process grow with upward and downwards fluctuations: downwards fluctuations delay the crossing of S.

2.3.6 Comparison between the two proposed scheduling

In order to understand what would be the best strategy (if we was free to chose between them) we summarize in Table 2.12 the results from the two strategies in the stochastic approach with $\sigma = 0.1$ and by choosing the best result in Strategy 1. From Table 2.12, it is evident that the second strategy is the best: it is preferable to apply the therapy just before the cancer mass crosses the control threshold. One can think that this contrasts with what we obtain from the results of Scheduling 1 because we suggested to apply the therapy as frequently as possible for some values of γ; but it is not so. The reason is that this criterion holds only if we have to use the Scheduling 1 (i.e. if we are forced to consider the same amplitude for each inter-jump interval) and not in comparison with Scheduling 2.
To explain better this, in Figure 2.19 we compare the mean of $X(t)$ for $\zeta = 1$ (blue line), $\zeta = 5$ (black line) by using the first strategy, while the other parameters are $\sigma = 0.1$, $\gamma = 0.1$, $S = 6 \cdot 10^8$ (red line). From figure 2.19, one has that for $\zeta = 5$ the mean cancer size crosses the threshold at the time 9.11, while for $\zeta = 1$ at the time 15.95. In particular, for $\zeta = 5$ the threshold's crossing occurs before the second application of the therapy because for big values of ζ we are forced to wait too long.

k	$\hat{t}_k$	ζ^a_{k+1}	τ^a_{k+1}	$\bar{t}$	ζ^b_{k+1}	τ^b_{k+1}	$\bar{t}$	ζ^c_{k+1}	τ^c_{k+1}	$\bar{t}$
0	5.68	5.11	5.11	9.23	5.40	5.40	9.51	5.63	5.63	9.74
1	4.11	3.70	8.82	12.09	3.90	9.31	12.58	4.07	9.70	12.97
2	3.27	2.94	11.76	14.50	3.11	12.42	15.15	3.24	12.94	15.68
3	2.73	2.46	14.23	16.58	2.59	15.02	17.37	2.33	15.65	18.01
4	2.35	2.12	16.35	18.42	2.23	17.25	19.33	0.74	17.98	20.05
5	2.07	1.86	18.21	20.06	1.96	19.22	21.08	0.61	20.03	21.89
6	1.85	1.66	19.88	21.55	1.75	20.98	22.66	0.61	21.87	23.54
7	1.67	1.50	21.39	22.91	1.59	22.57	24.10	0.61	23.53	25.05
8	1.52	1.37	22.76	24.17	1.45	24.03	25.43	0.61	25.04	26.44
9	1.40	1.26	24.03	25.33	1.33	25.36	26.67	0.61	26.43	27.73
10	1.30	1.17	25.20	26.41	1.23	26.60	27.81	0.61	27.71	28.93
11	1.21	1.09	26.29	27.43	1.15	27.75	28.89	0.61	28.92	30.06
12	1.13	1.02	27.31	28.38	1.07	28.83	29.90	0.61	30.05	31.11
13	1.06	0.96	28.27	29.28	1.01	29.85	30.85	0.61	31.10	32.11
14	1.00	0.90	29.18	30.13	0.95	30.80	31.75	0.61	32.10	33.05
15	0.95	0.85	30.04	30.94	0.90	31.71	32.61	0.61	33.04	33.95
16	0.90	0.81	30.85	31.71	0.85	32.57	33.43	0.61	33.94	34.80
17	0.86	0.77	31.63	32.45	0.81	33.38	34.20	0.61	34.79	35.61
18	0.82	0.73	32.37	33.15	0.77	34.16	34.95	0.61	35.60	36.39
19	0.78	0.70	33.07	33.82	0.74	34.91	35.66	0.61	36.38	37.13
20	0.75	0.67	33.75	34.47	0.71	35.62	36.34	0.61	37.12	37.84
21	0.72	0.64	34.40	35.09	0.68	36.31	37.00	0.61	37.84	38.53
22	0.69	0.62	35.02	35.69	0.65	36.97	37.63	0.61	38.52	39.19
23	0.66	0.60	35.62	36.27	0.63	37.60	38.24	0.61	39.18	39.83
24	0.64	0.57	36.18	36.80	0.61	38.19	38.81	0.61	39.80	40.42
25	0.62	0.55	36.74	37.34	0.58	38.78	39.38	0.61	40.41	41.01
26	0.60	0.54	37.28	37.86	0.57	39.35	39.93	0.61	41.01	41.59
27	0.58	0.52	37.80	38.36	0.55	40.46	11.27	0.61	41.58	42.15
28	0.56	0.50	38.31	38.85	0.53	40.44	40.98	0.61	42.14	42.68

Table 2.6: For $\alpha_k = 6.46 + \gamma k$, $\beta = 0.314$, $\gamma = 0.1$ and $\rho = 10^8$ the crossing times $\hat{t}$ and $\bar{t}$ through $S = 6 \cdot 10^8$ are listed.

k	$\hat{t}_k$	ζ^a_{k+1}	τ^a_{k+1}	$\bar{t}$	ζ^b_{k+1}	τ^b_{k+1}	$\bar{t}$	ζ^c_{k+1}	τ^c_{k+1}	$\bar{t}$
0	5.68	5.11	5.11	6.97	5.40	5.40	7.25	5.63	5.63	7.48
1	1.85	1.66	6.78	7.92	1.75	7.16	8.29	1.83	7.46	8.60
2	1.13	1.02	7.80	8.62	1.07	8.24	9.06	1.12	8.58	9.40
3	0.82	0.73	8.54	9.19	0.77	9.02	9.66	0.81	9.40	10.04
4	0.64	0.57	9.12	9.65	0.61	9.63	10.16	0.63	10.03	10.56

Table 2.7: As in Table 2.6 with $\gamma = 0.6$.

k	$\hat{t}_k$	ζ^a_{k+1}	τ^a_{k+1}	$\bar{t}$	ζ^b_{k+1}	τ^b_{k+1}	$\bar{t}$	ζ^c_{k+1}	τ^c_{k+1}	$\bar{t}$
0	2.27	2.04	2.04	3.91	2.16	2.16	4.03	2.25	2.25	4.12
1	1.87	1.68	3.73	5.32	1.77	3.93	5.53	1.85	4.10	5.69
2	1.59	1.43	5.16	6.55	1.51	5.45	6.84	1.57	5.68	7.07
3	1.38	1.25	6.41	7.64	1.31	6.77	8.00	1.37	7.05	8.29
4	1.23	1.10	7.52	8.63	1.16	7.94	9.04	1.21	8.27	9.38
5	1.10	0.99	8.52	9.52	1.05	8.99	9.99	1.09	9.37	10.37
6	1.00	0.90	9.42	10.34	0.95	9.94	10.86	0.99	10.36	11.28
7	0.91	0.82	9.90	11.09	0.87	10.82	11.66	0.91	11.27	12.12
8	0.84	0.76	10.25	11.80	0.80	11.62	12.41	0.83	12.11	12.90
9	0.78	0.70	11.01	12.45	0.74	12.37	13.10	0.77	12.89	13.62
10	0.73	0.66	11.72	13.07	0.69	13.07	13.75	0.72	13.62	14.30
11	0.68	0.61	12.38	13.64	0.65	13.72	14.37	0.68	14.30	14.94
12	0.64	0.58	13.00	14.19	0.61	14.33	14.95	0.64	14.94	15.55
13	0.61	0.54	14.13	14.71	0.58	14.91	15.49	0.60	15.54	16.12

Table 2.8: As in Table 2.6 with $S = 3 \cdot 10^8$.

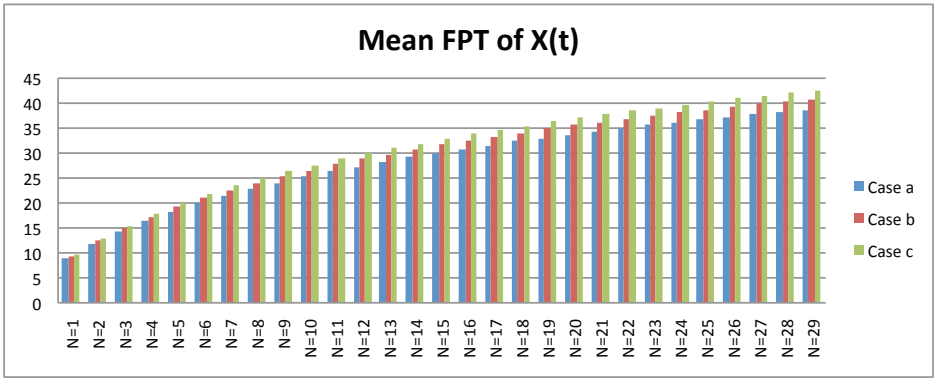

Figure 2.11: The mean FPT of $X(t)$ for the same choice of the parameters of Table 2.12.

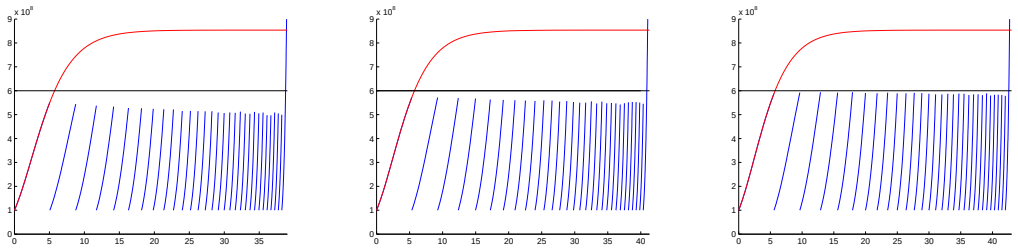

Figure 2.12: $E[X(t)|\tilde{X}_0(0) = \rho]$ (blue curve), $E[\tilde{X}_0(t)|\tilde{X}_0(0) = \rho]$ (red curve) and $S = 6 \cdot 10^8$ (black line) for the same parameters of Table 2.12 and for the Case (a), (b), (c) (from left to right).

k	$E[\tilde{T}_\rho^k(0)]$	ζ_{k+1}^a	τ_{k+1}^a	$E[T_\rho]$	ζ_{k+1}^b	τ_{k+1}^b	$E[T_\rho]$	ζ_{k+1}^c	τ_{k+1}^c	$E[T_\rho]$
0	5.63	5.06	5.06	9.18	5.34	5.34	9.46	5.57	5.57	9.69
1	4.11	3.70	8.77	12.05	3.91	9.26	12.54	4.07	9.65	12.93
2	3.28	2.95	11.73	14.47	3.12	12.38	15.12	3.25	12.90	15.64
3	2.74	2.47	14.20	16.56	2.61	14.99	17.35	2.71	15.62	17.98
4	2.36	2.12	16.33	18.41	2.24	17.23	19.31	2.34	17.96	20.04
5	2.08	1.87	18.20	20.06	1.97	19.21	21.07	2.05	20.02	21.88
6	1.85	1.67	19.87	21.55	1.76	20.98	22.66	1.83	21.86	23.54
7	1.68	1.51	21.38	22.92	1.59	22.57	24.11	1.66	23.52	25.06
8	1.53	1.38	22.76	24.17	1.45	24.03	25.44	1.51	25.04	26.45
9	1.41	1.26	24.03	25.34	1.34	25.37	26.67	1.39	26.44	27.74
10	1.30	1.17	25.21	26.43	1.24	26.61	27.83	1.29	27.73	28.95
11	1.21	1.09	26.30	27.44	1.15	27.77	28.90	1.20	28.93	30.07
12	1.13	1.02	27.33	28.40	1.08	28.85	29.92	1.12	30.06	31.13
13	1.06	0.96	28.29	29.30	1.01	29.86	30.87	1.05	31.12	32.13
14	1.00	0.90	29.20	30.15	0.95	30.82	31.78	0.99	32.12	33.07
15	0.95	0.85	20.06	30.96	0.90	31.73	32.64	0.94	33.07	33.97
16	0.90	0.81	30.87	31.74	0.86	32.59	33.45	0.89	33.96	34.82
17	0.86	0.77	31.65	32.47	0.81	33.41	34.23	0.85	34.82	35.64
18	0.82	0.74	32.39	33.18	0.78	34.19	34.98	0.81	35.63	36.42
19	0.78	0.70	33.10	33.85	0.74	34.94	35.69	0.77	36.41	37.16
20	0.75	0.67	33.78	34.50	0.71	35.65	36.38	0.74	37.15	37.88
21	0.72	0.65	34.43	35.12	0.68	36.34	37.03	0.71	37.87	38.56
22	0.69	0.62	35.05	35.72	0.65	37.00	37.67	0.68	38.56	39.23
23	0.66	0.60	35.65	36.30	0.63	37.63	38.28	0.66	39.22	39.86
24	0.64	0.57	36.21	36.83	0.61	38.23	38.85	0.63	39.83	40.46
25	0.62	0.55	36.77	37.37	0.59	38.82	39.42	0.61	40.45	41.05
26	0.60	0.54	37.31	37.90	0.57	39.39	39.97	0.59	41.05	41.63
27	0.58	0.52	37.84	38.40	0.55	39.94	40.50	0.57	41.62	42.18
28	0.56	0.50	38.34	38.89	0.53	40.47	41.02	0.55	42.18	42.72

Table 2.9: For $\alpha_k = 6.46 + \gamma k$, $\beta = 0.314$, $\gamma = 0.1$, $\sigma = 0.1$ and $\rho = 10^8$ the FPT means of $\tilde{X}_k(t)$ and of $X(t)$ through $S = 6 \cdot 10^8$ are listed.

k	$E[\tilde{T}_\rho^k(0)]$	ζ_{k+1}^a	τ_{k+1}^a	$E[T_\rho]$	ζ_{k+1}^b	τ_{k+1}^b	$E[T_\rho]$	ζ_{k+1}^c	τ_{k+1}^c	$E[T_\rho]$
0	5.63	5.06	5.06	6.92	5.34	5.34	7.20	5.57	5.57	7.43
1	2.08	1.67	6.74	7.87	1.76	7.11	8.25	1.83	7.41	8.55
2	1.30	1.02	7.76	8.58	1.08	8.19	9.01	1.12	8.54	9.36
3	0.95	0.74	8.50	9.15	0.78	8.97	9.62	0.81	9.35	10.00
4	0.75	0.57	9.08	9.61	0.61	9.59	10.12	0.63	9.99	10.52

Table 2.10: For $\alpha_k = 6.46 + \gamma k$, $\beta = 0.314$, $\gamma = 0.6$, $\sigma = 0.1$ and $\rho = 10^8$ the FPT means of $\tilde{X}_k(t)$ and of $X(t)$ through $S = 6 \cdot 10^8$ are listed.

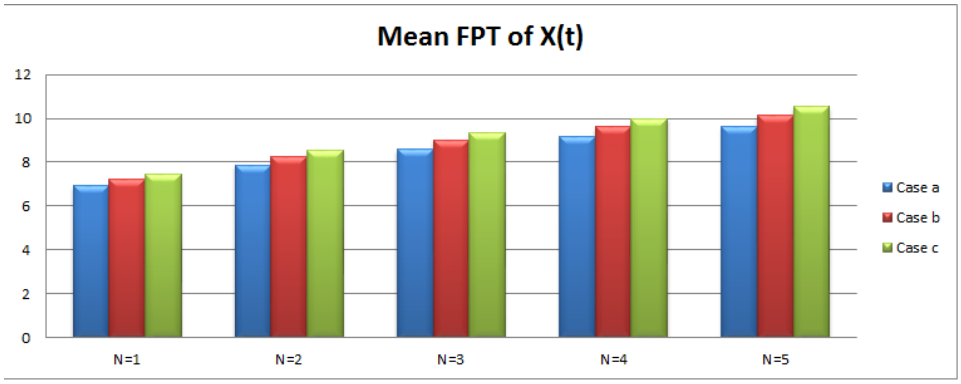

Figure 2.13: The mean FPT of $X(t)$ for the same choice of the parameters of Table 2.13.

k	$E[\tilde{T}_\rho^k(0)]$	ζ_{k+1}^a	τ_{k+1}^a	$E[T_\rho]$	ζ_{k+1}^b	τ_{k+1}^b	$E[T_\rho]$	ζ_{k+1}^c	τ_{k+1}^c	$E[T_\rho]$
0	2.28	2.05	2.05	3.93	2.16	2.16	4.07	2.25	2.25	4.13
1	1.87	1.69	3.74	5.34	1.78	3.95	5.55	1.86	4.11	5.72
2	1.60	1.44	5.18	6.58	1.52	5.47	6.86	1.58	5.70	7.09
3	1.39	1.25	6.44	7.67	1.32	6.79	8.03	1.38	7.08	8.32
4	1.23	0.99	7.55	8.66	1.17	7.97	9.08	1.22	8.30	9.41
5	1.11	0.90	8.55	9.55	1.05	9.02	10.03	1.09	9.40	10.41
6	1.10	0.82	9.45	10.38	0.95	9.98	10.90	0.99	10.40	11.32
7	0.92	0.76	10.28	11.13	0.87	10.85	11.70	0.91	11.31	12.16
8	0.85	0.71	11.05	11.84	0.80	11.66	12.45	0.84	12.15	12.94
9	0.78	0.66	11.76	12.49	0.74	12.41	13.15	0.78	12.93	13.67
10	0.73	0.62	12.42	13.11	0.69	13.11	13.80	0.72	13.66	14.35
11	0.68	0.58	13.04	13.69	0.65	13.77	14.41	0.68	14.35	14.99
12	0.64	0.55	13.62	14.24	0.61	14.38	14.99	0.64	14.99	15.60
13	0.61	0.52	14.18	14.76	0.58	14.96	15.54	0.60	15.59	16.17

Table 2.11: For $\alpha_k = 6.46 + \gamma k$, $\beta = 0.314$, $\gamma = 0.1$, $\sigma = 0.1$ and $\rho = 10^8$ the FPT means of $\tilde{X}_k(t)$ and of $X(t)$ through $S = 3 \cdot 10^8$ are listed.

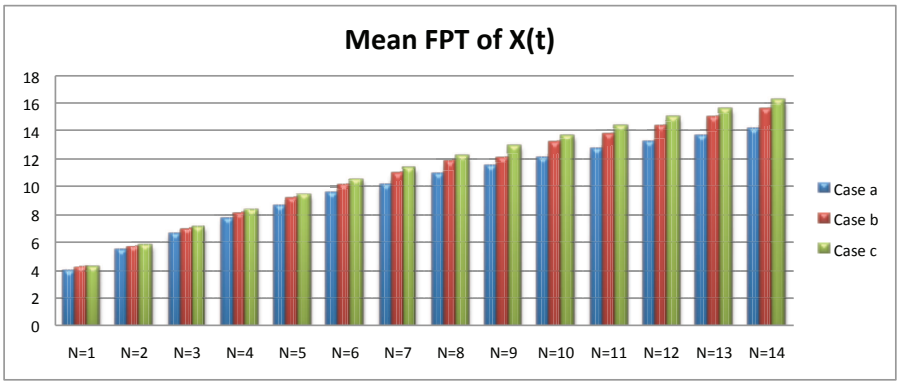

Figure 2.14: The mean FPT of $X(t)$ for the same choice of the parameters of Table 2.14.

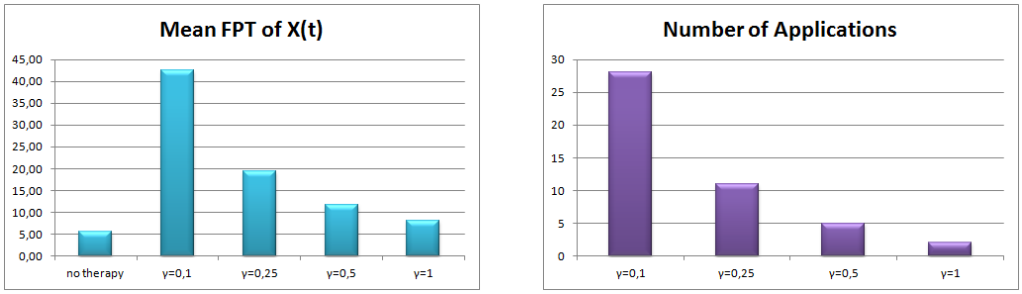

Figure 2.15: Case (c): means of T (on the left) and values of N (on the right) for $S = 6 \cdot 10^8$ and various choices of γ.

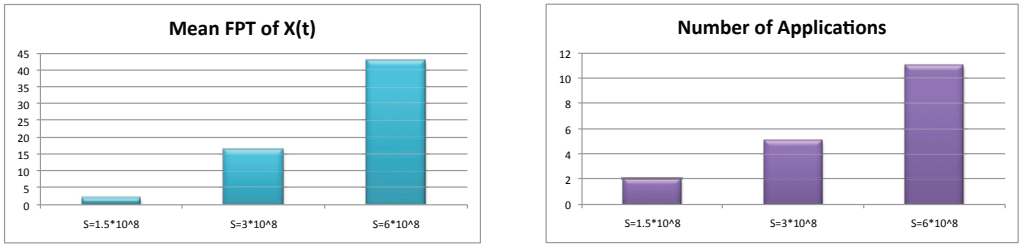

Figure 2.16: Case (c): means of T (on the left) and values of N (on the right) for $\gamma = 0.1$ and various choices of S.

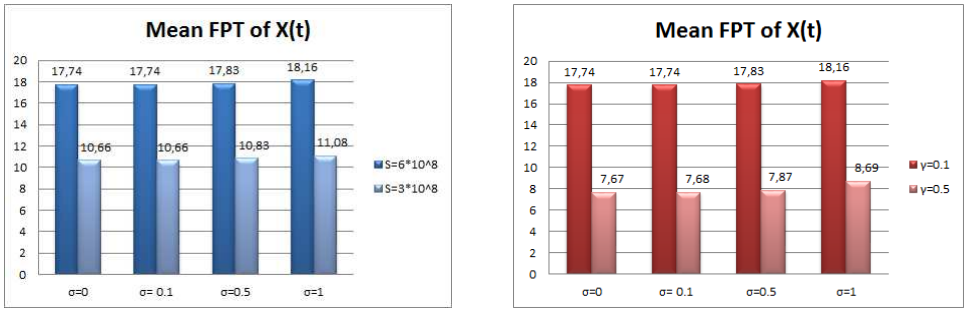

Figure 2.17: For the first scheduling the means of T for various values of σ are showed: on the left $\gamma = 0.1$, $\zeta = 1/12$ and $S = 3 \cdot 10^8, 6 \cdot 10^8$; on the right $S = 6 \cdot 10^8$ and for $\gamma = 0.1$, 0.5 we consider $\zeta = 1/12$, 5.6 respectively.

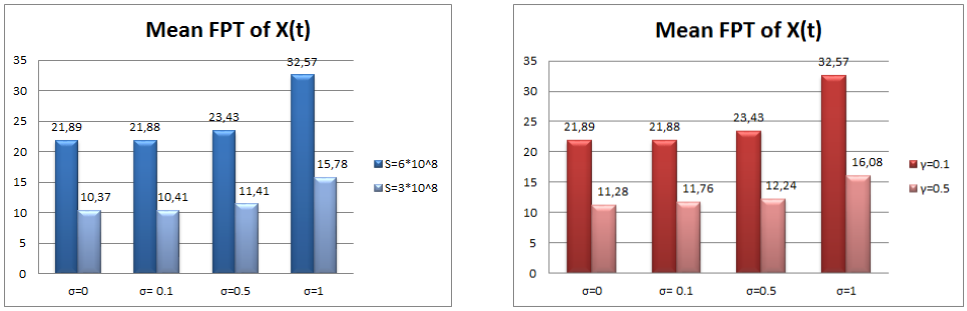

Figure 2.18: For the case (c) of the second scheduling: means of T for various values of σ and $N = 6$ with $\gamma = 0.1$ and $S = 3 \cdot 10^8, 6 \cdot 10^8$ (on the left) and with and $S = 6 \cdot 10^8$ and $\gamma = 0.1, 0.5$ (on the right).

	$S = 6 \cdot 10^8$ $\gamma = 0.1$	$S = 6 \cdot 10^8$ $\gamma = 0.5$	$S = 3 \cdot 10^8$ $\gamma = 0.1$	$S = 3 \cdot 10^8$ $\gamma = 0.5$
Scheduling 1	17.74	7.68	10.66	7.47
Scheduling 2	42.72	11.76	16.17	12.24

Table 2.12: The mean FPT of T for Scheduling 1 and Scheduling 2 for various choices of γ and S by considering in all cases the best results.

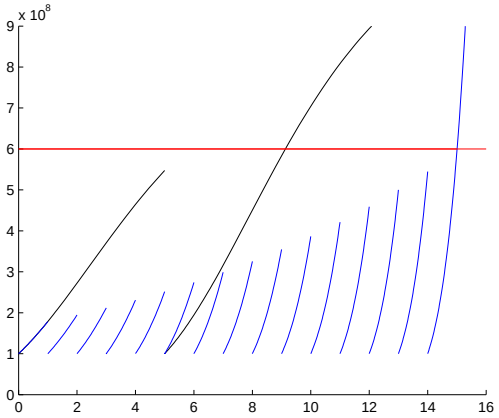

Figure 2.19: The mean of $X(t)$ for $\sigma = 0.1$, $\gamma = 0.1$, $S = 6 \cdot 10^8$ (red line) and $\zeta = 1$ (blue line), $\zeta = 5$ (black line).

Chapter 3

Return process with refractoriness for a non-homogeneous Ornstein-Uhlenbeck neuronal model

The neuron is the fundamental discrete unit of the central nervous system which is composed of brain and spinal cord. Each cell is separated from the external by a limiting permeable membrane. Between the external and the internal of the cell there is a potential difference (membrane potential) due to the different ionic concentrations. Before a neuron is stimulated, it has a slightly negative electric polarization: its interior has a negative charge compared with the extracellular fluid. This polarized state is called *resting membrane potential*; it is generated by a high concentration of positively charged sodium ions (Na+) outside the cell and high concentration of negatively charged chloride as well as a lower concentration of positively charged potassium (K+) inside. The resulting resting potential usually measures about -75 millivolts (mV); the minus sign indicates a negative charge inside. When a neuron is appropriately stimulated, there is an action potential, i.e. the cell membrane goes through a sequence of depolarization from its rest state followed by repolarization to that rest state, since the ions move through the membrane (via sparsely located specialized holes called *channels*). In such sequence, it actually reverses its normal polarity for a brief period before reestablishing the resting potential. The entire sequence last less than 6 milliseconds (ms) and can be divided in the following main steps (see Figure 3.1):

- A neuron is stimulated. This causes the Na+ channels to open. If the opening is sufficient to drive the interior potential from the resting state (-75mV) to

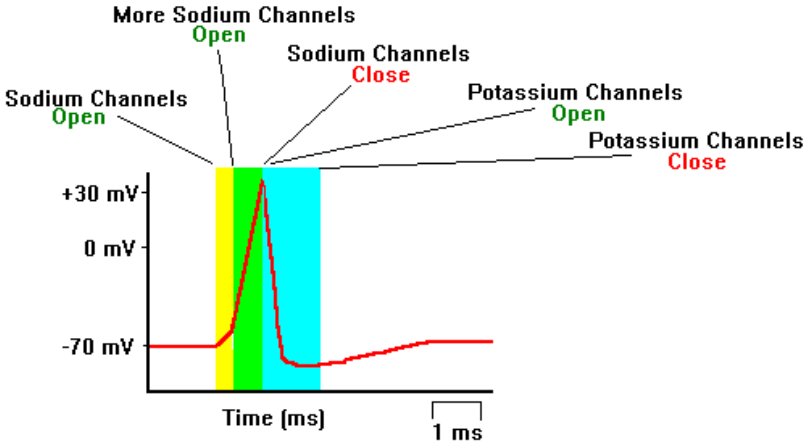

Figure 3.1: Transmission of an action potential.

the critical state, the process continues. The critical state is called *threshold potential* or *firing threshold* and measures about -55mV.

- For the reaching of the action threshold, more Na+ channels open. The Na+ influx drives the interior of the cell membrane up to about $+30$mV . The process to this point is called depolarization and the positive peak, reached in less than a millesecond, is called *spike* or *firing*.

- The Na+ channels close and the K+ channels open. Since the K+ channels are much slower to open, the depolarization has time to be completed.

- With the K+ channels opening, the membrane begins to repolarize back toward its resting potential.

- The repolarization typically overshoots the resting potential to about -90mV . This is called hyperpolarization and it prevents the neuron from receiving another stimulus during this time, or at least raises the threshold for any new stimulus. Moreover, hyperpolarization assures that the signal is proceeding in one direction.

- After hyperpolarization, the Na+/K+ pumps eventually bring the membrane back to its resting state.

During the transmission of an action potential, an interesting observed phenomenon is the refractory period: a short interval time following each spike and during which the neuron is completely or partially unable to respond to stimuli. In particular, as one area of membrane is being depolarized, the preceeding area of membrane is still in the depolarizing phase of its action potential, thus that area of membrane may not

be immediately stimulated to produce another action potential anyway. This period is called the *absolute refractory period*. In a period called *relative refractory period* that follows the absolute refractory period, the threshold is drastically increased, thus while not being impossible to generate another action potential, it requires a much stronger stimulus. This period is due to the sodium channels being closed and the potassium channels being open. So, exceptionally strong stimuli can cause more frequent generation of action potentials.

Various types of spiking neuron models exist, with different levels of details in the description. The starting point is the classical Gerstein-Mandelbrot model: in 1964 Gernstein and Mandelbrot proposed a model of neuronal activity based on the Wiener process ([37]). These authors demonstrated that with a suitable choice of parameters, the histograms of the interspike intervals (ISI), experimentally recorded, could be plotted with a good degree of approximation with the average of the FPT for a temporally homogeneous Wiener process. Since then various other models, based on diffusion stochastic processes, have been proposed to describe the evolution of the neuronal membrane potential. In particular, to take account of the exponential decay exhibited by the membrane potential in the absence of input of any type, in 1971 Capocelli and Ricciardi proposed a model based on the Ornstein-Uhlenbeck (OU) process (cf. [18]. This model has been used widely to describe the activity of a single neuron (see, for instance [16], [58], [76]). Several ways exist to derive this model, one of these consists of assuming that the neuron is subject to a sequence of inhibitory and excitatory postsynaptic potentials (PSP's) with constant amplitude that occur according to the Poisson's law. Further, it is assumed that, in the absence of input, the membrane potential decays exponentially to the resting potential, with a time constant which we denote by θ. When this constant diverges, the OU model yields to the Wiener model.
To describe the spikes train, we build a return process on an OU process in which the effect of random refractoriness is introduced. In this regard we recall that the first attempt to study the effect of refractoriness in a point process was made in [75] and in [84].

In the present chapter we assume that inputs, while remaining a constant amplitude, are characterized by time-dependent rates, meaning that some external stimulations are induced on the neuron; so that the involved Poisson process is not homogeneous. In Section 1 the model, based on a non-homogeneous OU process, is introduced. A comparison between the obtained OU model and the corresponding time-homogeneous process is done analyzing the trajectories of the two processes and considering the relative entropy of distributions characterizing the two models. Particular attention is paid to the FPT random variable because it represents the

"theoretical counterpart"of the neuronal firing time, so that the FPT's pdf describes the pdf of the firing time. In this regard it should be noted that for the OU process the FPT's pdf is not known in closed form if not for thresholds that are not of particular interest in the neuronal context, nonetheless, for the FPT pdf of the OU process is possible to make use of an asymptotic behavior of exponential type. To study the train of spikes, in Section 2, we build the return process. It is a process with jumps. The number of firings and the distribution of interspike intervals are studied under the assumption of exponential distribution for the firing time. We recall that the importance of interspike intervals is due to the generally accepted hypothesis that information transferred within the nervous system is usually encoded by timing of occurrence of neuronal spikes.
In Section 3, we introduce random downtimes which delay spikes, simulating the effect of refractoriness. A theoretical and numerical analysis of the return process in the presence of constant and exponential refractoriness is performed.

3.1 The model

To construct the model, we assume that the neuronal membrane potential is subject to a sequence of inhibitory and excitatory postsynaptic potentials characterized by constant magnitude ϵ occurring with time-dependent rates:

$$\alpha_i(t) = \frac{A_i(t)}{\epsilon} + \frac{\sigma^2}{2\,\epsilon^2}, \qquad \alpha_e(t) = \frac{A_e(t)}{\epsilon} + \frac{\sigma^2}{2\,\epsilon^2},$$

where $A_i(t)$, $A_e(t)$ are positive function of time and $\sigma^2 > 0$. Moreover, in the absence of inputs the membrane potential decays to the resting potential with a time constant $\theta > 0$. So, making use of a standard procedure (cf., for instance, [74]), it can be proved that the evolution of the neuronal membrane potential is described via a diffusion process $\{\tilde{X}(t),\ t \geq t_0 \geq 0\}$ defined in $\mathbb{R}$ whose infinitesimal moments are related to the rates. In particular, the drift and infinitesimal variance of $\tilde{X}(t)$ are

$$A_1(x,t) = -\frac{x}{\theta} + \mu(t), \qquad A_2 = \sigma^2,$$

respectively, with

$$\mu(t) = \lim_{\epsilon\to 0} \epsilon\,[\alpha_e(t) - \alpha_i(t)] = \mu + m(t), \qquad \sigma^2 = \lim_{\epsilon\to 0} \epsilon^2[\alpha_e(t) + \alpha_i(t)],$$

where $m(t)$ is a periodic and bounded function. We consider $m(t)$ periodic because this situation reflects some oscillatory effects of the environment acting on the neuron.

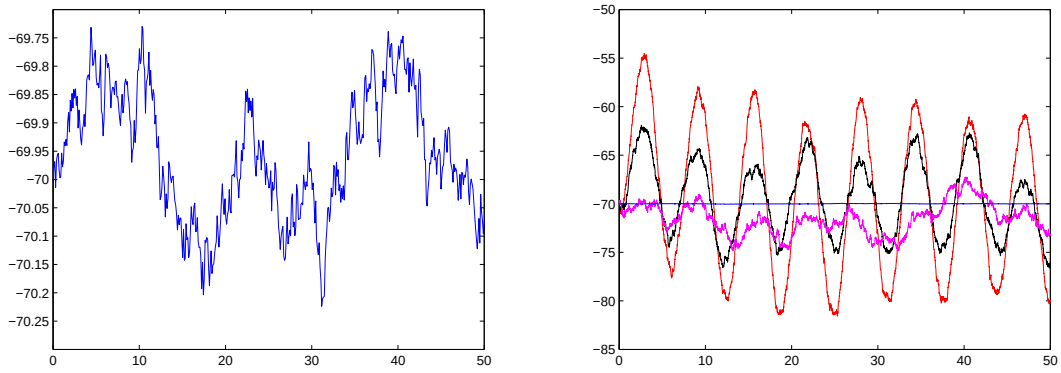

Figure 3.2: On the left a sample path of $\hat{X}(t)$ is plotted; on the right sample paths of $\hat{X}(t)$ (blue line) and of $\tilde{X}(t)$ with $m(t) = \sin t$ (magenta line), $m(t) = 5\sin t$ (black line) and $m(t) = 10\sin t$ (red line) are plotted. The chosen parameters are $\mu = -14$, $\theta = 5$, $\sigma = 1$ and $\eta = -70$.

Note that when θ diverges, $\tilde{X}(t)$ becomes a Wiener process with drift $\mu(t)$. Moreover, to give a quantitative information on the evolution of the membrane potential, we focus on the case $m(t) = A\sin t$.
In general, $\tilde{X}(t)$ is solution of the following stochastic equation:

$$d\tilde{X}(t) = \left[-\frac{\tilde{X}(t)}{\theta} + \mu + m(t)\right] dt + \sigma\, dB(t), \qquad \tilde{X}(t_0) = \eta, \tag{3.1}$$

where $B(t)$ is a standard Wiener process and η represents the resting potential. Equation (3.1) describes the evolution of the membrane potential.

To analyze the effect of the time dependent drift, in the following we denote by $\hat{X}(t)$ the process obtained from $\tilde{X}(t)$ when $m(t) = 0$. Hence, $\hat{X}(t)$ is described by the following equation:

$$d\hat{X}(t) = \left[-\frac{\hat{X}(t)}{\theta} + \mu\right] dt + \sigma\, dB(t), \qquad \hat{X}(t_0) = \eta. \tag{3.2}$$

$\hat{X}(t)$ is a time homogeneous OU process with drift $\hat{A}_1(x) = -x/\theta + \mu$ and infinitesimal variance $\hat{A}_2 = \sigma^2$. A sample path of $\hat{X}(t)$ is plotted on the left of Figure 3.2, while sample paths of $\hat{X}(t)$ and of $\tilde{X}(t)$ with periodic $m(t)$ are compared on the right. In particular, we choose $\mu = -14$ mV/ms, $\theta = 5$ ms, $\sigma = 1$ mV/ms$^{1/2}$, $\eta = -70$ mV and we consider various amplitudes of $m(t)$: $m(t) = \sin t$ (magenta line), $m(t) = 5\sin t$ (black line) and $m(t) = 10\sin t$ (red line). The sample path of $\hat{X}(t)$ is flat when it is compared to ones of $\tilde{X}(t)$, indeed the introduction of $m(t)$ makes the process more fluctuating. Moreover, by increasing A the sample paths of the process $\tilde{X}(t)$ become more and more oscillating.

Note that $\hat{X}(t)$ can be obtained from $\tilde{X}(t)$ via a transformation as shown in the following Remark.

Remark 5. *Let*

$$d(t) = -e^{-t/\theta} \int_{t_0}^{t} m(u)\, e^{u/\theta}\, du.$$

Then, the process

$$\hat{X}(t) = \tilde{X}(t) + d(t) \tag{3.3}$$

is a homogeneous OU process characterized by drift and infinitesimal variance

$$\hat{A}_1(x) = -x/\theta + \mu \qquad \hat{A}_2 = \sigma^2. \tag{3.4}$$

Proof. Let $v[\tilde{X}(t), t] = \hat{X}(t)$, from the Ito's lemma we have that $\hat{X}(t)$ satisfies the following stochastic equation

$$d\hat{X}(t) = \left(\frac{\partial v}{\partial t} + \frac{\partial v}{\partial x} F + \frac{1}{2}\, \sigma^2\, \frac{\partial^2 v}{\partial x^2} \right) dt + \frac{\partial v}{\partial x}\, \sigma\, dB(t),$$

where

$$\frac{\partial v}{\partial t} = -m(t) - \frac{d(t)}{\theta}, \qquad \frac{\partial v}{\partial x} = 1, \qquad \frac{\partial^2 v}{\partial x^2} = 0, \qquad F = -\frac{X(t)}{\theta} + \mu + m(t).$$

It follows that

$$d\hat{X}(t) = \left(-\frac{\tilde{X}(t) + d(t)}{\theta} + \mu \right) dt + \sigma\, dB(t) \equiv \left(-\frac{\hat{X}(t)}{\theta} + \mu \right) dt + \sigma\, dB(t)$$

is the Ito's equation for the diffusion process $\hat{X}(t)$ characterized by infinitesimal moments (3.4). □

In particular, by choosing $m(t) = A \sin(t)$ and $t_0 = 0$, we have

$$d(t) = \frac{A\theta}{1 + \theta^2} \left[\theta \left(\cos t - e^{-t/\theta} \right) - \sin t \right], \tag{3.5}$$

and $d(0) = 0$.

The transition pdf of $\tilde{X}(t)$ is a normal density:

$$\tilde{f}(x, t|y, \tau) = \frac{1}{\sqrt{2\,\pi\, V(t|\tau)}}\, \exp\left\{ -\frac{[x - M(t|y,\tau)]^2}{2\, V(t|\tau)} \right\} \tag{3.6}$$

with mean and variance

$$M(t|y,\tau) = \mu\theta + (y - \mu\theta)\, e^{-(t-\tau)/\theta} + e^{-t/\theta} \int_{\tau}^{t} m(u) e^{u/\theta}\, du,$$

$$V(t|\tau) = \frac{\sigma^2\theta}{2}\left[1 - e^{-2\,(t-\tau)/\theta}\right],$$

respectively. Note that if $m(t)$ is such that

$$m = \lim_{t\to\infty} e^{-t/\theta} \int_\tau^t m(u) e^{u/\theta}\, du,$$

exists and it is finite, then the steady state density of $\tilde{X}(t)$ is:

$$\tilde{W}(x) = \lim_{t\to\infty} \tilde{f}(x,t|y,\tau) = \frac{1}{\sqrt{\pi\sigma^2\theta}} \exp\left\{-\frac{[x-\mu\theta-m]^2}{\sigma^2\theta}\right\}.$$

Alternatively, when $m(t)$ is a periodic function with period Q it is possible to consider $\lim_{n\to\infty} \tilde{f}(x, t+nQ|y,\tau) = \tilde{W}(x,t)$; if this limit exists, $\tilde{W}(x,t)$ plays a role analogous to steady state density.

To analyze the influence of $m(t)$ on the transition pdf, we consider the relative entropy between $\tilde{f}(x,t|y,\tau)$ and $\hat{f}(x,t|y,\tau)$:

$$D(\tilde{f}|\hat{f}) = \int_{\mathbb{R}} \tilde{f}(x,t|y,\tau) \log \frac{\tilde{f}(x,t|y,\tau)}{\hat{f}(x,t|y,\tau)}\, dx, \tag{3.7}$$

where

$$\hat{f}(x,t|y,\tau) = \frac{1}{\sqrt{2\,\pi\, V(t|\tau)}} \exp\left\{-\frac{[x-\hat{M}(t|y,\tau)]^2}{2\,V(t|\tau)}\right\}, \tag{3.8}$$

with $\hat{M}(t|y,\tau) = y\, e^{-(t-\tau)/\theta} + \mu\theta[1 - e^{-(t-\tau)/\theta}]$, represents the transition pdf of $\hat{X}(t)$. The relative entropy, although it is not symmetrical, is used as a measure of the "distance" between $\tilde{f}$ e $\hat{f}$. Making use of (3.6) and (3.8), from (3.7) we have

$$D(\tilde{f}|\hat{f}) = \frac{[M(t|y,\tau) - \hat{M}(t|y,\tau)]^2}{2V(t|\tau)^2}. \tag{3.9}$$

In Figure 3.3 for $\mu = -14$, $\theta = 5$ and $\sigma = 2$, we plot on the left the time functions $\hat{f}(-65,t|-70,0)$ (blue line) and $\tilde{f}(-65,t|-70,0)$ with $m(t) = A\sin t$ by choosing $A = 1$ (magenta line), $A = 2$ (black line) and $A = 3$ (red line). The function $\tilde{f}(-65,t|-70,0)$ fluctuates around $\hat{f}(-65,t|-70,0)$ and the width of the fluctuations increases as A increases. On the right of Figure 3.3 the relative entropy (3.9) is plotted. Note that the relative entropy vanishes at times in which $\tilde{f} = \hat{f}$, moreover it increases as A increases according to the behavior shown on the left of Figure 3.3.

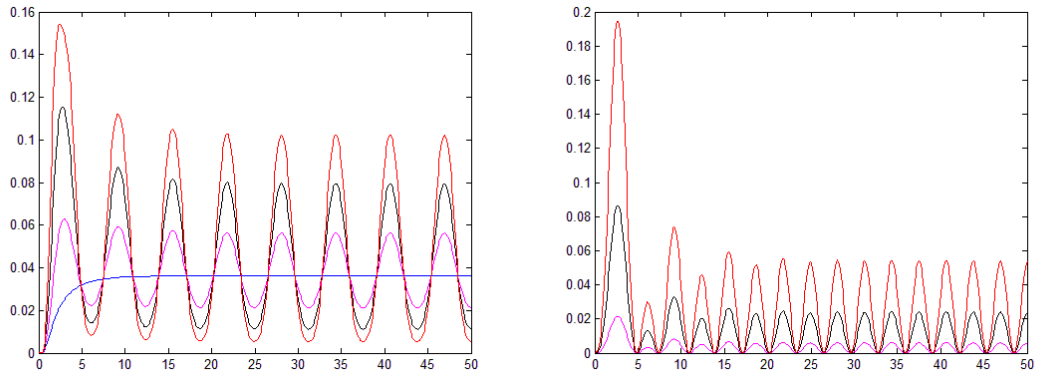

Figure 3.3: On the left, the functions $\hat{f}(-65, t| -70, 0)$ (blue line) and $\tilde{f}(-65, t| -70, 0)$ with $m(t) = A \sin t$ by choosing $A = 1$ (magenta line), $A = 2$ (black line) and $A = 3$ (red line) are plotted. On the right, $D(\tilde{f}|\hat{f})$ is plotted with $m(t) = \sin t$ (magenta line), $m(t) = 5 \sin t$ (black line) and $m(t) = 10 \sin t$ (red line). The chosen parameters are $\mu = -14$, $\theta = 5$ and $\sigma = 2$.

Let $\tilde{S} \in \mathbb{R}$ be the state of the process $\tilde{X}(t)$ representing the firing threshold. Let

$$\tilde{T}_y(\tau) = \inf\{t \geq \tau : \tilde{X}(t) > \tilde{S}\}, \qquad \tilde{X}(\tau) = y < \tilde{S}$$

be the FPT through $\tilde{S}$ and let $\tilde{g}(\tilde{S}, t|y, \tau)$ be its pdf. The random variable $\tilde{T}_y(\tau)$ describes the time of occurrence of neuronal spike and $\tilde{g}(\tilde{S}, t|y, \tau)$ is the theoretical counterpart of the firing pdf for the neuron. Making use of Remark 5, we can study the FPT problem of $\tilde{X}(t)$ through $\tilde{S}$ via the FPT problem of $\hat{X}(t)$ through

$$\hat{S}(t) = \tilde{S} + d(t) = \tilde{S} - e^{-t/\theta} \int^t m(u)\, e^{u/\theta}\, du. \tag{3.10}$$

In particular, denoting by $\hat{g}[\hat{S}(t), t|\hat{y}, \tau]$ the FPT pdf of $\hat{X}(t)$ from $\hat{y} = y + d(\tau)$ through $\hat{S}(t)$, we have that $\tilde{g}(\tilde{S}, t|y, \tau) = \hat{g}[\hat{S}(t), t|\hat{y}, \tau]$; so we focus on $\hat{g}[\hat{S}(t), t|\hat{y}, \tau]$. Unfortunately, the FPT pdf $\hat{g}$ is known analytically only in particular cases that are not of interest in the present context. However, numerical approximations for FPT pdf can be obtained via the appropriate algorithm described in the Subsection 1.1.3 of Chapter 1.
Furthermore, since $\hat{X}(t)$ admits steady state density

$$\hat{W}(x) = \lim_{t\to\infty} \hat{f}(x, t|y, \tau) = \frac{1}{\sqrt{\pi\sigma^2\theta}} \exp\left\{-\frac{[x - \mu\theta]^2}{\sigma^2\theta}\right\}, \tag{3.11}$$

the FPT pdf exhibits an exponential behavior for large times when the boundary is far from the starting point, as we showed in the Chapter 1. In particular, two cases

can be distinguished:

1. if $\hat{S}(t)$ admits limit $\hat{S} = \lim_{t\to\infty} \hat{S}(t)$, then for large times one has:

$$\hat{g}[\hat{S}(t), t|\tau] \sim R(\hat{S})\, \exp\{-R(\hat{S})\,(t-\tau)\}$$

where

$$R(\hat{S}) = \left[\frac{\hat{S}}{\theta} - \mu\right] \hat{W}(\hat{S});$$

2. if $\hat{S}(t)$ is a periodic function of period Q, then for sufficiently large time the following approximation holds

$$\hat{g}[\hat{S}(t), t|\tau] \sim \lambda(t)\, \exp\left\{-\Lambda_\tau(t)\right\}, \tag{3.12}$$

where

$$\lambda(t) = \left\{-U'(t) + \frac{U(t)}{\theta} - \mu\right\} \hat{W}[U(t)] \quad \text{and} \quad \Lambda_\tau(t) = \int_\tau^t \lambda(u)\, du, \tag{3.13}$$

with $U(t) = \lim_{n\to\infty} \hat{S}(t + n\,Q)$ and $\hat{W}(x)$ defined in (3.11).

If $m(t) = A\sin(t)$, one has $U(t) = \tilde{S} + d(t)$ with $d(t)$ given in (3.5), hence it follows:

$$\lambda(t) = \left(A\sin(t) + \frac{\tilde{S} + d(t)}{\theta} - \mu\right) \frac{1}{\sqrt{\pi\sigma^2\theta}} \exp\left\{-\frac{[\tilde{S} + d(t) - \mu\theta]^2}{\sigma^2\theta}\right\}.$$

In Figure 3.4 the approximation of the FPT pdf $\hat{g}[\hat{S}(t), t|\tau]$ obtained via (3.12) is plotted for $\hat{S}(t) = -60 + d(t)$, where $d(t)$ is given in (3.5) with $A = 1$, and for $\mu = -14$, $\theta = 5$, $\sigma = 2$ on the left and $\sigma = 3$ on the right.

3.2 The return process

In this Section the return process constructed on $\hat{X}(t)$ is studied to describe the train of spikes characterizing the neuronal activity. Note that if the firing threshold is asymptotically constant, the firing time mean is time independent. This situation has been widely studied in [33], so that in the following we will analyze the return process constructed on $\hat{X}(t)$ making use of the exponential approximation of the FPT pdf (3.12).

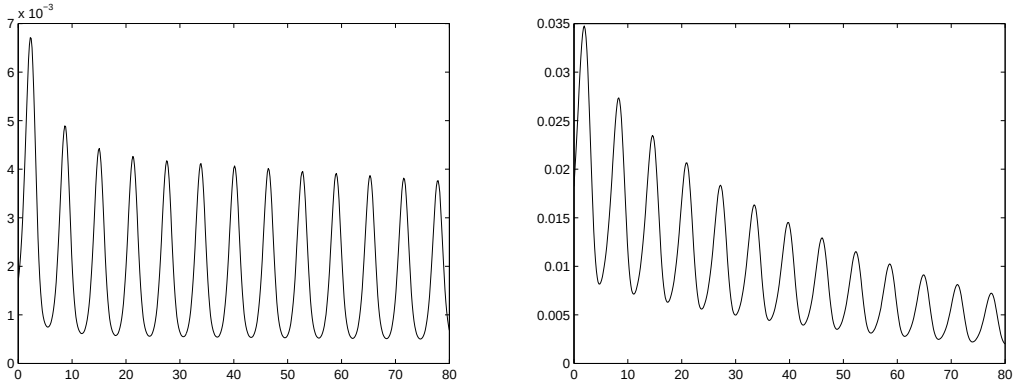

Figure 3.4: For the process $\hat{X}(t)$ with $\mu = -14$, $\theta = 5$, $\sigma = 2$ on the left and $\sigma = 3$ on the right, the approximation of FPT pdf (3.12) is plotted for $\hat{S}(t) = -60 + d(t)$ where $d(t)$ is given in (3.5) with $A = 1$.

3.2.1 Description of the process

Let $X(t)$ be the return process constructed from $\hat{X}(t)$ in the following way. Starting at $X(0) = \hat{X}(0) = \eta$, the process goes on as described by (3.2) until the threshold $\hat{S}(t)$, defined in (3.10), is reached for the first time. After this time the process is instantaneously reset to η and then evolves as described by (3.2) until $\hat{S}(t)$ is reached again, and so on.

The process $X(t)$ consists of recurrent cycles $\mathcal{I}_1,\ \mathcal{I}_2,\ \ldots$ of random durations $I_1,\ I_2,\ \ldots$. The random variable I_1 is the waiting time for the first firing and, for $i = 2, 3, \ldots$, I_i measures the time interval elapsing between the $(i-1)$-th and the i-th firing.

The sample path of $X(t)$ is solution of the following stochastic equation:

$$dX(t) = \left(-\frac{X(t)}{\theta} + \mu\right) dt + \sigma\, dB(t) - d[(\hat{S}(t) - \eta)\, P(t)]$$

where $B(t)$ is a standard Wiener process, $P(t)$ is a non-homogeneous Poisson process with intensity $\lambda(t)$, given in (3.13), and the term $\hat{S}(t) - \eta$ represents the amplitude of the jumps. In this context, η represents the resting potential and each return, occurring simultaneously with a jump, represents a neuronal spike.

Figures 3.5-3.6 show the sample-paths of $X(t)$ assuming that the process returns on the starting point η when the boundary $\hat{S}(t)$ is reached. In Figure 3.5, for $\mu = -10$ and $\theta = 5$, we have on the left $\sigma = 1$ and $\hat{S}(t) = -50 + d(t)$, where $d(t)$ is given in (3.5) with $A = 1$, so the distance between the starting point $\eta = -70$ and the threshold is approximatively 20; moreover η is different from the equilibrium point of the process being $\mu\theta = -50$. On the right of Figure 3.5, the threshold

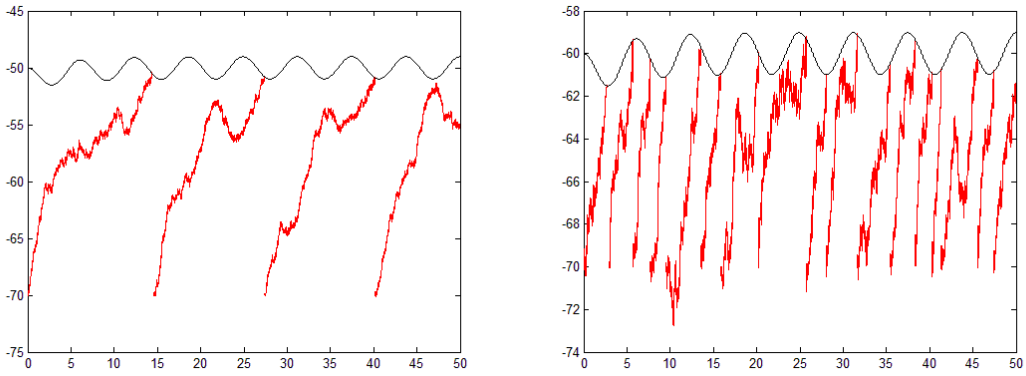

Figure 3.5: For $\eta = -70$, $\mu = -10$ and $\theta = 5$, a sample path of $X(t)$ is plotted assuming $\hat{S}(t) = \tilde{S} + d(t)$ (black curve) with $\sigma = 1$ and $\tilde{S} = -50$ on the left, with $\sigma = 2$ and $\tilde{S} = -60$ on the right; $d(t)$ is given in (3.5) with $A = 1$.

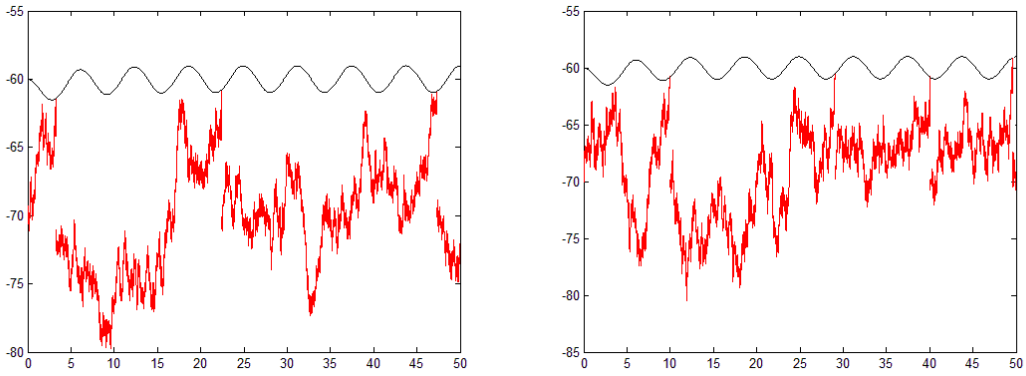

Figure 3.6: For $\eta = -70$, $\mu = -14$ and $\theta = 5$, a sample path of $X(t)$ is plotted assuming $\hat{S}(t) = \tilde{S} + d(t)$ (black curve) with $\sigma = 3$ and $\tilde{S} = -60$ on the left, with $\sigma = 4$ and $\tilde{S} = -60$ on the right; $d(t)$ is given in (3.5) with $A = 1$.

$\hat{S}(t) = -60 + d(t)$ has been approached to $\eta = -70$, simultaneously the width of the environmental oscillations $\sigma = 32$ has been increased, consequently the frequency of the jumps increases. In Figure 3.6, for $\mu = -14$ and $\theta = 5$, we consider $\eta = \mu\theta = -70$ and $\hat{S}(t) = -50 + d(t)$ such that $|\hat{S}(t) - \eta| \approx 10$. Note that on the left of Figure 3.6 the threshold is rarely reached although $\sigma = 3$; the frequency of the jumps increases when σ grows, as shown on the right of Figure 3.6, where $\sigma = 4$.

3.2.2 Analysis of interspike intervals (ISI)

To analyze the sequence of the spikes we denote with $\mathbf{T} = (T_1, T_2, \ldots, T_n)$ the random vector representing the instants of time in which firings occur. Note that T_i is a FPT random variable and the variables T_i $(i = 1, \ldots, n)$ conditioned from $T_{i-1} = t_{i-1}$ are independent and distributed according to $\hat{g}[\hat{S}(t), t|t_{i-1}]$. Now we study the joint density of $\mathbf{T}$.
For $t_0 < t_1 < t_2 < \ldots < t_n$ it follows:

$$\begin{aligned} f_{\mathbf{T}}(t_1, t_2, \ldots, t_n) &= \prod_{i=1}^{n} \lambda(t_i) \exp\{-\Lambda_{t_{i-1}}(t_i)\} \qquad (3.14) \\ &= \exp\{-\sum_{i=1}^{n} \Lambda_{t_{i-1}}(t_i)\} \prod_{i=1}^{n} \lambda(t_i) = \exp\{-\Lambda_{t_0}(t_n)\} \prod_{i=1}^{n} \lambda(t_i). \end{aligned}$$

From (3.15) the marginal density and the distribution function of the i-th element T_i of $\mathbf{T}$ can be determined. Indeed, one has

$$\begin{aligned} f_{T_i}(t_i) &= \int_{t_0}^{t_i} dt_{i-1} \int_{t_0}^{t_{i-1}} dt_{i-2} \ldots \int_{t_0}^{t_2} dt_1 \, f_{T_1, T_2, \ldots, T_i}(t_1, t_2, \ldots, t_i) \\ &= \int_{t_0}^{t_i} dt_{i-1} \int_{t_0}^{t_{i-1}} dt_{i-2} \ldots \int_{t_0}^{t_2} dt_1 \, \exp\{-\Lambda_{t_0}(t_i)\} \prod_{j=1}^{i} \lambda(t_j), \end{aligned}$$

and, after $k < i$ integrations, it follows:

$$f_{T_i}(t_i) = \frac{\exp\{-\Lambda_{t_0}(t_i)\}\lambda(t_i)}{k!} \int_{t_0}^{t_i} \lambda(t_{i-1}) dt_{i-1} \ldots \int_{t_0}^{t_{k+2}} \lambda(t_{k+1}) [\Lambda(t_{k+1})]^k dt_{k+1}.$$

Hence, it results:

$$f_{T_i}(t_i) = \lambda(t_i) \, \frac{[\Lambda_{t_0}(t_i)]^{i-1}}{(i-1)!} \, \exp\{-\Lambda_0(t_i)\}. \qquad (3.15)$$

From (3.15) the marginal distribution function of T_i can be determined. In particular one has:

$$F_{T_i}(t) = \int_{t_0}^{t} \exp\{-\Lambda_{t_0}(t_i)\} \, \lambda(t_i) \, \frac{[\Lambda_{t_0}(t_i)]^{i-1}}{(i-1)!} \, dt_i;$$

placing $x = \Lambda_{t_0}(t)$ so that $dx = \lambda(t)dt$, it follows:

$$F_{T_i}(t) = \int_{t_0}^{\Lambda_{t_0}(t)} \frac{x^{i-1}}{(i-1)!}\, e^{-x}\, dx.$$

Therefore

$$F_{T_i}(t) = 1 - \sum_{k=0}^{i-1} \frac{[\Lambda_{t_0}(t)]^k}{k!}\, \exp\{-\Lambda_{t_0}(t)\}. \tag{3.16}$$

We use (3.16) to determine the probability of occurrence of k firings up to time t. To this aim, we denote by $M(t)$ the stochastic process that counts the number of firings records in (t_0, t). It results that $M(t)$ is a Poisson process with intensity $\Lambda_{t_0}(t)$. Indeed,

$$\begin{aligned} P[M(t) = k | M(t_0) = 0] \\ &= P[M(t) \geq k | M(t_0) = 0] - P[M(t) \geq k+1 | M(t_0) = 0] \\ &= F_{T_k}(t) - F_{T_{k+1}}(t) = \frac{[\Lambda_{t_0}(t)]^k}{k!}\, \exp\{-\Lambda_{t_0}(t)\}. \end{aligned}$$

To analyze the ISI distribution we assume that $T_0 = t_0$ and for $n = 0, 1, \ldots$ we denote with $I_{n+1} = T_{n+1} - T_n$ the random variable describing the duration of the $(n+1)$-th ISI, i.e. the duration of the time interval between the n-th and $(n+1)$-th firing. One has:

$$\begin{aligned} F_{I_{n+1}|T_n}(x|t_n) &= P[I_{n+1} \leq x | T_n = t_n] = 1 - P[I_{n+1} > x | T_n = t_n] \\ &= 1 - P[T_{n+1} > x + t_n | T_n = t_n] = \int_{t_n}^{x+t_n} \hat{g}[\hat{S}(t), t | t_n]\, dt, \end{aligned}$$

so, assuming that (3.12) holds, it follows that

$$F_{I_{n+1}|T_n}(x|t_n) = 1 - \exp\{-\Lambda_{t_n}(t_n + x)\}.$$

Therefore, I_{n+1} conditioned from $T_n = t_n$ $(n = 0, 1, \ldots)$ is distributed according to a pdf with hazard function $\lambda(t_n + x)$ and integrated hazard function $\Lambda_{t_n}(t_n + x)$, that is:

$$f_{I_{n+1}|T_n}(x|t_n) = \frac{\partial}{\partial x} F_{I_{n+1}|T_n}(x|t_n) = \lambda(t_n + x) \exp\{-\Lambda_{t_n}(t_n + x)\}.$$

3.3 The effect of refractoriness

The refractoriness is the time interval of variable duration that follows a spike during which the neuron is incapable of responding to input signals. We introduce refrac-

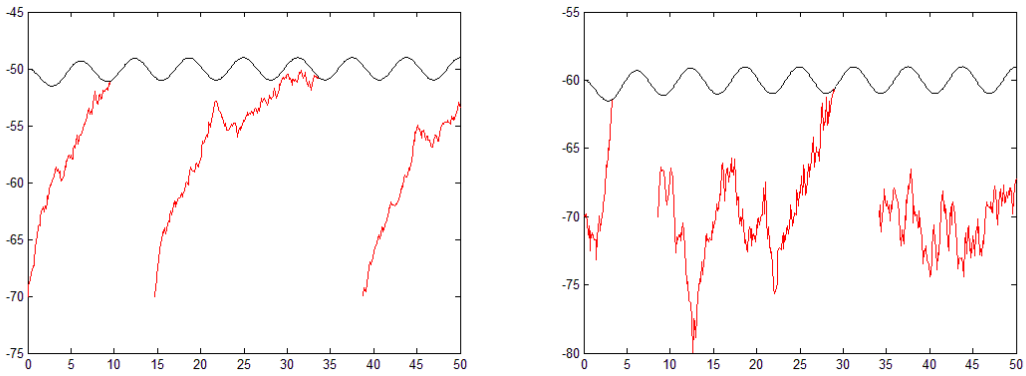

Figure 3.7: A sample path of $X^R(t)$ is plotted with a constant refractoriness of 5 ms and for $\eta = -70$, $\theta = 5$. On the left $\mu = -10$, $\tilde{S} = -50$, $\sigma = 1$, while on the right $\mu = -14$, $\tilde{S} = -60$, $\sigma = 3$. The black line is the threshold $\hat{S}(t) = -50 + d(t)$ on the left and $\hat{S}(t) = -60 + d(t)$ on the right, with $d(t)$ defined in (3.5) for $A = 1$.

toriness periods in the return process so that the interspike's interval, starting from the second one, can be considered as consisting of the sum of two terms: the first one represents the refractory period following the firing, the second term describes the time for firing from the state η. Therefore we construct a new process $X^R(t)$ describing the evolution of membrane potential in the presence of refractoriness as follows. Starting at $X^R(0) = \hat{X}(0) = \eta$, a firing takes place when $\hat{X}(t)$ attains for the first time the firing threshold $\hat{S}(t)$, defined in (3.10), after which the neuron is unable to fire again for a period of refractoriness of random duration. At the end of this period, $X^R(t)$ is instantaneously reset to η. The subsequent evolution of the process goes on as described by $\hat{X}(t)$, until the boundary is again reached. A new firing then occurs, followed by the period of refractoriness, and so on.
The process $X^R(t)$ consists of recurrent cycles $\mathcal{F}_0$, $\mathcal{R}_1$, $\mathcal{F}_1$, $\mathcal{R}_2, \ldots$ each of random duration. The duration of cycle $\mathcal{F}_i$ is represented by the random variable F_i described by the FPT pdf of $\hat{X}(t)$ through $\hat{S}(t)$ starting from η. Moreover, for $i = 1, 2, \ldots$, the refractory period $\mathcal{R}_i$ is represented by the random variable R_i. The pdf of R_i is denoted with $h_{t_i}(t)$ and it depends on the time t_i in which the last spike occurs. In particular, for $i = 0, 1, \ldots$, the duration F_i of $\mathcal{F}_i$ denotes the time interval elapsing between the i-th reset of the membrane potential at the value η and the $(i+1)$-th FPT from η to $\hat{S}(t)$. Instead, for $i = 1, 2, \ldots$, R_i indicates the duration of the i-th refractory period. Note that the random variables F_i are not independent and identically distributed because they depend on the instant of the last reset as well as $R_1, R_2, \ldots$ depend on the last firing time.

In Figure 3.7 sample paths of $X^R(t)$ are shown with a constant refractoriness of 5 ms and for $\eta = -70$, $\theta = 5$. On the left $\mu = -10$, $\sigma = 1$, while on the right

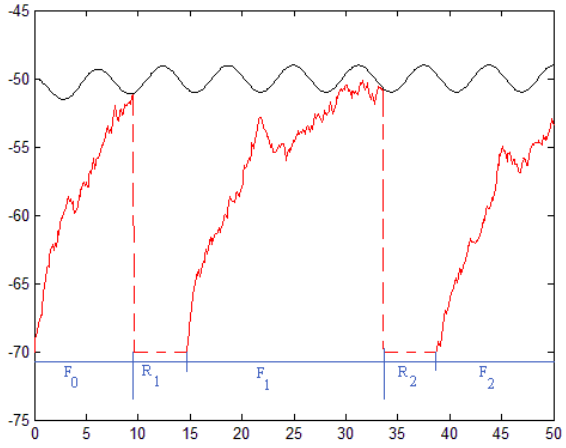

Figure 3.8: The random variables that describe the ISI are represented; the same sample path of the process plotted on the left of Figure 3.7 is considered.

$\mu = -14$, $\sigma = 3$. The black line is the threshold $\hat{S}(t) = -50 + d(t)$ on the left and $\hat{S}(t) = -60 + d(t)$ on the right, with $d(t)$ defined in (3.5) for $A = 1$. For the chosen parameters, we can compare the left side of Figure 3.7 with the left side of Figure 3.5 and the right side of Figure 3.7 with the left side of Figure 3.6. Since in Figures 3.6 and 3.5 sample paths of the process $X(t)$ without refractoriness are considered, the sample path of $X^R(t)$ reaches the thresholds less times than $X(t)$ during 50 ms. The random variables that describe the ISI are given by:

$$I_1^R = F_0, \qquad I_{n+1}^R = R_n + F_n \quad (n = 1, 2, \ldots);$$

they are represented in Figure 3.8 in which we consider the same sample path of the process plotted on the left of Figure 3.7.

To study the ISI pdf's we denote by $\mathbf{T^R} = (T_1^R, T_2^R, \ldots, T_n^R)$ the random vector that represents the instants of time in which single firings occur during the evolution of $X^R(t)$. Note that $T_1^R = I_1^R$ is a FPT random variable, moreover $T_n^R = \sum_{k=1}^n I_k^R$. Let

$$F_{I_{n+1}^R|T_n^R}(x|t_n) = P[I_{n+1}^R \leq x | T_n^R = t_n]$$

be the ISI distribution conditioned by the occurrence of the last firing at time t_n.

Proposition 5. *For $n = 1, 2, \ldots$ the ISI conditional distribution is:*

$$F_{I_{n+1}^R|T_n^R}(x|t_n) = \int_{t_n}^{x+t_n} h_{t_n}(r)\,[1 - \exp\{-\Lambda_r(x + t_n)\}]\; dr \tag{3.17}$$

and the ISI conditional pdf results:

$$f_{I^R_{n+1}|T^R_n}(x|t_n) = \int_{t_n}^{x+t_n} h_{t_n}(r)\lambda(t_n+x)\,\exp\{-\Lambda_r(x+t_n)\}\,dr. \tag{3.18}$$

Proof. To obtain the distribution $F_{I^R_{n+1}|T^R_n}(x|t_n)$ we note that x represents the width of the interval (t_n, t_n+x). So, after the instant of the n-th firing, occurred at time t_n, there is a refractory period that can have width at most x and ends at a certain time r. In the remaining interval (r, t_n+x) another firing occurs. It follows that:

$$F_{I^R_{n+1}|T^R_n}(x|t_n) = \int_{t_n}^{x+t_n} dr\, h_{t_n}(r) \int_r^{x+t_n} du\,\lambda(u)\,\exp\left\{-\int_r^u \lambda(v)\,dv\right\}, \tag{3.19}$$

from which, recalling (3.13), equation (3.17) immediately follows.
By taking the derivative with respect to x in (3.19), we get:

$$\begin{aligned} f_{I^R_{n+1}|T^R_n}(x|t_n) &= \frac{\partial}{\partial x}\int_{t_n}^{x+t_n} [h_{t_n}(r)\,(1-\exp\{-\Lambda_r(x+t_n)\})]\,dr \\ &= h_{t_n}(t_n+x)\,[1-\exp\{-\Lambda_{t_n+x}(t_n+x)\}]\,\frac{\partial(t_n+x)}{\partial x} \\ &- h_{t_n}(t_n)\,[1-\exp\{-\Lambda_{t_n}(t_n+x)\}]\,\frac{\partial(t_n)}{\partial x} \\ &+ \int_{t_n}^{x+t_n} h_{t_n}(r)\lambda(t_n+x)\,\exp\{-\Lambda_r(x+t_n)\}\,dr, \end{aligned}$$

that leads to (3.18). □

In the following we consider two types of refractoriness. In the first case the refractoriness is constant and its duration is $1/\zeta$, whereas in the second case we consider a refractoriness period of random duration characterized by exponential distribution with parameter ζ, so that its mean duration is the same of the constant case.

3.3.1 Constant refractory period

We assume that the refractoriness period is constant and of duration $1/\zeta$, with $\zeta > 0$. So, assuming that the last spike occurs at τ, one has:

$$h_\tau(t) = \delta\left(t-\tau-\frac{1}{\zeta}\right), \tag{3.20}$$

where $\delta(x)$ is the Dirac delta function. From Proposition 5, the ISI distribution can be evaluated. In particular, from (3.17), recalling (3.20) and making use of the properties of the Dirac delta function, it follows that:

$$F_{I^R_{n+1}|T^R_n}(x|t_n) = \int_{t_n}^{t_n+x} \delta\left(r - t_n - \frac{1}{\zeta}\right)\left[1 - \exp\left\{-\Lambda_r(t_n+x)\right\}\right] dr$$

$$= \begin{cases} 1 - \exp\left\{-\Lambda_{t_n+\frac{1}{\zeta}}(t_n+x)\right\}, & \text{if } x > \frac{1}{\zeta} \\ 0, & \text{if } x < \frac{1}{\zeta}, \end{cases}$$

with $\Lambda_\tau(t)$ defined in (3.13). Hence, one has:

$$F_{I^R_{n+1}|T^R_n}(x|t_n) = H\left(x - \frac{1}{\zeta}\right)\left[1 - \exp\left\{-\Lambda_{t_n+\frac{1}{\zeta}}\left(t_n+x\right)\right\}\right],$$

where $H(x)$ is the Heaviside unit step function. Furthermore, the ISI pdf is:

$$f_{I^R_{n+1}|T^R_n}(x|t_n) = H\left(x - \frac{1}{\zeta}\right)\left[\lambda(t_n+x)\exp\left\{-\Lambda_{t_n+\frac{1}{\zeta}}\left(t_n+x\right)\right\}\right]. \tag{3.21}$$

In Figures 3.9-3.10 the ISI pdf's in the presence of constant refractoriness are plotted

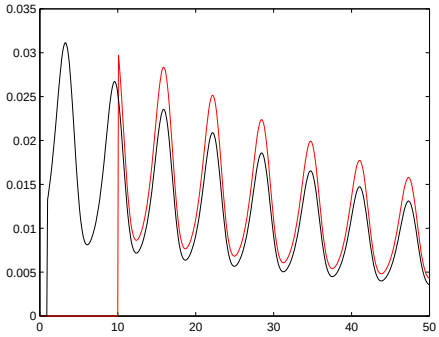

Figure 3.9: For the same parameters of the left side in Figure 3.7 and t_n= 5 ms, the ISI pdf's in the presence of constant refractoriness, given in (3.21), are plotted for $\zeta = 1$ (black line) and $\zeta = 0.1$ (red line).

with the same parameters of the left side in Figure 3.7. In Figure 3.9, we choose $\zeta = 0.1$ (red line), which represents a refractoriness of 10 ms, and $\zeta = 1$ (black line). Note that when the refractoriness period is longer (red line) the ISI pdf assumes higher values at times greater than 10 ms. Indeed, for a fixed time $x \geq 10$, the spikes are more frequent for shorter refractoriness, consequently, the distribution of the ISI decreases when ζ increases. The ISI pdf without refractoriness $f_{I_{n+1}|\hat{T}_n}$ (blue line) and the ISI pdf in the presence of constant refractoriness $f_{I^R_{n+1}|T^R_n}$ (red line), with $1/\zeta = 10$ ms, are compared in Figure 3.10. From the left of Figure 3.10, one can observe that, assuming the last spike occurs at the same time t_n, the ISI pdf

with refractoriness is not shifted with respect to that without refractoriness, as one would expect. This is due to the assumption that the two densities are evaluated for the same instant t_n. Indeed, if we consider the ISI pdf without refractoriness evaluated in $t_n + 1/\zeta$, we have the ISI pdf with refractoriness is shifted with respect to that without refractoriness, as shown on the right of Figure 3.10.

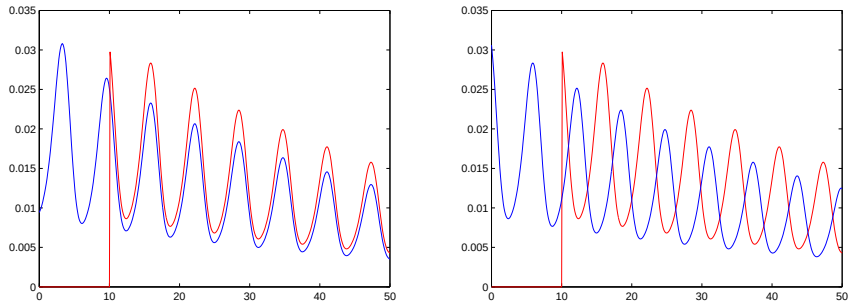

Figure 3.10: For the same parameters of Figure 3.9, on the left the ISI pdf's $f_{I_{n+1}|\hat{T}_n}(x|t_n)$ (blue line) and $f_{I^R_{n+1}|T^R_n}(x|t_n)$ with $\zeta = 0.1$ ms (red line) are plotted, on the right the ISI pdf's $f_{I^R_{n+1}|T^R_n}(x|t_n)$ and $f_{I_{n+1}|\hat{T}_n}(x|t_n + \frac{1}{\zeta})$ are compared.

3.3.2 Exponential refractory period

We suppose that the refractory period is a random variable having an exponential distribution of parameter ζ. Hence, assuming that the last firing occurs at time τ one has:

$$h_\tau(t) = \begin{cases} \zeta \exp\{-\zeta(t-\tau)\}, & \text{if } t > \tau \\ 0, & \text{if } t \leq \tau. \end{cases} \tag{3.22}$$

To determine the ISI distribution we make use of the Proposition 5. In particular, from (3.17), recalling (3.22), one has:

$$F_{I^R_{n+1}|T^R_n}(x|t_n) = \int_{t_n}^{t_n+x} \zeta e^{-\zeta(r-t_n)}[1 - \exp\{-\Lambda_r(t_n + x)\}]\, dr \qquad (x > \tau),$$

from which it follows:

$$F_{I^R_{n+1}|T^R_n}(x|t_n) = 1 - e^{-\zeta x} - \zeta e^{\zeta t_n} \int_{t_n}^{t_n+x} \exp\{-\zeta r - \Lambda_r(t_n + x)\}\, dr \qquad (x > \tau),$$

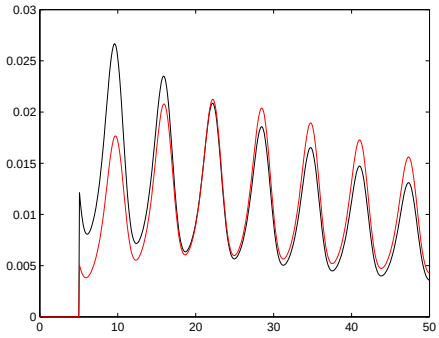

Figure 3.11: For the same parameters of Figure 3.9 and t_n= 5 ms, the ISI pdf given in equation (3.23) with $\zeta = 1$ (black line) and with $\zeta = 0.1$ (red line) are plotted.

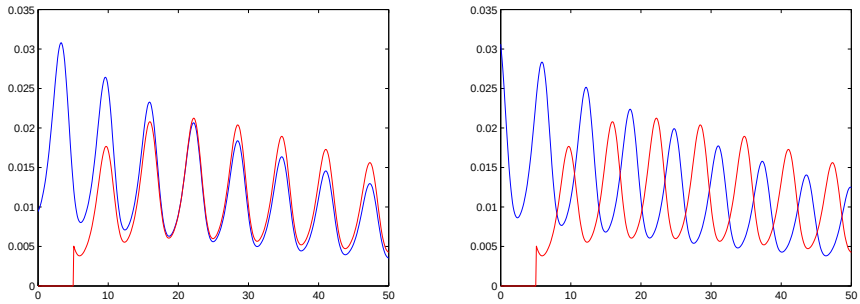

Figure 3.12: For the same parameters of Figure 3.10, on the left the ISI pdf's $f_{I_{n+1}|\hat{T}_n}(x|t_n)$ (blue line) and $f_{I^R_{n+1}|T^R_n}(x|t_n)$ (red line) given in equation (3.23) with $\zeta = 0.1$ are plotted; on the right, the densities $f_{I_{n+1}|\hat{T}_n}(x|t_n + \frac{1}{\zeta})$ (blue line) and $f_{I^R_{n+1}|T^R_n}(x|t_n)$ (red line) are compared.

where $\Lambda_\tau(t)$ is defined in (3.13). Moreover, the ISI density in the presence of exponential refractoriness is

$$f_{I^R_{n+1}|T^R_n}(x|t_n) = \zeta e^{\zeta t_n} \lambda(t_n + x) \int_{t_n}^{t_n+x} \exp\left\{-\zeta r - \Lambda_r(t_n + x)\right\} dr \qquad (x > \tau). \tag{3.23}$$

In Figures 3.11-3.12, the ISI pdf's in the presence of exponential refractoriness, obtained from equation (3.23), are plotted for the same parameters of Figure 3.9-3.10, respectively. From Figure 3.11, where $\zeta = 0.1$ (red line) and $\zeta = 1$ (black line), we note that for small amplitudes (small values of x) the ISI pdf for $\zeta = 1$ exceeds the density for $\zeta = 0.1$ and then this behavior reverses, differently from the case of constant refractoriness (cf. Figure 3.9). Indeed, since the refractoriness mean is $1/\zeta$ ms, one has that for small values of x, corresponding to small ISI durations, it is more likely that the neuron with smaller mean refractoriness fires. As in the case of

constant refractoriness we compare the ISI densities with and without refractoriness. From Figure 3.12, where $\zeta = 0.1$, we note that, also in this case, the curves are not shifted, whereas this property is verified when we compare $f_{I_{n+1}|\hat{T}_n}(x|t_n + \frac{1}{\zeta})$ and $f_{I^R_{n+1}|T^R_n}(x|t_n)$ at least for great values of x as we can see on the right of Figure 3.12.

Conclusions and future developments

In this thesis we have studied evolutionary processes subject to jumps and we have considered various applications of interest in different areas.
A jump, or catastrophe, is considered as a random event that shifts the state of the process in a certain level from which the process can re-start. We have introduced the effect of jumps in deterministic models for rumor spreading, in time non-homogeneous Markov chains and in stochastic diffusion processes with particular attention to the Gompertz model for cancer evolution and to the non-homogeneous Ornstein-Uhlenbeck process for neuronal activity.
In the following, we summarize the performed studies and we provide some possible developments.

- We have firstly analyzed rumor spreading mechanisms, during which one can consider the effect of an external entity that denies the rumor so that the process is reset to the initial state consisting in a unique spreader that renews the spreading process. The denials are random and they occur according to a Poisson process with parameter ξ.
  Two rumor spreading models with denials have been studied. In both models the population has been divided into three groups: the spreaders (who know and transmit the rumor), the ignorants (who do not know the rumor) and the stiflers (who know the rumor but do not transmit it). The rumor spreads through pair-wise contacts between spreaders and the other people occurring with rate λ.
  We have considered the well-known DK model with denials (model A), and an alternative model in which denials occur and each spreader can transmit the rumor at most k times (model B). For both models, we have focused on the asymptotic percentage of ignorants to identify the density of the population that knows the rumor.
  We have noted that, in both cases the asymptotic percentage of ignorants increases when the rate of the denials grows respect to the rate of the contacts;

in particular, if the size of the population is large and $\xi \geq \lambda$, the rumor does not spread at all.

For the model B, the density of individuals that knows the rumor increase with k, since the rumor has more chance to spread. Moreover, the model B behaves like the model A when k increases, in particular a good match is found already for $k = 6$. In both models, we have obtained that at most the half of the population can be informed about the rumor.

Future work would consists in studying the corresponding stochastic processes and in constructing other models that follows different rules.

- Concerning the time non-homogeneous Markov chains, we have considered the effect of catastrophes which occur at random times and that empty instantaneously the system reducing to zero the number of customers.

  Catastrophes occur according to a time non-homogeneous Poisson process; in particular, the catastrophe's rates depend on time and on the number of customers in the queue.

  We have analyzed the system by studying the transition probabilities and the moments of the number of customers in the system. We have focused on the problem of FVT to zero state with particular attention to busy period of the service center, i.e the time interval during which at least one server is busy. Specifically, we have paid attention to the case in which the catastrophe intensity is a periodic function of time obtaining some properties of asymptotic distribution and of the FVT density. We have studied the $M/M/1$ queueing systems to perform an example of the obtained results.

- In Chapter 1, *Stochastic diffusion processes with random jumps*, we construct diffusion processes with jumps by supposing that catastrophes occur at time interval following a general distribution and the return points are randomly chosen. Moreover, we have considered the possibility that, after each jump, the process can evolve with a different dynamics respect to the previous processes; we have also supposed that the inter-jump intervals and the return points are not identically distributed. For this type of process, we analyze the pdf, its moments and the FPT problem. We have also studied the Wiener process with jumps, as example.

- In Chapter 2, **A Gompertz model with jumps for an intermittent treatment in cancer growth**, to analyze the effect of a therapeutic program that provides intermittent suppression of cancer cells, we have constructed a Gompertz process with jumps for which a jump represents an application of the therapy.

Firstly, we have considered a simple model in which the Gompertz process has the same characteristics between two consecutive jumps, the return points and the inter-jump intervals are random and identically distributed. For this model, we have studied the transition pdf, the average state of the system and the number of therapeutic applications to be carried out in time intervals of fixed amplitude. We have considered the degenerate and the exponential distribution for the inter-jump intervals and we have studied three different distributions of the return point (degenerate, uniform and bi-exponential). We have noted that the obtained results for different distribution are comparable, so, in the following studies, we have considered only the degenerate case without loss of generality.

After this first step, we have constructed a more realistic model. Specifically, we have assumed: the therapeutic program has a deterministic scheduling, so that jumps occur at fixed and conveniently chosen time instants; the return points are deterministic; therapeutic treatments weaken an ill organism and when a therapy is applied there is a selection event in which only the most aggressive clones survive (for example this perspective could be applied to targeted drugs that have a much lower toxicity for the patient).

Taking into consideration these aspects, we have constructed the deterministic and the stochastic processes with jumps.

Two possible scheduling have been proposed in order to control the cancer growth. In the first scheduling, we have assumed that inter-jump intervals have equal size. We have also supposed that the return points are all equal after each jump. In this case, we have obtained interesting properties which allow to choose the most appropriate application times, when the toxicity of the drug is fixed.

In the second scheduling, we have suggested to apply the therapy just before the cancer mass reaches a fixed control threshold S. To this aim, we have studied the FPT problem through S and we have provided information on how to choose the application times so that the cancer size remains bounded during the treatment. The goodness of the obtained results has been measured via the increase of the mean FPT of the process through S. The performed analysis have shown that better results are obtained when the therapy is applied as later as possible, for higher control thresholds and smaller weakening rates. Moreover, we have compared the deterministic and stochastic approaches noting that, for both scheduling, the mean FPT through S increases as the amplitude of random fluctuations increases.

We have also provided a comparison between the two proposed scheduling

concluding that the second strategy is the best, i.e. it is preferable to apply the therapy just before the cancer mass crosses the control threshold.
Future study would consist the inclusion of delay times after each therapeutic application. Indeed, it is reasonable to think that the effect of an application is not instantaneous, but it needs a time interval to observe the effect of the treatment. Such interval can have random duration imagining that the reaction times are variable for different individuals.

- In Chapter 3, **Return process with refractoriness for a non-homogeneous Ornstein-Uhlenbeck neuronal model**, we have considered a diffusion stochastic process with jumps for the neuronal activity.
  To describe the input-output behavior of a single neuron subject to a diffusion-like dynamics, we have modeled the neuronal membrane potential via the Ornstein-Uhlenbeck (OU) diffusion process. We have assumed that inputs, while remaining a constant amplitude, are characterized by time-dependent rates. In particular, we have considered an OU process characterized by a time-dependent drift in which appears a periodic function $m(t)$ representing some oscillatory effects of the environment acting on the neuron.
  A return process has been constructed on such time non-homogeneous OU process as follows. Starting from a value representing the resting potential, the neuronal membrane potential follows the non-homogeneous OU process as long as a threshold (the action threshold) is reached for the first time. In correspondence to the reaching of this peak, a neuronal spike occurs resetting the process to the resting potential. Then, the membrane potential evolves as before until the threshold is reached again causing another neuronal spike, and so on. This process describes the spike train. In order to study the ISI distribution, we have studied the FPT random variable of the non-homogeneous OU process because it represents the theoretical counterpart of the neuronal firing time, so that the FPT's pdf describes the pdf of the firing time. In this regard, for the FPT pdf of the OU process we have made use of an asymptotic behavior of exponential type for the firing time.
  Concerning this return process, we have studied the ISI distribution and the number of firings occurring until a fixed time.
  Moreover, we have taken into account the effect of the refractoriness on the model. Hence, we have introduced random downtimes which delay spikes, simulating the effect of refractoriness. We have provide the expression of the ISI distribution also for the process with refractoriness. This distribution is conditioned by the time in which the last fire occurs.
  A theoretical and numerical analysis of the return process in the presence of

constant and exponential refractoriness has been performed.
Some similarities between the ISI pdf with refractoriness and without refractoriness have been observed. In particular, our analysis has shown that the ISI pdf in the presence of refractoriness is shifted with respect to the ISI pdf in the absence of refractoriness provided the latter is suitably conditioned.
Future research may investigate the behavior of the model with different external inputs (different choices of the function $m(t)$) as well as different refractoriness distributions.

Bibliography

[1] Abundo M, Rossi C (1989) Numerical simulation of a stochastic model for cancerous cells submitted to chemotherapy. Journal of Mathematical Biology 27, No. 1: 81-90

[2] Abundo M, Rossi C, Rubiu O (1993) Estimation of parameters for stochastic model of tumoral cells treated with anticancer agents. Journal of Experimental & Clinical Cancer Research 12, No. 2: 81-90

[3] Abundo M (2010) First-passage problems for one dimensional diffusions with random jumps from boundary. Stochastic Analysis and Applications 29, No. 1: 121-145

[4] Albano G, Giorno V (2006) A stochastic model in tumor growth. Journal of Theoretical Biology 242, No.2: 229-236

[5] Albano G, Giorno V, Saturnino C (2007) A prey-predator model for immune response and drug resistence in tumor growth. In Computer Aided SystemsTheory EUROCAST 2007 (Moreno-Diaz R.,Pichler F.R. and Quesada-Arencibia A., eds.) Lecture Notes in Computer Science, Vol. 4739, Springer-Verlag, Berlin. ISBN: 3-540-75866-2, 171-178

[6] Albano G, Giorno V (2008) Towards a stochastic two-compartment model in tumor growth. Scientiae Mathematicae Japonicae 67, No. 2: 305-318

[7] Albano G, Giorno V, Román-Román P, Torres-Ruiz F (2011) Inferring the effect of therapy on tumors showing stochastic Gompertzian growth. Journal of Theoretical Biology 276: 67-77

[8] Albano G, Giorno V, Román-Román P, Torres-Ruiz F (2012) Inference on a stochastic two-compartment model in tumor growth. Computational Statistics & Data Analysis 56: 1723-173

[9] Albano G, Giorno V, Román-Román P, Torres-Ruiz F (2013) On the effect of a therapy able to modify both the growth rates in a Gompertz stochastic model. Mathematical Biosciences 245: 12-21

[10] Albano G, Giorno V, Román-Román P, Román-Román S, Torres-Ruiz F (2014) Estimating and determining the effect of a therapy on tumor dynamics by a modified Gompertz diffusion process. Journal of Theoretical Biology 364C: 206-219. doi: 10.1016/j.jtbi.2014.09.014

[11] Bettencourt L M A, Cintron-Arias A, Kaiser D I, Castillo-Chavez C (2006) The power of a good idea: quantitative modeling of the spread of ideas from epidemiological models. Physica A 364: 513-536

[12] Brockwell P J, Gani J, Resnick S I (1982) Birth, immigration and catastrophes processes. Advances in Applied Probability 14: 709-731

[13] Brockwell P J (1985) The extinction time of a birth, death and catastrophe process and of a related diffusion model. Advances in Applied Probability 17: 42-52

[14] Brockwell P J (1986) The extinction time of a general birth and death process with catastrophes. Journal of Applied Probability 23: 851-858

[15] Buonocore A, Nobile A G, Ricciardi L M (1987) A new integral equation for the evaluation of first-passage-time probability densities. Advances in Applied Probability 19: 784-800

[16] Buonocore A, Caputo L, Pirozzi E (2008) On the evaluation of firing densities for periodically driven neuron models. Mathematical Biosciences 214: 122-133

[17] Cameron D A (1997) Mathematical modelling of the response of breast cancer to drug therapy. Journal of Theoretical Medicine 2: 137-151

[18] Capocelli R M, Ricciardi L M (1971) Diffusion approximation and first passage time problem for a model neuron. Kybernetik (Berlin) 8: 214-223

[19] Chao X, Zheng Y (2003) Transient analysis of immigration birth-death processes with total catastrophes. Probability in Engineering and Informational Sciences 17: 83-106

[20] Daley D J, Gani J (1999) Epidemic Modelling: An Introduction. Cambridge University Press, Cambridge

[21] Daley D J, Kendall D G (1964) Epidemics and rumors. Nature 204: 11-18

[22] Daley D J, Kendall D G (1965) Stochastic rumors. Journal of the Institute of Mathematics and its Applications 1: 42-55

[23] de Vladar H P, Gonzalez J A, Rebolledo M (2003) New-late intensification schedules for cancer treatments. Acta Cient Venez 54: 263-276

[24] de Vladar H P, Gonzalez J A (2004) Dynamics response of cancer under the influence of immunological activity and therapy. Journal of Theoretical Biology 227: 335-348

[25] Di Cesare R, Giorno V, Nobile A G (2009) Diffusion Processes Subject to Catastrophes. Lecture Notes in Computer Science 5717: 129-136

[26] Di Crescenzo A, Giorno V, Nobile A G, Ricciardi L M (2003) On the M/M/1 queue with catastrophes and its continuous approximation. Queueing Systems 43: 329-347

[27] Di Crescenzo A, Giorno V, Nobile A G, Ricciardi L M (2008) A note on birth-death processes with catastrophes. Statistic & Probability Letters 78: 2248-2257

[28] Di Crescenzo A, Giorno V, Nobile A G, Ricciardi L M (2010) On time non-homogeneous stochastic processes with catastrophes. In Cybernetics and Systems 2010 (Trappl R., ed.). EMCSR 2010. Austrian Society for Cybernetics Studies, Vienna, 169-174, ISBN 978-3-85206-178-8

[29] Di Crescenzo A, Giorno V, Krishna Kumar B, Nobile A G (2012) A double-ended queue with catastrophes and repairs, and a jump-diffusion approximation. Methodology and Computing in Applied Probability 14: 937-954

[30] Ditlevsen S, Lansky P (2005) Estimation of the input parameters in the Ornstein-Uhlenbeck neuronal model. Physical Review E 71: 011907

[31] Ditlevsen S, Lansky P (2008) Comparison of statistical methods for estimation of the input parameters in the Ornstein-Uhlenbeck neuronal model from first-passage times data. In Collective Dynamics: Topics on Competition and Cooperation in the Biosciences (eds. L. M. Ricciardi, A. Buonocore and E. Pirozzi), AIP Conf. Proc., 1028, Amer. Inst. Phys., Melville, NY: 171-185

[32] Economou A, Fakinos D (2003) A continuous-time Markov chain under the influence of a regulating point process and applications in stochastic models with catastrophes. European Journal of Operational Research 149: 625-640

[33] Esposito G, Giorno V, Nobile A G, Ricciardi L M, Valerio C (2006) Neuronal modeling in the presence of random refractoriness. Scientiae Mathematicae Japonicae 64: 1-36

[34] Feller W (1952) The parabolic differential equations and the associated semigroups of transformations. Annals of Mathematics 55: 468-518

[35] Feller W (1954) Diffusion processes in one dimension. Transactions of the American Mathematical Society 77: 1-31

[36] Gerlee P (2013) The Model Muddle: In Search of Tumor Growth Laws. Cancer Research 73(8): 2407-2411

[37] Gerstein G L, Mandelbrot B (1964) Random walk models for the spike activity of a single neuron. Biophysical Journal 4: 41-68

[38] Giorno V, Nobile A G, Ricciardi L M, Sato S (1989) On the evaluation of first-passage-time probability densities via nonsingular integral equations. Advances in Applied Probability 21: 20-36

[39] Giorno V, Nobile A G, Ricciardi L M (1990) On the asymptotic behaviour of first-passage-time densities for one-dimensional diffusion processes and varying boundaries. Advances in Applied Probability 22: 883-914

[40] Giorno V, Nobile A G, Saura A (2003) Prendiville stochastic growth model in the presence of catastrophes. Cybernetics and Systems, Vol. I, Austrian Society for Cybernetic Studies, Vienna

[41] Giorno V, Nobile A G, Saura A (2008) Loss system in the presence of catastrophes. In Cybernetics and Systems 2008. Trappl R., ed. EMCSR 2008. Austrian Society for Cybernetics Studies, Vienna: 261-266

[42] Giorno V, Spina S (2013) A Stochastic Gompertz Model with Jumps for an Intermittent Treatment in Cancer Growth. In: R. Moreno-Diaz, F.R. Pichler, A. Quesada-Arencibia (Eds.), Computer Aided Systems Theory - EUROCAST 2013, Lecture Notes in Computer Science 8111 : 61-68, Springer-Verlag

[43] Giorno V, Nobile A G, Spina S (2014) A note on time non-homogeneous adaptive queue with catastrophes. Applied Mathematics and Computation: 220-234

[44] Giorno V, Spina S (2014) On the return process with refractoriness for a non-homogeneous Ornstein-Uhlenbeck neuronal model. Mathematical Biosciences and Engineering, Volume 11, Number 2: 285-302

[45] Giorno V, Spina S (2014) Rumor spreading with denials. Pre-print

[46] Giorno V, Spina S (2015) A model of tumor dynamics subject to an intermittent treatment involving reduction of tumor size and rise of growth rate. To appear on: R. Moreno-Diaz, F.R. Pichler, A. Quesada-Arencibia (Eds.), Computer Aided Systems Theory - EUROCAST 2015, Lecture Notes in Computer Science, Springer-Verlag

[47] Giorno V, Spina S (2015) Analysis of a cancer growth model subject to a treatment applied at constant intervals. Work in progress

[48] Spina S, Giorno V, Román-Román P, Torres-Ruiz F (2014) A Stochastic Model of Cancer Growth Subject to an Intermittent Treatment with Combined Effects: Reduction of Tumor Size and Rise of Growth Rate. Bulletin of Mathematical Biology 76(11): 2711-36. doi: 10.1007/s11538-014-0026-8

[49] Hausten V, Schumacher U (2012) A dynamic model for tumor growth and metastasis formation. Journal of Clinical Bioinformatics 2: 11

[50] Hirata Y, Bruchovsky N, Aihara K (2010) Development of a mathematical model that predicts the outcome of hormone therapy for prostate cancer. Journal of Theoretical Biology 264: 517-527

[51] Karlin S, Taylor H M (1981) A Second Course in Stochastic Processes. Gulf Professional Publishing

[52] Kawachi K (2008) Deterministic models for rumor transmission. Nonlinear Analysis: Real World Applications 9: 1989-2028

[53] Kawachi K, Seki M, Yoshida H, Otake Y, Warashina K, Ueda H (2008) A rumor transmission model with various contact interactions. Journal of Theoretical Biology 253: 55-60

[54] Kozusko F, Bajzer Z (2003) Combining Gompertzian growth and cell population dynamics. Mathematical Biosciences 185: 153-167

[55] Kyriakidis E G (1994) Stationary probabilities for a simple immigration-birth-death process under the influence of total catastrophes. Statistics & Probability Letters 20: 239-240

[56] Kyriakidis E G (2004) Optimal control of a simple immigration-emigration process through total catastrophes. European Journal of Operational Research (Stochastic and Statistics) 155: 198-208

[57] Krishna Kumar B, Krishnamoorthy A, Pavai Madheswari S, Sadiq Basha S (2007) Transient analysis of a single server queue with catastrophes, failures and repairs. Queueing Systems 5: 133-141

[58] Lansky P, Sacerdote L (2001) The Ornstein-Uhlenbeck neuronal model with signal-dependent noise. Physics Letters A 285: 132-140

[59] Lansky P, Sanda P, He J (2006) The parameters of the stochastic leaky integrate-and-fire neuronal model. Journal of Computational Neuroscience 21: 211-223

[60] Lefevre C, Picard P (1994) Distribution of the final extent of a rumor process. Journal of Applied Probability 31: 244-249

[61] Lo C F (2007) Stochastic Gompertz model of tumor cell growth. Journal of Theoretical Biology 248: 317-321

[62] Lo C F (2010) A modified stochastic Gompertz model for tumor cell growth. Computational and Mathematical Methods in Medicine 11(1): 3-11

[63] Maki D P, Thomson M (1973) Mathematical Models and Applications, with Emphasis on Social, Life, and Management Sciences, Prentice. Hall, Englewood Cliffs, NJ

[64] Maronski R (2008) Optimal strategy in chemotherapy for a Gompertzian model of cancer growth. Acta of Bioengineering and Biomechanics 10 No. 2: 81-84

[65] Marusic M, Bajzer Z, Vul-Pavlovic S, Freyer J (1994) Tumor growth in vivo and as multicellular spheroids compared by mathematical models. Bulletin of Mathematical Biology 56, No. 4: 617-631

[66] Migita T, Narita T, Nomura K (2008) Activation and Therapeutic Implications in Non-Small Cell Lung Cancer. Cancer Research 268: 8547-8554

[67] Nobile A G, Ricciardi L M (1980) Growth and extinction in random environment. Appl. Inform. Control Syst.: 455-465

[68] Noymer A (2001) The transmission and persistence of urban legends: Sociological application of age-structured epidemic models. Journal of Mathematical Sociology 25: 299-323

[69] Norton L (1988) A Gompertzian Model of Human Breast Cancer Growth. Cancer Research 48: 7067-7071

[70] Pakes A G (1997) Killing and resurrection of Markov processes. Communications in Statistics Stochastic Models 13: 255-269

[71] Parfitt A M, Fyhrie D P (1997) Gompertzian growth curves in parathyroid tumors: further evidence for the set-point hypothesis. Cell Proliferation 30: 341-349

[72] Pittel B (1990) On a daley-kendall model of random rumors. Journal of Applied Probability 27: 14-27

[73] Ricciardi L M (1979) On the conjecture concerning population growth in random environment. Biological Cybernetics 32: 95-99

[74] Ricciardi L M, Di Crescenzo A, Giorno V, Nobile A G (1999) An outline of theoretical and algorithmic approches to first passage time problems with applications to biological modeling. Mathematica Japonicae 50: 247-322

[75] Ricciardi L M, Esposito F (1966) On some distribution functions for non-linear switching elements with finite dead time. Kybernetik 3: 148-152

[76] Ricciardi L M, Sacerdote L (1979) The Ornstein-Uhlenbeck process as a model for neuronal activity. Biological Cybernetics 35: 1-9

[77] Román-Román P, Torres-Ruiz F (2012) Inferring the effect of therapies on tumor growth by using diffusion processes. J. Theor. Biol., 314: 34-56

[78] Siegert A J F (1951) On the first passage time probability problem. Physical Review 81: 617-623

[79] Speer J F, Petrosky V E, Retsky M W, Wardwell R H (1984) A stochastic numerical model of breast cancer growth that simulates clinical data. Cancer Research 44: 4124-4130

[80] Spratt J A, von Fournier D, Spratt J S, Weber E E (1992) Decelerating Growth and Human Breast Cancer. Cancer 71 No. 6: 2013-2019

[81] Sudbury A (1985) The proportion of the population never hearing a rumor. Journal of Applied Probability 22: 443-446

[82] Swift R J (2001) Transient probabilities for a simple birth-death immigration processes under the influence of total catastrophes. International Journal of Mathematical Sciences 25: 689-692

[83] Tanaka G, Hirata Y, Goldenberg S L, Bruchovsky N, Aihara K (2010) Mathematical modelling of prostate cancer growth and its application to hormone therapy. Philosophical Transaction of the Royal Society A 368: 5029-5044

[84] Teich M C, Matin L, Cantor B I (1978) Refractoriness in the maintained discharge of the cat's retinal ganglion cell. Journal of the Optical Society of America 68: 386-402

[85] Trpevski D, Tang W K S, Kocarev L (2010) Model for rumor spreading over networks. Physical Review E 81, 056102

[86] Wang J, Tucker L A, Stavropoulos J (2007) Correlation of tumor growth suppression and methionine aminopetidase-2 activity blockade using an orally active inhibitor, Global pharmaceutical Research and Development, Abbott Laboratories. Edit by Brian W. Matthews, University of Oregon; Eugene, OR

[87] Weedon-Fekjaer H, Lindqvist B H, Vatten L J, Aalen O O, Tretli S (2008) Breast cancer tumor growth estimated through mammography screening data. Breast Cancer Research 10: R41. doi: 10.1186/bcr2092

[88] Zhang J (1991) The transient solution of time-dependent $M/M/1$ queues. IEEE Transactions on Information Theory 31(6): 1690-1696

[89] Zhao L, Wang J, Chen Y, Wang Q, Cheng J, Cui H (2012) SIHR rumor spreading model in social networks. Physica A 391: 2444-2453

Ringraziamenti

Un primo ringraziamento va alla Prof.ssa Virginia Giorno che ha creduto in me e mi ha accompagnata in questo viaggio. La ringrazio per avermi sempre lasciata libera di esprimere le mie idee e di fare le mie scelte, permettendomi di cimentarmi negli ambiti a me più favoriti e congeniali. Grazie soprattutto per essere stata contemporaneamente mentore e guida dei miei passi.
I miei più sinceri ringraziamenti vanno anche ai Professori Amelia G. Nobile e Antonio Di Crescenzo che mi hanno permesso di crescere notevolmente durante questi anni.
Ringrazio la mia famiglia e le mie più care amiche, Serena e Valeria, per avermi sostenuta incondizionatamente con il loro amore.
Il mio più sentito grazie va a colui che mi ha supportato e sopportato in questo percorso dimostrandosi il mio più accanito sostenitore. Il confronto umano e accademico con lui è stato fondamentale per la mia crescita; senza di lui non sarebbe stata la stessa cosa. GRAZIE Giuseppe!
E, infine, grazie a ME STESSA per l'impegno e la passione spesi giorno dopo giorno nella realizzazione di questo lavoro.